

STRUCTURAL INTERPRETATION OF THE MORENCI MINING DISTRICT,
GREENLEE COUNTY, ARIZONA

by

Mary Amelia Walker

THESIS

Presented to the Faculty of the Graduate School of

New Mexico Institute of Mining and Technology

in Partial Fulfillment of the Requirements

for the Degree of

MASTER OF SCIENCE

NEW MEXICO INSTITUTE OF MINING AND TECHNOLOGY
SOCORRO, NEW MEXICO
December 1995

ACKNOWLEDGMENTS

Working in the Morenci mining district has been a special experience. There have been many great minds that have gone before me and to follow in their footsteps was a great challenge. Waldemar Lindgren was the first. In 1905, he came to this district to learn about and document the geology of one of the southwestern North America porphyry copper deposits. He set the stage for nearly 100 years of geologists to follow. Times change, theories change, and knowledge grows, but the fundamental basics of the science we call geology, the science of the earth, remain intact. The most important lesson that I have learned while researching and writing this thesis is this one simple fact. To all the great geologists who have come before me, I thank you for the heritage.

There are always many people who contribute their knowledge, patience, and time in any undertaking such as this. I would like to propose a toast to some of the people who have given a part of themselves to me: To Fred J. Menzer, for the chance, Laurel B. Goodwin, for the patience, Richard K. Preece, for the insight; Charles E. Chapin, for the humor; William X. Chavez, for the impulse; David B. Johnson, for the rules; and M. Steven Enders, for the time. Also, a very special acknowledgment to Ron and Amie and Daniel, who at times were ready to trade me in for a new model.

Far better it is to dare mighty things, to win glorious triumphs even though checkered by failure than to take rank with those poor spirits who neither enjoy much nor suffer much because they live in the gray twilight that knows not victory nor defeat.

Theodore Roosevelt

STRUCTURAL INTERPRETATION OF THE MORENCI MINING DISTRICT,
GREENLEE COUNTY, ARIZONA

by

Mary Amelia Walker

ABSTRACT

The Morenci mining district, located on the southeastern edge of the Transition Zone physiographic province of Arizona, hosts the largest producing porphyry copper deposit in North America. The district is approximately 90 km² and appears as a roughly triangular window of Precambrian through early Tertiary rocks units surrounded by middle Tertiary volcanic rocks and Miocene through Quaternary basin fill deposits. Multiple deformational episodes are recorded in the complex geological terrain of this district.

Relative stability prevailed, in this district, during most of the Paleozoic through late Cretaceous. The first marked disturbance of Paleozoic through late Cretaceous sedimentary rocks exposed in the Morenci mining district occurred in association with Paleocene to early Eocene porphyry intrusions. Main-stage alteration and mineralization is associated in time and space with emplacement and cooling of part of this system of intrusions. Regional tectonism during the Laramide orogeny exerted a strong control on

the nature and distribution of the Morenci district porphyry copper system, as demonstrated by the consistently 040° to 020°-striking Laramide-age normal faults, veins, dikes, and stocks. These regularly oriented structures record NW to NNW extension during the Laramide orogeny

Evidence for Laramide-age faulting also occurs along east-striking faults and one NW-striking fault. Slickensides on fault surfaces of the east-striking Coronado fault record a complex history of strike-slip, oblique-slip and dip-slip motion. Further, fault zone deformation features and cross-cutting relationships suggest that the Coronado fault and other east-striking faults acted as conduits for hydrothermal fluids and/or constrained the distribution of hypogene mineralization and subsequent supergene enrichment. Fault zone deformation features associated with the NW-striking Kingbolt fault record pre-intrusion, syn-mineralization and post-Laramide movement.

Regional extension dominated the tectonic regime of the southwestern United States from the late Oligocene through the late Miocene. The Morenci mining district lies between the relatively structurally intact Colorado Plateau and the highly extended terrain of the southern Basin and Range province. Evidence for metamorphic core complex-type deformation occurs within 25 km southwest of the Morenci mining district. A series of NE-striking structural zones that accommodated moderate to strong extension define the southeastern edge of the Colorado Plateau. These structural zones extend to the northeast from this district.

The Laramide-age structures in the Morenci district are cut by a series of NW-striking faults. The district is bounded to the southwest by the NW-striking Eagle Creek fault. This fault juxtaposes Paleozoic through Cretaceous sedimentary rocks and Laramide-age intrusives against middle Tertiary volcanic rocks and/or conglomerates. Fault-zone deformation features and cross-cutting relationships associated with many NW-striking faults in the district indicate that movement occurred subsequent to Laramide-age deformation. Extension accommodated by the NW-striking Eagle Creek fault system may have been associated with metamorphic core complex deformation that was active in this region from the latest Oligocene through early Miocene.

Although the majority of NE-striking structures in this district record Laramide-age deformation, the NE-striking San Francisco fault either represents a younger episode of faulting or was reactivated during late Oligocene through Miocene extensional tectonism. The San Francisco fault bounds the southeastern portion of the district and cuts all other faults to the north and northwest. Surface mapping and drill hole data indicate that the San Francisco fault is the bounding fault of a half-graben filled with Gila Group conglomerates. Gila Group conglomerates and Precambrian granite and granodiorite are therefore juxtaposed across this fault. Extension along the San Francisco fault is believed to be related to the NE-striking structural zone that defines the southeastern edge of the Colorado Plateau.

The north-striking Chase Creek fault is associated with the mountainous region to the north of the district. Slickensides on the fault surface record dip-slip motion that

placed middle Tertiary volcanic rocks on the east against Precambrian granite on the west. Faulting along the Chase Creek fault system is interpreted to have formed in response to structural adjustments that occurred within the transition zone between the highly extended terrain of the southern Basin and Range and the stable Colorado Plateau.

TABLE OF CONTENTS

INTRODUCTION

The Morenci Mining District.....	1
Method of Study.....	4

GEOLOGIC SETTING

Precambrian through Late Cretaceous Stratigraphy of the Morenci Mining District.....	6
The Laramide Orogeny.....	12
Late Paleocene to Eocene Intrusion in the Morenci Mining District.....	15
Hydrothermal Alteration and Mineralization.....	23
Evidence for Laramide-age Extension Directions in the Morenci Mining District.....	27
First Generation of Supergene Enrichment in the Morenci Mining District.....	30
Middle Tertiary Tectonism.....	33
Middle to Late Miocene Extension.....	45
Second Generation of Supergene Enrichment in the Morenci Mining District.....	46

STRUCTURAL DESCRIPTION AND ANALYSIS OF THE MORENCI MINING DISTRICT

Introduction.....	47
Terminology.....	48
Evidence of Laramide-age Faulting.....	50
Northwest-Striking Faults.....	78
Northeast-Striking Faults.....	91

North-Striking Faults.....	95
Summary and Discussion.....	104
CONCLUSIONS.....	110
REFERENCES.....	115

LIST OF TABLES

Table 1. Radiometric age determinations from selected rocks and minerals from the Morenci mining district	20
Table 2. Depths estimated from the pressures determined from coexisting liquid-rich and vapor-rich inclusions in stockwork veins. Maximum depths were derived assuming pure hydrostatic head, minimum depths were derived assuming pure lithostatic head	26
Table 3. Radiometric age determinations for middle Tertiary volcanic rocks near the Morenci mining district. Numbers on table correspond numbered locations in Figure 10.....	35

LIST OF FIGURES

Figure 1. Regional location of the Morenci mining district. Insert described in Figure 2.	3
Figure 2. Generalized distribution of rocks that crop out in the Morenci mining district. The Morenci porphyry copper deposit lies within the Precambrian through early Tertiary units.....	5
Figure 3. Graphical representation, generalized descriptions and regional correlations of the Precambrian, Paleozoic and Cretaceous sedimentary units in the Morenci mining district.	9
Figure 4. Index map to porphyry copper deposits in Arizona, New Mexico, and Sonora, Mexico. Modified from Titley (1982).	16
Figure 5. Paleocene to early Eocene intrusives and associated breccias in the Morenci mining district. Note the northeast migration of intrusive centers over time. A key to the map is shown on the following page; coordinates shown on map correspond with the Morenci mining district survey grid. See also Plate 1 Modified from Preece and others (1984).	18
Figure 6. Lower hemisphere equal-area plots of poles to mesoscopic intrusive contacts, main-stage veins and late fissure veins in the Morenci mining district. Modified from Preece (1986).....	25

- Figure 7. Summary of fluid inclusion homogenization temperatures for the major vein types in the Morenci mining district. A systematic progression of fluid characteristics is observed through time (see text). L = Liquid, V = Vapor, b = bars, Qtz-Kspar = quartz-Kfeldspar veins, Qtz-Moly = quartz-molybdenite veins, Qtz-Ser-Cpy-Py = quartz-sericite-chalcopyrite-pyrite veins, Qtz-Ser-Py = quartz-sericite-pyrite veins, Ag-Mn Vein = Silver-Manganese vein. From Preece (1986). 26
- Figure 8. Simplified map of the Eocene-age monzonite porphyry and older granite porphyry stocks and comagmatic dikes. The arrows point in the direction of extension and the dashed lines are oriented along an average strike direction of the stocks and dikes. Modified from Preece and others (1984). 29
- Figure 9. Map showing distribution of Eocene uplifts and basins in western New Mexico and eastern Arizona. Modified from Cather and Johnson (1984). 31
- Figure 10. Middle Tertiary volcanic rocks near the Morenci Mining District. Numbers correspond with Table 3. 35
- Figure 11. Generalized tectonic map of New Mexico and eastern Arizona showing the relationship of the Mogollon Rim and Mogollon slope to regional structural elements. Provinces and domains of moderate Cenozoic extension are shown in white. Crustal provinces and blocks that have generally resisted Cenozoic extension are shaded grey. From Chamberlain and Cather (1994). 37
- Figure 12. Map and cross section showing major middle Tertiary tectonic features in part of southeastern Arizona. See text for details. Map and cross section modified from Spencer and Reynolds (1989). 39
- Figure 12.1. Aerial view looking southwest, the Morenci mining district in the foreground and the Pinaleno Mountains on the horizon. The intervening mountains are composed of middle Tertiary volcanic flows that dip gently toward the northeast. 40
- Figure 13. Simplified map, placing the major faults in the Morenci mining district in context with the northeast-striking faults that are part of the Morenci-Reserve fault zone, the northwest-trending basins of the southern Basin and Range province and the southeastern edge of the Colorado Plateau. Stippled pattern indicates late Cenozoic

basins. Faults are shown by heavy lines, ball on the down dropped side. Compiled from Ratte (1994), Houser (1994), Simons (1964), and unpublished maps obtained from Phelps Dodge Morenci, Inc	43
Figure 14. Major faults of the Morenci mining district. Arrows point in the direction of dip, numbers indicate average dip angle.	49
Figure 15. The Coronado fault and surrounding geologic relationships.	51
Figure 16. View looking east from the Matilda shaft. Strongly silicified brecciated zone of the Coronado fault in foreground, fault zone shown is approximately 25m wide. Metcalf open-pit in background.	53
Figure 16.1. View looking west from the Matilda shaft. Arrows point to exposures of the silicified breccia zone that forms resistant ribs along strike of the Coronado fault. Middle Tertiary volcanic rocks, hills in background, overlie the Coronado fault and lie approximately three kilometers west from fault zone in foreground.....	53
Figure 17. Coronado fault breccia. Highly fractured, angular to sub-rounded clasts of Cambrian quartzite and Precambrian granite.	54
Figure 17.1. Slab from the Coronado fault showing breccia clasts within a breccia.	54
Figure 18. Slabs of Coronado fault breccia showing pervasive quartz \pm sericite \pm pyrite \pm hematite alteration.	55
Figure 19. Slabs of Coronado fault breccia showing oxidized pyrite with quartz in matrix and in quartz veins that cut across fragments.	56
Figure 20. Well developed northeast-striking faults and fractures north of the Coronado fault. View looking southwest.	58
Figure 21. Northeast-striking faults that are splays to the Coronado fault. View looking north	58
Figure 22. Slickenside striations coated and accentuated by hematite staining from the Coronado fault.	60
Figure 23. Lower hemisphere, equal-area plot. Poles to the Coronado fault are indicated by points (n=28). Strike-slip slickenside striae are	

indicated by diamonds (n=11); oblique-slip slickenside striae are indicated by stars (n=12); dip-slip slickenside striae are indicated by stars (n=9).....	61
Figure 24. Anticipated Riedel shear geometries. 1. Left-lateral motion on the Coronado fault. 2. Existing geometries along the Coronado fault are not consistent with right-lateral movement.	63
Figure 25. Anticipated behavior of faults during the Laramide orogeny based on the orientations of the faults in the Morenci mining district and the known extension and shortening directions. Average direction of shortening during Laramide deformation is indicated by straight arrows. NW-striking faults are expected to be reverse (040° dike orientation) or right-lateral transpressional faults (020° dike orientation). East-striking faults are expected to be left-lateral and/or left-lateral transpressional faults. NE-striking faults (not shown) are expected to be normal faults.	64
Figure 26. Photos showing the mineralized breccia of the Producer fault. Note the quartz-sericite halo surrounding the leached center. The bottom photograph is an enlargement of the area outlined in top photograph.....	66
Figure 27. Simplified geology of the Morenci open-pit. Modified from Preece and others (1984).....	68
Figure 28. Deep mining in the Morenci open-pit has exposed large volumes of Laramide diabase that intruded along the strike of the Quartzite fault. Diabase is dark grey rock exposed on the wall of the open-pit. Trace of the fault indicated on photo. The view is looking south, Paleozoic sedimentary rocks are exposed in the benches above the diabase.	70
Figure 29. Slab showing monzonite porphyry forming matrix around clasts of Precambrian granite in the Kingbolt fault breccia.....	72
Figure 30. Slabs from Kingbolt fault showing stringers of quartz-molybdenite and pyrite-chalcopyrite ± chalcocite veins wrapping around clasts and filling void spaces in the matrix	73
Figure 31. Slabs from Kingbolt fault showing clasts of monzonite porphyry, clasts of Precambrian granite, and clasts of veins. The clasts range	

in size from <1mm to >2cm. The matrix includes stringers of pyrite-chalcopyrite ± chalcocite veins and monzonite porphyry.	75
Figure 32. Striated quartz-molybdenite and pyrite-chalcopyrite ± chalcocite veins typical of striated surfaces along the Kingbolt fault.	76
Figure 33. Lower hemisphere, equal-area plots. Poles to the Kingbolt fault are indicated by points (n=15). Dip-slip slickenside striae indicated by diamonds (n=10)..	77
Figure 34. Slab of brecciated zone exposed along the splay of the Eagle Creek fault. Clasts are of immature, feldspathic sandstone; matrix is composed of fragments similar to the clasts.....	79
Figure 35. View looking south along the plane of the Apache fault. Highly argillized monzonite porphyry dike (left side of photos) is cut off by the fault.....	83
Figure 36. Simplified geology map showing the Copper Mountain fault and the Apache fault near the southern edge of the Morenci open-pit. Modified from unpublished maps obtained from Phelps Dodge Morenci, Inc.	84
Figure 37. Two parallel slip planes along the trace of the Copper Mountain fault.	85
Figure 38. Breccia zone along the Copper Mountain fault. Clasts of mineralized and hydrothermally altered Paleozoic sedimentary rocks and monzonite porphyry in a moderately cemented matrix of clay.....	86
Figure 39. Aerial view looking north-northwest toward the half-graben formed by the San Francisco fault. Precambrian granite is exposed in the mountains along the footwall side of the fault. Gila Group conglomerates fill the valley that is occupied by the San Francisco river in the center of the photo. Beds of gently dipping middle Tertiary volcanic rocks crop out in the foreground	92
Figure 40. The Chase Creek fault, Garfield fault and the surrounding geological relationships.	96
Figure 41. Aerial view looking west. Middle Tertiary volcanics in the foreground. Cambrian Coronado quartzite capping Coronado Mountain forms the distinctive ridge, top center. Precambrian	

- granite crops out west of the Chase Creek fault. The fault strikes north in the center of the photo. Trace of the fault indicated by dashed line. The Northwest Extension open-pit mine is visible in the left center of the photo. 97
- Figure 42. View looking north from southern boundary of the Morenci open-pit. The middle Tertiary volcanic rocks, located east and on the horizon, dip 10-15° west-northwest into the Chase Creek fault. The fault is obscured by dumps in the left-center of the photo..... 98
- Figure 43. Lower hemisphere, equal-area plots. Poles of the Chase Creek fault are indicated by points. Dip-slip slickenside striae indicated by squares..... 100
- Figure 44. Gouge and breccia zones of the Chase Creek fault..... 101
- Figure 45. Slabs of the matrix-supported breccia zone of the Las Terrazas fault. The matrix is predominantly azurite, malachite and chrysocolla. Very fine, sharp edged azurite crystals line vugs within the matrix. Note breccia clasts in the breccia, which indicates multiple episodes of brecciation. 102
- Figure 46. Major faults in the Morenci mining district. Approximate direction of extension for each of the fault systems that record movement beginning around latest Oligocene is indicated by small arrows. Overall extension accommodated by NE-striking, NW-striking, and N-striking faults is indicated by large arrows..... 105
- Figure 47. Distribution of Precambrian volcanic and sedimentary rocks in Arizona in relation to the three major lithologic belts - Northwest Gneiss Belt, Central Volcanic Belt, and Southeast Schist Belt- that make up the Proterozoic crust. Rocks of dominantly sedimentary origin are shown in black, rocks of volcanic origin are stippled, rocks of mainly volcanosedimentary origin in the Southeast Schist Belt are shown in dotted outlines, the Mazatzal Group is vertically ruled, and terranes remobilized by younger events are denoted "R". From P. Anderson, 1989. 108
- Figure 48. Distribution of Proterozoic granite complexes of North America. Modified from J. L. Anderson, 1989..... 108
- Figure 49. Map showing distribution of Neogene basin-fill and rift-flank deposits and selected structural features. Abbreviations for the

basins (from north to south) are CBb, Circle Bar Basin; SRb, Split Rock Basin; BPb, Browns Park Basin; NPs, North Park syncline; Tb, Troublesome Basin; GFb, Granby-Fraser basin; UAb, Upper Arkansas Basin; SLb, San Luis Basin; Eb, Espanola Basin; nAb, northern Albuquerque Basin; sAb, southern Albuquerque Basin; Pb, Popotosa basin; ASb, Abbe Springs Basin. Abbreviations from accommodation zones are VGaz, Villa Grove; Eaz, Embudo; SAaz, Santa Ana; Taz, Tijeras; Saz, Socorro. From Chapin and Cather, 1994

INTRODUCTION

The Morenci Mining District

Porphyry copper deposits are widely distributed throughout the rim of the Pacific basin. These deposits are commonly of great economic and scientific importance and as a result have been the subject of extensive investigation. Pertinent characteristics associated with porphyry copper deposits include tectonic setting, age and evolution of the deposit type. These subjects have been considered on a variety of scales. Studies range from regional geologic analyses and plate tectonic interpretations to detailed geologic and engineering investigations of local deposits. Regional scale evaluations place these deposits in a geologic setting in which the igneous intrusions can be related in time, space and composition. More detailed analyses, including style and process of mineralization, hydrothermal alteration, and secondary enrichment have furthered the understanding of these important metallogenic occurrences.

The porphyry copper deposits of southwestern North America are located in a region that has been tectonically active since Precambrian time. Multiple episodes of mountain building and igneous activity are recorded in a complex geological terrain. The intrusions responsible for copper mineralization are, with few exceptions, associated with mountain building and igneous arc activity which swept toward the interior of the North American continent during the Laramide orogeny, 80-40 m.y. ago, (Coney, 1971, 1972, 1976; Coney & Reynolds, 1977; Dickinson & Snyder, 1978; Keith, 1978). The Laramide orogeny was followed by middle to late Tertiary volcanism and extension. From 80 m.y. ago to the present, virtually continuous deformational and igneous activity throughout southwestern North America has resulted in complex overprinting relationships. A clear understanding of the

geological evolution of many of the porphyry copper deposits, both during and after emplacement, is greatly hindered by this overprinting. However, each episode of deformation and igneous activity has distinguishable characteristics that have been researched and documented throughout the southwest. Through careful study of geological relationships, integrated with data on these multiple regimes, the geologic history for specific deposits can be assembled.

The Morenci mining district, located in southeastern Arizona, hosts the largest producing porphyry copper deposit in North America and the second largest copper-producing operation in the world. The mining complex, owned and operated by Phelps Dodge Corporation, consists of the Morenci, Metcalf, and Northwest Extension open-pits, two concentrators with a combined capacity of 116,000 tons of ore per day and the worlds largest solvent extraction/electrowinning facility. In 1994, the Morenci mining district produced 407,400 tons of copper (Phelps Dodge Corp., annual report, 1995).

Historically, this district boasts tales similar to many of the old west mining camps. Mining began in the late 1800's with underground operations targeting high-grade oxide and sulfide mineralization. These underground operations gave way to open-pit mining technology by the late 1930's. Approximately 1.1 billion tons of concentrator ore averaging 0.9% Cu, as well as 1.8 billion tons of leach-grade and low-grade material have been produced from the Morenci mining district in the last 120 years.

The Morenci mining district is located on the southeastern edge of the Transition Zone physiographic province of Arizona (Figure 1). The Colorado Plateau province lies roughly 30

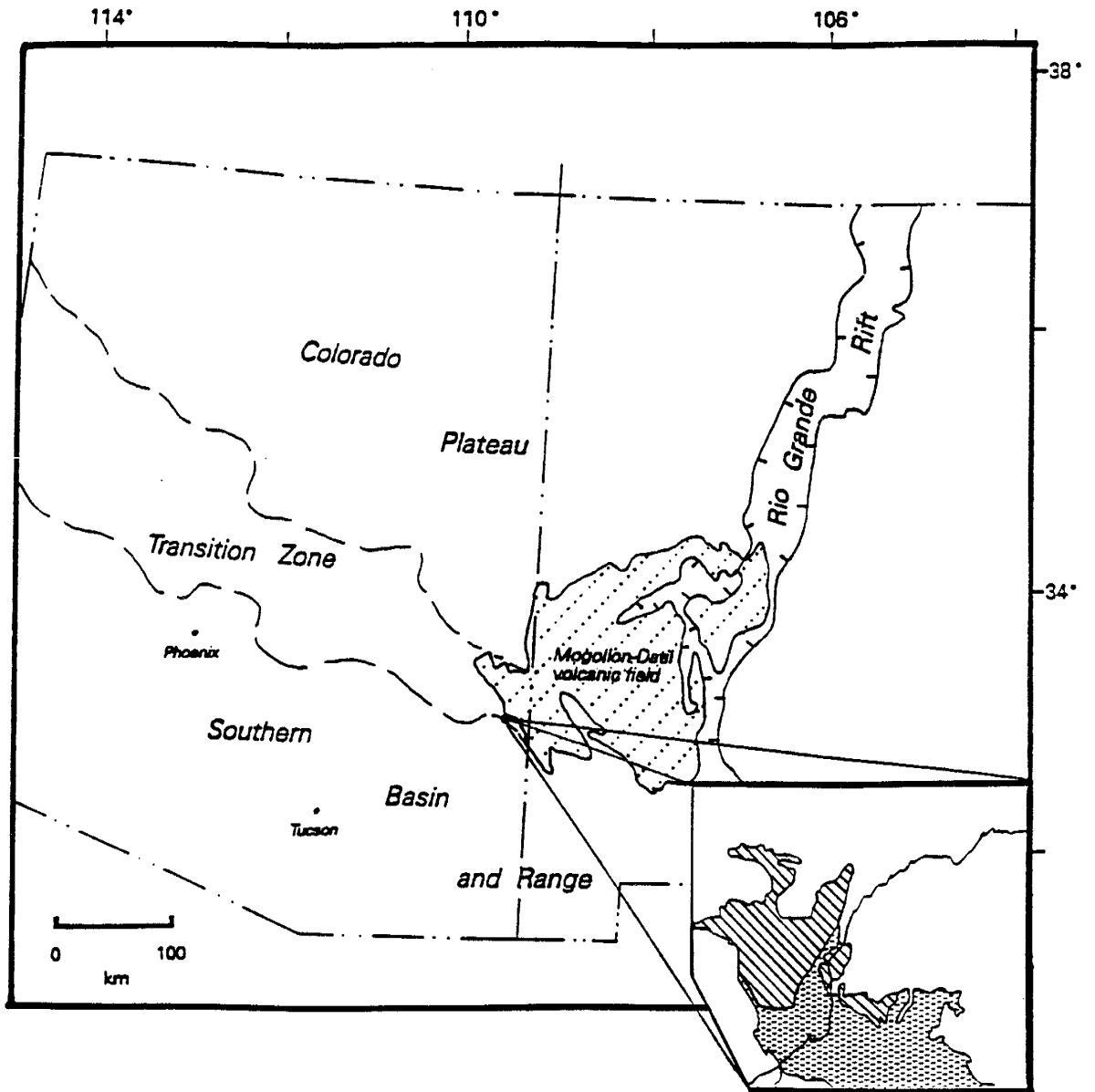


Figure 1. Regional location of the Morenci mining district. Insert described in Figure 2.

km to the north, the Basin and Range province of southeastern Arizona and southwestern New Mexico borders the district to the south and southeast. The district appears as a roughly triangular window of Precambrian through early Tertiary rock units surrounded by middle Tertiary volcanic rocks and Miocene through Quaternary basin fill (Figure 2). A combination of complex deformation events, from the latest Cretaceous to the present, have produced the current configuration of this district.

Methods of Study

The focus of this study is to examine the deformational history of the Morenci mining district. The nature and timing of movement of major and minor structures throughout the district are evaluated and this information is integrated with reference to the current understanding of the regional tectonic history of eastern Arizona. Comparisons of local structures with regional structural trends aid in constraining the timing and nature of deformation in this district. The process of unraveling the structural history was accomplished through several methods.

One method of study included researching and compiling the existing data on the district. Development of the Morenci mining district has been accomplished through detailed geologic and engineering analysis of specific areas. Data included maps and reports from numerable pre-1930 underground operations, drill hole data, surface and mine maps, and scientific studies aimed toward establishing and defining the ore-forming processes of the Morenci porphyry copper deposit. These data had not been previously integrated and this

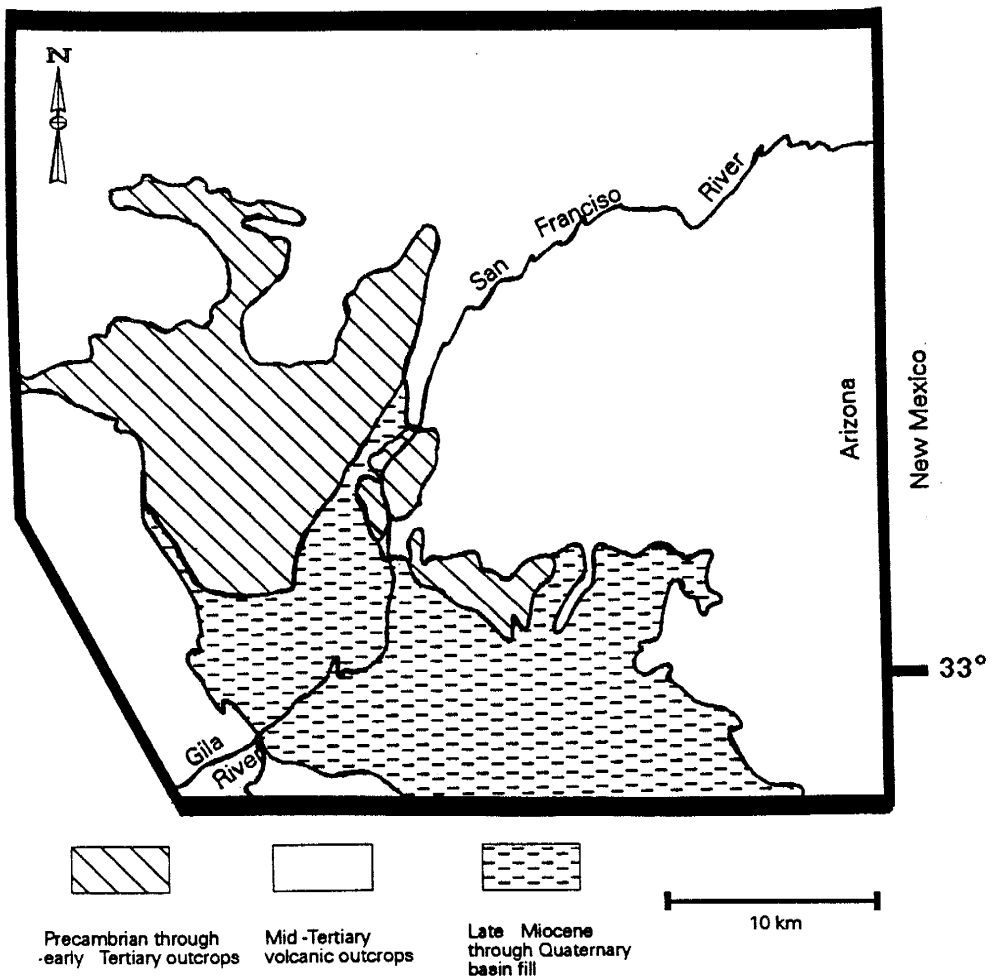


Figure 2. Generalized distribution of rocks that crop out in the Morenci mining district. The Morenci porphyry copper deposit lies within the Precambrian through early Tertiary units.

valuable information served to provide documentation of geological relationships that have since been obscured and/or eliminated by mining and helped to guide district-wide interpretations of the faulting history.

The second method of study involved field examination of major and minor faults, including documentation of fault-zone deformation features and crosscutting relationships. Evidence established from field studies was used to evaluate the nature and timing of faulting in this district. Limited petrographic analysis was used to aid in interpretation of fault-zone deformation features. Using a variety of scales, data is presented in maps, cross sections, photographs and diagrams. The major structures of the district are characterized in order to aid in explaining the kinematic history and data is inventoried in a relative chronological order using pertinent geological relationships.

The nature and timing of deformation in the Morenci mining district is examined in the context of the current understanding of the tectonic history of the surrounding region. Correlation between faults found locally and regional trends are discussed. This evaluation develops a more comprehensive understanding of the tectonic setting, age and evolution of this important porphyry copper deposit.

GEOLOGIC SETTING

Precambrian through Late Cretaceous Stratigraphy of the Morenci Mining District

The district geology was first described by Waldemar Lindgren (1905), who established the geologic framework and nomenclature that is still used today. Descriptions of

district geology can also be found in Reber (1916), Moolick and Durek (1966), Langton (1973), and Bennett (1975). Rocks ranging from Early Proterozoic schists and granite through Paleozoic and Cretaceous sedimentary sequences are overlain and intruded by early to middle Tertiary igneous rocks with subsequent erosion forming large Quaternary basin-fill deposits (Figure 2). An overview of the geological history of southwestern North America, as related to this particular area and the geologic units found here, follows. This review will help facilitate interpretations regarding the complex geological evolution of this mining district.

Extensive Proterozoic terrains occur throughout the southern Cordillera and include voluminous granitic batholiths, widespread calc-alkaline volcanic rocks and associated metamorphic belts (Dickinson, 1981). Precambrian basement in the Morenci mining district consists of a granodiorite, underlying the east and southeast portion of the district, and a granite, located in the northern half of the district (Plate 1). The intrusives are compositionally and texturally similar to the 1440 Ma Ruin Granite of the Globe District, Arizona, and the Oracle Granite, of similar age, in the northern Santa Catalina Mountains, Arizona (Silver & others, 1981). These similarities suggest that the Precambrian intrusives in the Morenci district, Globe district, and other areas are of similar age (Preece & Menzer, 1992). A quartz-sericite schist and metaquartzite occur 5 km north of the mining district. This unit has been correlated with the early Proterozoic Pinal Schist (Lindgren, 1905), which is present throughout the southeastern third of Arizona. Initial consolidation of continental crust had occurred throughout the southwest by the middle Proterozoic (Condie, 1982), and passive continental margins evolved along the Cordilleran and Ouachita margins of the craton

(Dickinson, 1989). These continental margins were gradually submerged and the sea transgressed onto both the eastern and western platforms. Cambrian, Ordovician, Silurian, Devonian and Mississippian sediments in this region were deposited in shelf seas and related environments that fringed and covered the continental platform (Dickinson, 1989). The distribution of undifferentiated Paleozoic rocks in the Morenci district are shown on Plate 1.

The pre-Pennsylvanian stratigraphic sequence in Arizona is characterized by repetitive transgressions and regressions of marine waters. Cambrian strata throughout the southwest are time-transgressive sandstone bodies, dominantly quartzose in composition. The Cambrian unit present in the Morenci mining district, the Coronado Quartzite (Lindgren, 1905), has been correlated with the lower three members, or sandy facies, of the Middle Cambrian Abrigo Formation to the west (Figure 3) (Hayes, 1978). Hayes interprets these units to represent beach sands and/or dune sands deposited near the strand line of the Cambrian Abrigo Sea.

Accumulation of shelf sediments continued in this region through the Ordovician, and are represented by the shallow marine units of the El Paso Limestone and the Second Value Dolomite (Hayes, 1978). These formations were originally assigned to the Longfellow Limestone by Lindgren (1905). Although the term El Paso is recognized to refer to the lower Ordovician rocks of the Morenci district, the original nomenclature of Lindgren (1905) is retained to maintain consistency with older maps and reports (Figure 3). The base of the Longfellow Formation is a 20 to 30 m thick Late Cambrian member. This member is correlative with the Copper Queen Member of the Abrigo Formation to the west and to the lower two-thirds of the Bliss Sandstone of western New Mexico (Hayes, 1978). The Second

Morenci Stratigraphy
Lindgren (1905)

Regional Correlations
References cited in text

Upper Cretaceous
Pinkard Formation
total thickness unknown
maximum known thickness: 65 m
lower portion consists of black shales; the upper portion contains alternating shales and sandstones

Lower Mississippian
Modoc Formation
thickness: 50 to 55 m
coarse, blue-gray crinoidal limestone with subordinate strata of quartz arenite

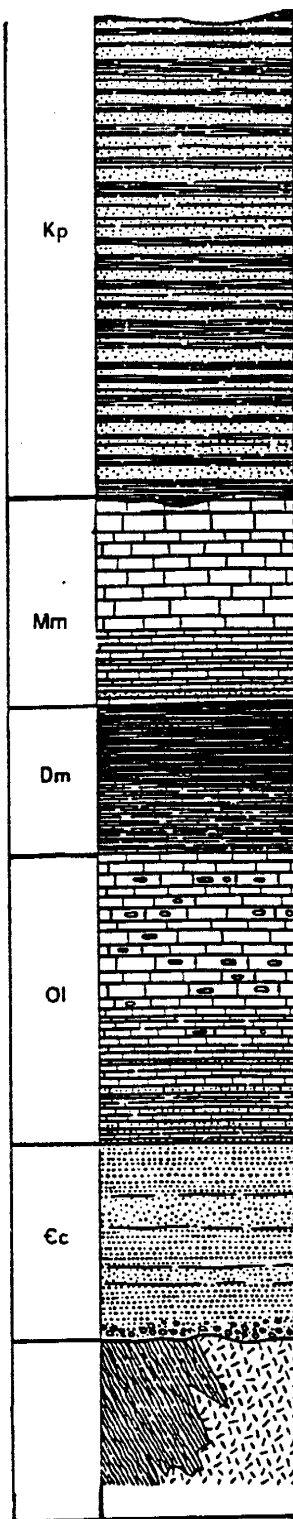
Middle to Upper Devonian
Morenci Formation
thickness: 45 to 80 m
upper member consists of brown shales; lower member is a fine-grained argillaceous limestone

Ordovician
Longfellow Formation
thickness: approx. 120 m
thin-bedded limestone and/or dolomite, chert nodules present

The lower portion of Lindgren's Longfellow Formation is a 20 to 30 m Late Cambrian member

Cambrian
Coronado Quartzite
thickness: 45 to 75 m
quartzose to locally arkosic sandstone with a 1-15 m basal conglomerate

Precambrian
granite, granodiorite, schist



Dakota Sandstone
Mancos Shale

Escabrosa Limestone

Percha Formation
Martin Formation

El Paso Limestone

Copper Queen Member
Abrigo Formation

Lower three members
Abrigo Formation

Ruin Granite
Oracle Granite
Pinal Schist

1 cm = 20 m

Figure 3. Graphical representation, generalized descriptions and regional correlations of the Precambrian, Paleozoic and Cretaceous sedimentary units in the Morenci mining district.

Value Dolomite of the Montoya Group (approx. 5 m thick) is present only near Morenci and represents the only record of latest Middle and Late Ordovician shelf accumulation in Arizona (Hayes, 1978) (not shown on stratigraphic column). This unit disconformably overlies the El Paso and is characterized as a dark-weathering sandy dolomite.

No rocks of Silurian or early Devonian age occur in the Morenci district, with the base of the Devonian System marking a major unconformity. Devonian sedimentation began during the lower Frasnian and is represented in the Morenci mining district by the lower member of the Morenci Formation (Figure 3). This limestone unit is time-equivalent and lithologically similar to the Martin Formation occurring in other areas of southeastern Arizona (Schumacher, 1978; Beus, 1989). Interpretation of isopach data (Schumacher, 1978) indicate that the Morenci district may represent the depositional limit for the late Devonian sea due to a topographic high to the northeast. This topographic high is thought to be part of the stable cratonic Transcontinental Arch (Frazier & Schwimmer, 1987).

The upper portion of the Morenci Formation represents a transgression, characterized by tidal-flat to lagoonal accumulations, that occurred throughout this region during the late Famennian. Regional relationships suggest that this unit can be correlated with the shale member of the Percha Formation to the west and with the Percha Shale of New Mexico (Schumacher, 1978).

The Early Mississippian marks the beginning of renewed marine encroachment. By middle Early Mississippian, an epicontinental sea covered northern and eastern Arizona and adjacent New Mexico. This Early Mississippian sea is represented in the Morenci District by

the Modoc Formation (Lindgren, 1905) (Figure 3). The Modoc Formation is correlative with the lower Mississippian Escabrosa Limestone (Armstrong & Mamet, 1978). Stable platform sedimentation began to wane by the end of the Mississippian and fundamental changes were initiated on the southern Cordillera and Ouachita margins of the North American continent.

Pennsylvanian, Permian, Triassic and Jurassic rocks are not found in the Morenci mining district; however, during the Late Triassic and Jurassic, major changes in plate tectonic regimes accompanied the breakup of Pangaea II (Dickinson, 1989). From the early Jurassic to the end of the Cretaceous a sequence of events occurred which resulted in a major Andean-type orogenic belt to the west and broad, open oceans to the east, south and north of the continent. By the middle Mesozoic, a persistent regime of subduction and arc magmatism had been established along the western borders of North and South America (Dickinson, 1989).

The nature of cratonic sedimentation changed dramatically in the early Cretaceous from the patterns present since the Mississippian. A sizable marine transgression took place between the Cordillera and the midcontinent and, by the late Cretaceous, a Paleozoic-style eperic sea flooded the midcontinent, extending from the Arctic Ocean to the Gulf of Mexico.

Deposition of Cretaceous strata did not occur in northeastern Arizona until upper Cretaceous time. By the middle Turonian, maximum marine transgression had been achieved and shallow marine, coastal plain and fluvial sediments were being deposited along the western margin of the Western Interior Seaway (Nations, 1989). Marine and non-marine upper Cretaceous rocks are exposed in the Morenci mining district (Plate 1 & Figure 3). The Pinkard Formation (Lindgren, 1905) overlies the Paleozoic sediments. Cobban and Hook (1984)

assign a late Cenomanian age to the Pinkard Formation and consider it to be correlative with the Twowells Tongue of the Dakota Sandstone and the Whitewater Arroyo Tongue of the Mancos Shale in western New Mexico.

The Laramide Orogeny

Magmatism and tectonism associated with the Laramide orogeny occurred between 80 and 40 Ma (Coney, 1971). Deformation and arc magmatism began to sweep toward the interior parts of the western Cordillera during the late Cretaceous (Coney & Reynolds, 1977; Dickinson & Snyder, 1978; Keith, 1978). By the late Paleocene to middle Eocene both deformation and igneous activity had migrated well into the continental interior (Coney, 1971, 1972, 1976; Tweto, 1975; Coney & Reynolds, 1977; Dickinson & Snyder, 1978; Keith, 1978; Dickinson, 1981; Spencer & Reynolds, 1990; Foster & others, 1990).

Detailed analysis of the style and timing of Laramide uplifts and adjacent basins in the modern Rocky Mountain region has been instrumental in developing a synthesis of the dynamics of late Cretaceous to early Tertiary tectonism (e.g. Chapin & Cather, 1981; Blackstone, 1983; Gries, 1983; Blackstone, 1983; Cather & Chapin, 1990). Differences in early and late Laramide strain patterns are attributed to changes in the sense of rotation of the rigid Colorado Plateau block (Chapin & Cather, 1981; Dickinson, 1981; Lowell, 1983; Bird, 1984; Cross, 1986; Cather & Chapin, 1990; Livaccari, 1991). The first stage of deformation (80-55 Ma), was characterized by east-northeast shortening and was associated with plate convergent stresses that caused the rigid Colorado Plateau block to be driven east-

northeastward. Most of the uplifts and basins of the Colorado Plateau and Rocky Mountain foreland were blocked out during this time (Chapin & Cather, 1981, Davis, 1978; Gries, 1983). The second stage of deformation, beginning in the latest Paleocene to earliest Eocene, is thought to have been extremely rapid, causing major uplift of mountain blocks and subsidence of basins (Chapin & Cather, 1981). Regional extensional collapse of orogenically thickened crust in the southern Cordillera is hypothesized to have occurred during this time (Livaccari, 1991). The second stage of Laramide deformation coincides with a shift in the axis of regional shortening in the southwestern United States from east-northeast to northeast. The Colorado Plateau block rotated slightly clockwise and was driven north-northeastward during this time (Chapin & Cather, 1981; Cather & Chapin, 1990).

The segment of the North American Cordillera that underwent classic Laramide tectonism along its eastern side was the same segment that experienced a pronounced Paleogene lull in magmatism farther west (Armstrong, 1974). This lull in igneous activity has been interpreted as a temporary gap in the continuity of the magmatic arc that was evolving within the Cordillera in response to subduction along the Pacific margin of the continent (Dickinson & Snyder, 1978). The Paleogene lull in arc magmatism to the west was accompanied by migration of the inland limit of arc activity. Coney and Reynolds (1977) describe the relationship between the surface manifestations of arc activity and the dip-angle of a descending slab. They document, for the region south of the Colorado Plateau, a sweep of magmatism inboard in excess of 1000 km, and then back again, between late Cretaceous and middle Tertiary time. It is now widely accepted that the Paleogene magmatic lull and the

inboard sweep of arc magmatism were due to a shallowing of the dip-angle of the descending Farallon plate. The progressive flattening of the Benioff zone beneath southwestern North America began in the late Cretaceous, reaching its shallowest angle in latest Paleocene to earliest Eocene time (Keith, 1978). Rapid convergence between the North American plate and the subducting Farallon plate is thought to be responsible for the shallowing of the angle of descent (Coney & Reynolds, 1977).

The dynamic effects of a subhorizontally subducted plate, transmission of plate-convergence stresses across thickened hinterland crust, and extensional collapse are proposed as the causal mechanisms of Laramide deformation (Dickinson & Snyder, 1978; Livaccari, 1991). Similar deformation styles have been documented for zones within the modern Andean Mountain system of South America and the Tien Shan Mountains of northwestern Tibet (Jordan & others, 1983; Dewey, 1988; Molar & Lyon-Caen, 1988; Cross, 1986).

In southeastern Arizona and southwestern New Mexico, the folding and faulting associated with Laramide tectonism has been the subject of ongoing controversy (Jones, 1966; Lowell, 1974; Mayo & Davis, 1976; Rehrig & Heidrick, 1976; Drewes, 1978 & 1981; Davis, 1979). Structural interpretations are complicated in this region due to multiple, superimposed deformational episodes.

Associated magmatism occurred in an unusually wide belt of interspersed centers of intra-arc volcanic and plutonic activity. This magmatic activity left one of the richest metallogenic provinces on earth: the porphyry copper province of southeastern Arizona and southwestern New Mexico includes at least thirty-five separate significant occurrences of

porphyry-related concentrations of copper (Figure 4) (Titley, 1982). With few exceptions, these deposits formed between 75 and 55 m.y. ago. Most of the known porphyry copper systems appear to be systematically distributed, either along the axis of a north-northwest-trending arc orogen, or along transverse belts of northeast strike (Heidrick & Titley, 1982).

Structural analyses of the orientations of Laramide intrusive rocks, detailed in extensive field studies, reveal systematic trends. Rehrig & Heidrick (1972, 1976) and Heidrick & Titley (1982) discussed mesoscopic and megascopic structural data collected in and around numerous plutons throughout Arizona and New Mexico. Strikes of mineralized and unmineralized joint sets, veins, fault-veins, dikes and elongate intrusions were summarized on strike histograms. They document a regional pattern of dominant east-northeast and very minor west-northwest fracture and dike systems, which have been noted in all but one local domain (Goodwin & Haxel 1990). This pattern is consistent with Laramide tectonism. In general, dilatant structural elements have a pronounced east-northeast trend, indicating that north-northwest extension accompanied east-northeast shortening. That is, regional east-northeast shortening was operative during emplacement of the Laramide-age plutons. (Heidrick & Titley, 1982).

Late Paleocene to Eocene Intrusions in the Morenci Mining District

Laramide intrusive activity is recorded in the Morenci mining district by a series of Paleocene to early Eocene hypabyssal intrusions. The Laramide stocks, laccoliths, and associated dikes and sills are a comagmatic, calc-alkaline series of porphyritic intrusions, ranging in composition from diorite to granodiorite to quartz monzonite and granite (Moolick

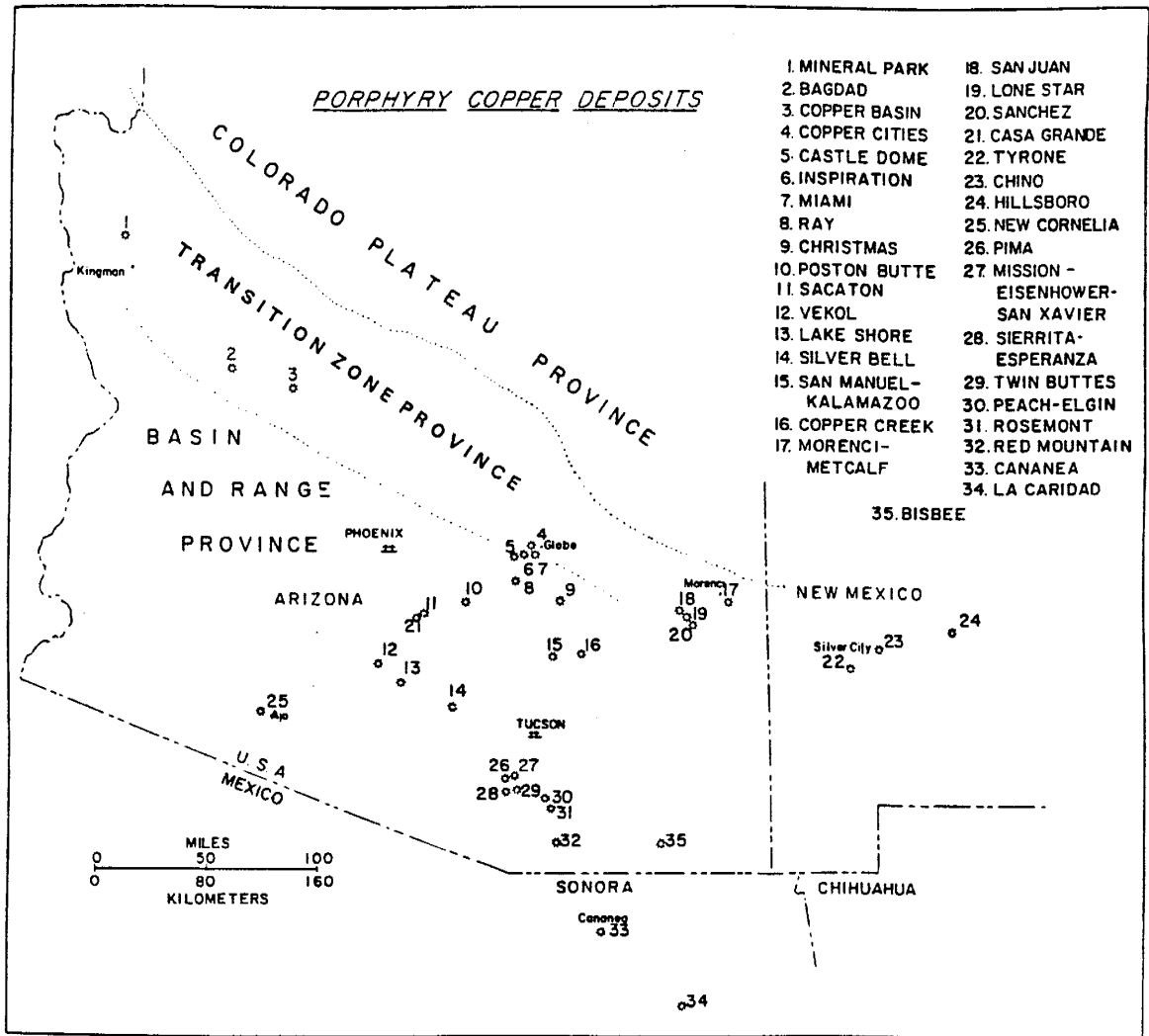


Figure 4. Index map to porphyry copper deposits in Arizona, New Mexico, and Sonora, Mexico. Modified from Titley (1982).

& Durek, 1966; Preece & Menzer, 1992) (Plate 1 & Figure 5). The following descriptions are a compilation of work done by numerous geologists in the Morenci district.

Textural and fluid inclusion evidence pertaining to the intrusive complex in the Morenci district indicate rapid cooling and emplacement at shallow crustal levels, approximately 2-3 km depth, into host rocks that show no evidence of regional metamorphism (Richard K. Preece, pers. comm., 1994). This suggests that K-Ar dates should approximate the emplacement ages of the stocks, laccoliths and associated dikes and sills. The Paleocene to early Eocene radiometric ages shown in Table 1 are therefore interpreted to be emplacement ages of the porphyries. The timing of the related mineralization is constrained by a Re-Os date on molybdenite (Table 1), as well as field relationships.

The earliest Laramide intrusive, dated at approximately 64 Ma (Table 1), is a hornblende diorite porphyry that occurs as small plugs, laccoliths and radiating dikes, intruding Precambrian basement and Paleozoic and Cretaceous sediments in the southwestern portion of the district (Plate 1 & Figure 5). This early intrusion is relatively unmineralized, alteration is predominantly propylitic and it is interpreted as pre-main stage mineralization (Moolick & Durek, 1966; Menzer, 1980; Preece & Menzer, 1992)

Main stage alteration and mineralization is associated in time and space with the emplacement and cooling of a biotite monzonite porphyry and a granite porphyry, both dated at 56 to 57 Ma (Table 1). The monzonite porphyry occurs as a NE-striking elongate stock in the vicinity of the Morenci open-pit (Plate 1 & Figure 5). The stock grades laterally and along strike into a dike swarm that extends to the southwest and northeast for greater than 13 km.

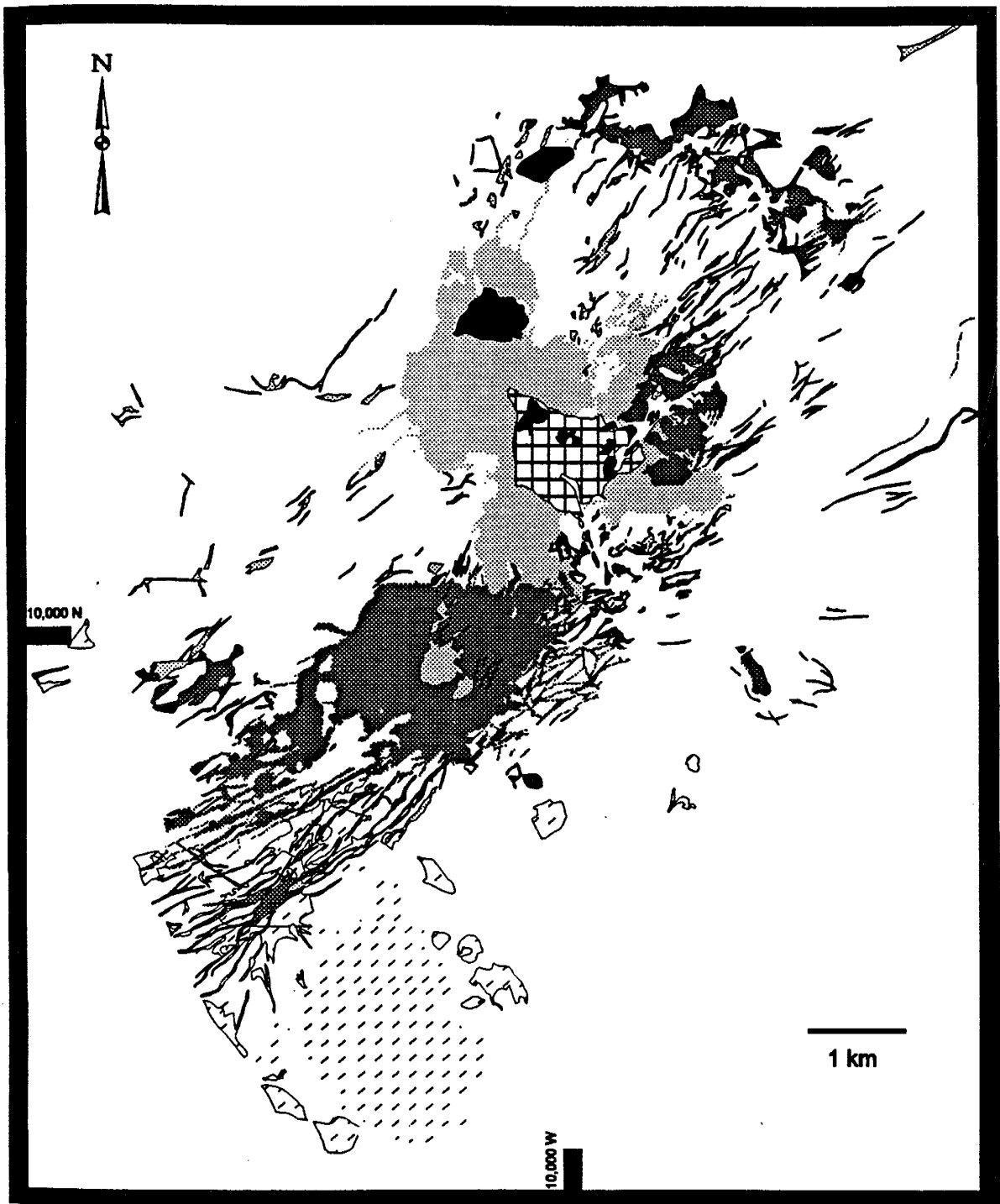


Figure 5. Paleocene to early Eocene intrusives and associated breccias in the Morenci mining district. Note the northeast migration of intrusive centers over time. A key to the map is shown on the following page; coordinates shown on the map correspond with the Morenci mining district survey grid. See also Plate 1. Modified from Preece and others (1984).

Paleocene to early Eocene intrusives and associated breccias in the Morenci mining district

Key to Figure 5

K-Ar dates on Table 1



Breccias: undifferentiated



Younger granite porphyry and younger rhyolite porphyry: (ygp and yrp)
 ygp - large, euhedral, bipyramidal quartz phenocrysts and highly seritized and argillized euhedral plagioclase phenocrysts, in a groundmass of pervasively seritized quartz, orthoclase and albite.
 yrp - nearly equigranular, shardy and broken phenocrysts of quartz and plagioclase in a very fine matrix of quartz, plagioclase and sericite.



Older Granite Porphyry: (ogp) two phases recognized
 ogp 1- 3 to 7 volume %, small (less than 4 mm) subhedral quartz phenocrysts and crowded rectangular feldspar phenocrysts, commonly andesine in composition. The groundmass is aphanitic and consists of plagioclase, quartz and orthoclase.
 ogp 2- 5 to 10 volume % bipramidal quartz phenocrysts that are as large as 1cm in diameter, with matrix-supported feldspar phenocrysts.



Monzonite Porphyry: (mp) Small closely spaced phenocrysts of plagioclase and biotite in a microcrystalline groundmass of quartz and feldspar. Plagioclase ranges from andesine to oligoclase. Primary biotite is found locally.



Diorite Porphyry: (dp) Large phenocrysts of hornblende and plagioclase with subordinate quartz and biotite, in a microcrystalline groundmass of chlorite, epidote, montmorillite and plagioclase.

Modified from Moolick and Durek, (1966); Menzer, (1980); Preece and Menzer, (1992)

Rock/Mineral	Age (Ma)	Method	Reference
Diorite Porphyry	63.0±1.9	K-Ar (hornblende)	McDowell, 1971
	64.7 ± 2.0	K-Ar (hornblende)	McDowell, 1971
Monzonite Porphyry	56.5± 1.7	K-Ar (biotite)	McDowell, 1971
Older Granite Porphyry	57.6 ±2.2	K-Ar (biotite)	Bennett, 1975
Molybdenite	55.8± 1.0	Re-Os (molybdenite)	McCandless & others, 1993
Candelaria Breccia	52.8± 2.0	K-Ar (sericite)	Bennett, 1975
Andesite Dike	30.0 ±0.7	K-Ar (biotite)	Cook, 1994
Alunite (Metcalf open-pit)	9.9± 0.3	K-Ar (alunite)	Cook, 1994
Alunite (Coronado)	7.2± 0.3	K-Ar (alunite)	Cook, 1994

Table 1. Radiometric age determinations from selected rocks and minerals from the Morenci mining district.

Within the orebody, the monzonite porphyry generally displays abundant quartz-sericite stockwork veining and pervasive quartz + sericite alteration. Subsequent supergene argillic alteration commonly overprints and obliterates original rock textures (Moolick & Durek, 1966; Menzer, 1980; Griffin & others, 1993)

The granite porphyry consists of several irregular stocks and NNE-striking dikes that overlap the northeastern edge of the monzonite porphyry stock (Plate 1 & Figure 5). Two phases of granite porphyry are recognized and referred to as Older Granite Porphyry 1 and Older Granite Porphyry 2 (Bennett, 1975). Contacts between the two phases are both transitional and intrusive. The granite porphyry displays main-stage mineralization and alteration characteristics. A well developed stockwork fracture system, healed to produce quartz-sericite stockwork veining along with pervasive quartz + sericite alteration, is common in both phases of the granite porphyry. Alteration zones in the granite porphyry and surrounding rocks range from potassic to intense quartz-sericite, grading to generally propylitic at the perimeter of the district (Moolick & Durek, 1966; Menzer, 1980; Preece & Menzer, 1992; Griffin & others, 1993; Preece & others, 1993)

Several breccia bodies are associated with the intrusion of the Older Granite Porphyry. The Morenci Breccia, located in the Morenci open-pit, is an oblate lenticular mass approximately 76 m wide, 23 to 62 m thick, 488 m long with a 20 to 25° plunge to the north (Bennett, 1975). The Candelaria Breccia, dated at approximately 53 Ma (Table 1), occurs in the northernmost portion of the district. This breccia pipe cuts the Older Granite Porphyry stock with sharp contacts and is 550 by 825 m in maximum dimensions. The breccia formed

following quartz-sericite veining in the Older Granite Porphyry (Bennett, 1975).

A series of irregular diabase dikes and sills occur throughout the district. The dikes were intruded along east-striking faults. Sills often occur within the Precambrian granite. Although these dikes and sills are minor in abundance, they form continuous zones, 3 to 30 m wide, with strike lengths of several km. The diabase dikes have not been dated, but field relationships indicate that some diabase intrudes monzonite porphyry and is cut by Older Granite Porphyry dikes. The diabase and the rock it intrudes is typically strongly mineralized and highly altered (Moolick & Durek, 1966; Menzer, 1980; Preece & Menzer, 1992; Griffin & others, 1993; Preece & others, 1993).

Following the Older Granite Porphyry suite and main-stage district alteration and mineralization, a Younger granite porphyry and rhyolite porphyry complex represent the final Laramide intrusive event in the district (Plate 1, Figure 5). This complex is characterized by a lack of through-going veinlets and, although no unaltered material has been recovered for radiometric dating, field relations indicate an age younger than mineralization. The complex forms a laccolith-shaped plug and occurs in the central portion of the mining district (Preece & Menzer, 1992; Griffin & others, 1993; Preece & others, 1993).

Several breccias are believed to have formed contemporaneously with the younger porphyry intrusions (Bennett, 1975). The Metcalf Breccia developed as the younger porphyry intruded the Older Granite Porphyry stock and forms a rind along the margins of the laccolith. The King Breccia, located near the southeastern edge of the Younger granite porphyry plug, forms a nearly cylindrical pipe between the older porphyries and the younger intrusions.

Hydrothermal Alteration and Mineralization

The effects of hydrothermal alteration and mineralization are superimposed on both the causative intrusions and the district host rocks as is typical of porphyry copper systems. The style and sequence of hydrothermal alteration and mineralization in the Morenci district has been described from district-wide vein assemblage relationships. Potassium-silicate alteration and quartz-molybdenite veining are followed by main stage quartz-sericite alteration. Hypogene protore accompanied intense phyllic alteration. Multiple fracturing events are recorded in the crosscutting nature of these vein assemblages. Vein paragenesis and fluid inclusion thermometry reveal a consistent trend toward progressively younger vein alteration assemblages (Preece, 1986).

The earliest alteration event is generally restricted to the vicinity of the monzonite porphyry and the Older Granite Porphyry. This event is characterized by several veining assemblages, limited wall-rock alteration, and variable vein orientations. Earliest veins are quartz-K-feldspar, although, locally in the more mafic igneous rocks, biotite + magnetite veins preceded quartz-K-feldspar veins. Selectively pervasive biotite alteration is also present, with hydrothermal biotite replacing pre-existing mafic minerals in igneous rocks, but its distribution and importance is not known. Quartz-molybdenite veins are also included in the early phase of alteration and mineralization, as this vein assemblage cuts and offsets quartz-K-feldspar structures. Sphene, rutile and apatite are common accessory minerals associated with this early alteration phase (Preece, 1986).

The most volumetrically important alteration within the Morenci porphyry system is the development of quartz and sericite replacement of rock-forming silicates. This pervasive alteration is termed main-stage and was accompanied by multiple generations of quartz + sericite + pyrite \pm chalcopyrite stockwork veins. These veins commonly exhibit a uniform northeast to east-northeast strike orientation (Figure 6), occur throughout the district and are often the only vein assemblage in a given area (Preece, 1986; Preece & Menzer, 1992).

Large, through-going quartz + sulfide fissure veins appear to represent the latest hydrothermal event and exhibit district-wide NE strikes (Figure 6). Vein widths are 10 cm to more than 1 m, with individual strike lengths on the order of hundreds of meters. Geochemical analyses and polished section microscopy have indicated that the veins often contain relatively high-grade Cu-Zn-Au-Ag mineralization, in addition to the ubiquitous quartz + pyrite (Preece & Menzer, 1992; Preece & others, 1993)

A reconnaissance fluid inclusion study was conducted by Preece (1986) to determine fluid characteristics of the major vein types. Figure 7 and Table 2 summarize his conclusions. A systematic progression of fluid characteristics was observed through time. Early quartz-K-feldspar veining resulted from reactions between rock and locally derived high-salinity fluids. Molybdenite mineralization occurred during a transition from high-salinity to low-salinity fluids with otherwise similar attributes to the early potassic vein formation. Sulfide deposition was concomitant with the introduction of low-salinity fluids that were far from equilibrium with the host rock and in sufficient quantities to control water/rock reactions (Preece, 1986). In addition, coexisting liquid- and vapor-rich, two-phase inclusions provide evidence of low-

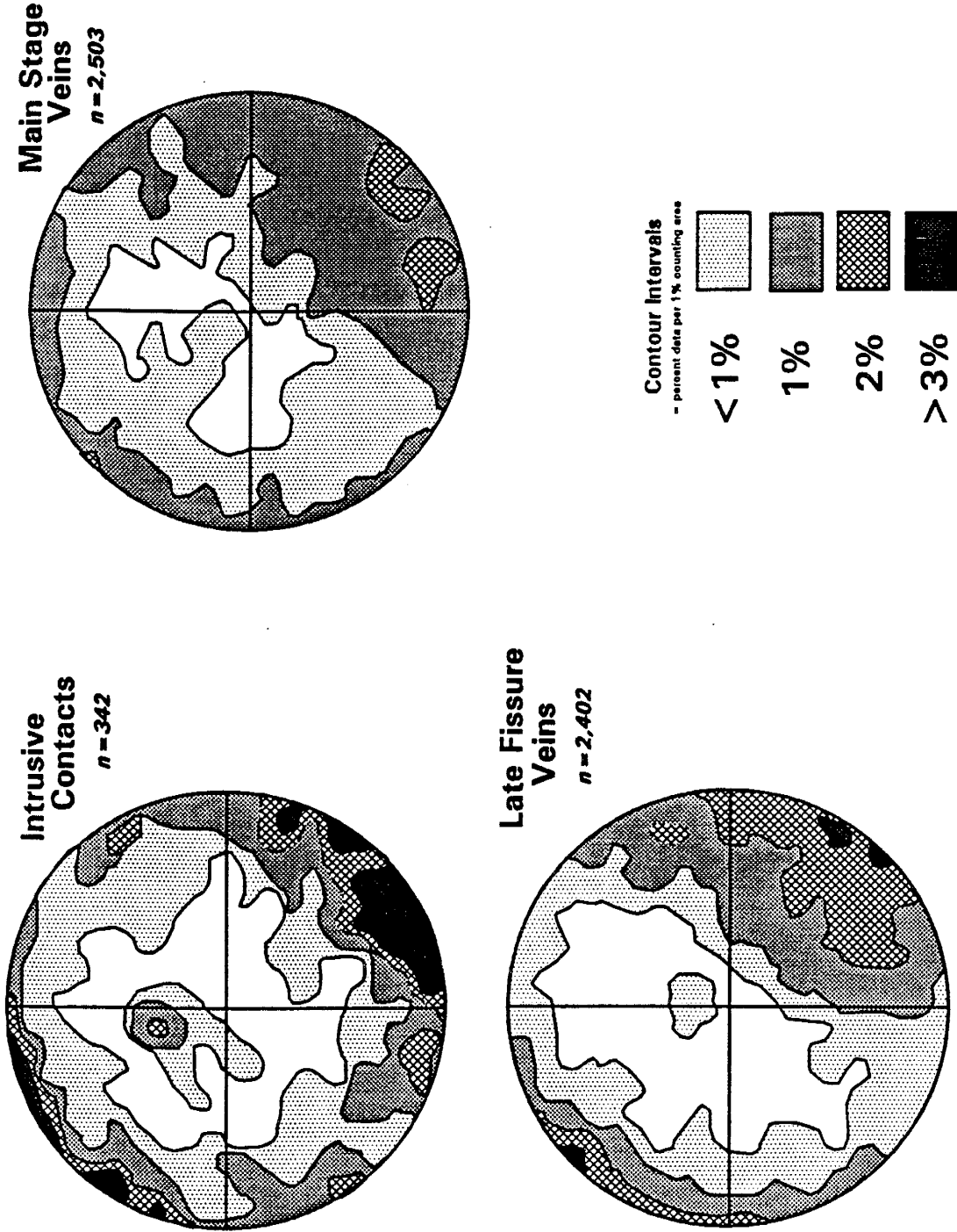


Figure 6. Lower hemisphere equal-area plots of poles to mesoscopic intrusive contacts, main-stage veins and late fissure veins in the Morenci mining district. Modified from Preece (1986).

Summary of Fluid Inclusion Homogenization Temperatures

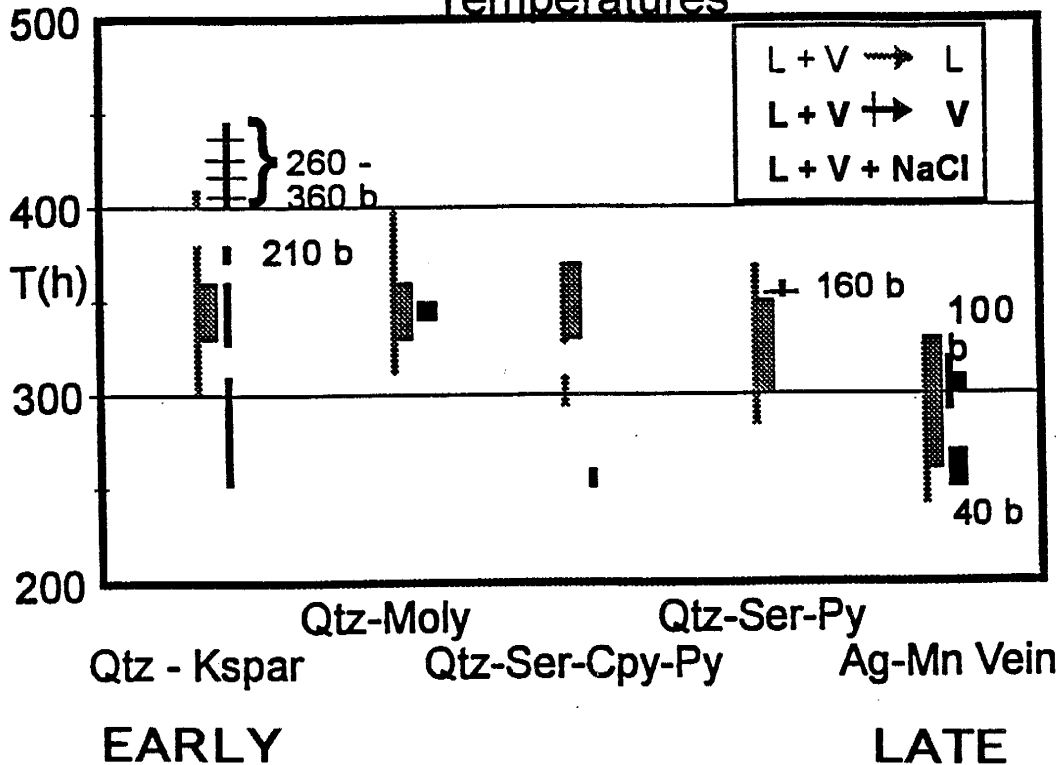


Figure 7. Summary of fluid inclusion homogenization temperatures for the major vein types in the Morenci mining district. A systematic progression of fluid characteristics is observed through time (see text). L = Liquid, V = Vapor, b = bars, Qtz-Kspar = quartz-Kfeldspar veins, Qtz-Moly = quartz-molybdenite veins, Qtz-Ser-Cpy-Py = quartz-sericite-chalcopyrite-pyrite veins, Qtz-Ser-Py = quartz-sericite-pyrite veins, Ag-Mn Vein = Silver-Manganese vein. From Preece (1986).

<u>Pressure</u>	<u>Maximum Depth</u>	<u>Minimum Depth</u>	<u>Depth to top of Cretaceous Sediments</u>
260-30 b	3.2-4.4 km	1.1-1.5 km	0.7 km
210 b	2.6 km	0.9 km	0.7 km
160 b	1.9 km	0.7 km	0.7 km

Table 2. Depths estimated from the pressure determined from coexisting liquid-rich and vapor-rich inclusions in stockwork veins. Maximum depths were derived assuming pure hydrostatic head, minimum depths were derived assuming pure lithostatic head. From Preece (1986).

salinity fluids that boiled at 375° and at 400-450° C, indicating pressures of 210 and 260-360 bars respectively (Preece, 1986). Limited evidence of boiling consisted of a single pair of liquid-rich and vapor-rich inclusions that homogenized at 354° C, indicating 160 bars pressure (Preece, 1986). Depths of burial can be estimated from the pressures determined from coexisting liquid-rich and vapor-rich inclusions in the stockwork veins (Table 2). The estimated depths suggest that the reconstructed Paleozoic plus Mesozoic stratigraphic column is not sufficient to account for the pressures required by the fluid inclusion evidence of boiling. The additional rock mass required is most likely to be from a coeval andesitic volcanic pile attending Laramide-age intrusive activity (Preece, 1986).

Evidence for Laramide-age Extension Directions in the Morenci Mining District

The Laramide intrusive center in the Morenci district migrated nearly 9 km northeast along an arcuate 040° to 020° trend, over approximately 13 Ma (Plate 1, Figure 5 & Table 1). The early, 64 Ma, diorite porphyry pluton, which occurs in the southwestern portion of the district, displays weak concentric and radial fracturing patterns. This fracturing style typically reflects stresses that are presumed to be related to the thermal effects of pluton emplacement at high levels, (Knapp & Norton, 1981; Koide & Bhattacharji, 1975). By approximately 57 Ma, the intrusive center had migrated nearly 5 km northeast and the elongate monzonite porphyry stock and cogenetic dike swarm display a highly regular orientation of 040° (Plate 1). With the next pulse of magmatism, represented by the Older Granite Porphyry, the intrusive center had migrated further toward the north-northeast. The southern portion of the Older Granite

Porphyry stock and cogenetic dike swarm exhibits a 040° orientation, similar to the monzonite porphyry intrusions. However, in the northern portion of the district, the Older Granite Porphyry stock and associated dikes are more commonly oriented 020°.

Regularly oriented fractures, dikes, veins and elongate stocks, with approximately planar margins, are commonly interpreted as extension fractures or fillings of extension fractures. Extension fractures may form in tensional or compressional regimes. The regular orientations of the Laramide stocks, dikes and veins in the Morenci district are the most obvious indicators of the extension directions and magnitudes during this time period (Plate 1 & Figure 6).

During the early stages of igneous activity, local stresses related to pluton emplacement appear to have been dominant. As the intrusive system developed, regional stresses became more important. The systematic east-northeast strike of extensional elements in this district correlates with the pronounced east-northeast direction of structures documented in association with many of the Laramide porphyry occurrences throughout the southwest (Rehrig & Heidrick, 1972, 1976; Heidrick & Titley, 1982). This suggests that regional tectonism exerted a strong control on the nature and distribution of the Morenci Laramide porphyry copper system. Further, evidence from the Morenci district suggests that the direction of extension rotated counterclockwise from NW-SE to WNW-SSE at approximately 57 Ma (Figure 8). The timing of the counterclockwise rotation of the extension direction in this district coincides with the second stage of Laramide deformation. This episode of foreland deformation has been attributed both to a shift in the axis of regional shortening to

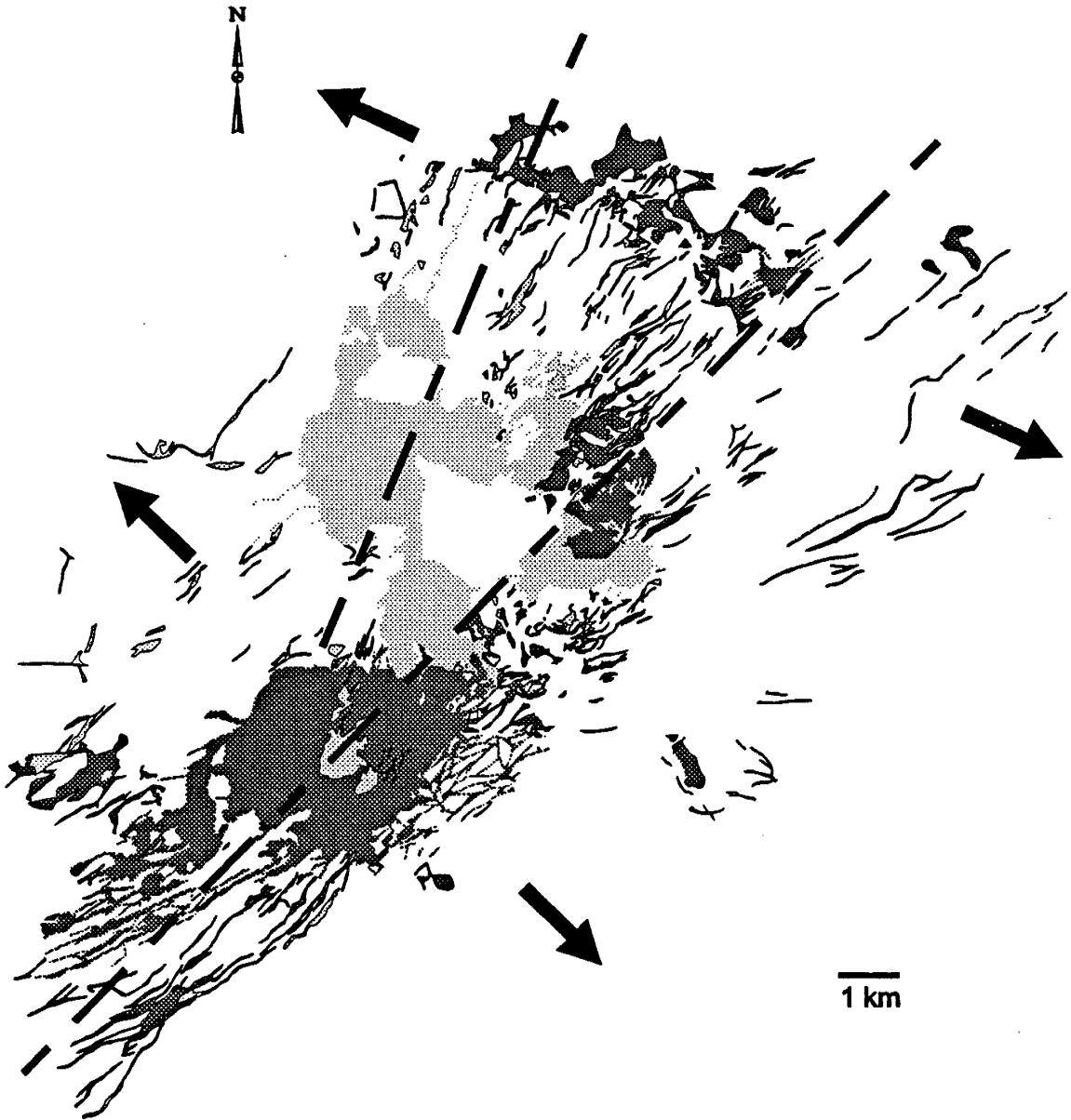


Figure 8. Simplified map of the Eocene-age monzonite porphyry and older granite porphyry stocks and comagmatic dikes. The arrows point in the direction of extension and the dashed lines are oriented along an average strike direction of the stocks and dikes. Modified from Preece and others (1984).

approximately 045° resulting in slight clockwise rotation of the rigid Colorado Plateau block (Chapin & Cather, 1981; Cather & Chapin, 1990) and to region-wide extensional collapse that may have driven the Colorado Plateau north-northeast (Livaccari, 1991).

First Generation of Supergene Enrichment in the Morenci Mining District

Maximum strain rates and the structural culmination of Laramide deformation began in latest Paleocene to earliest Eocene time (Chapin & Cather, 1981). Abundant evidence from basins formed during this time suggests that a period of weathering and erosion pre-dated the onset of middle Tertiary magmatism (Epis & Chapin, 1975; Peirce & others, 1979; Cather, 1980; Cather & Johnson, 1984). This period of intense weathering and erosion is also considered to be responsible for initial supergene leaching and enrichment in many of the southwestern United States porphyry copper deposits (Livingston & others, 1968; Lowell, 1974; Peirce & others, 1979).

Formations included in the Eocene Baca basin of west-central New Mexico and east-central Arizona (Figure 9) contain clasts of Laramide volcanic rocks and show evidence of a north-northeast-trending drainage system that was active during deposition (Pierce & others, 1979; Cather & Johnson, 1984). This evidence has been interpreted as a record of rapid erosion of Laramide highlands to the south and southwest and stripping of overlying sedimentary and volcanic rocks that probably unroofed some of the copper deposits of this age that lie to the south and southwest (Peirce & others, 1979; Cather & Johnson, 1984). The sedimentological and stratigraphic record within the Baca basin provides important clues to the

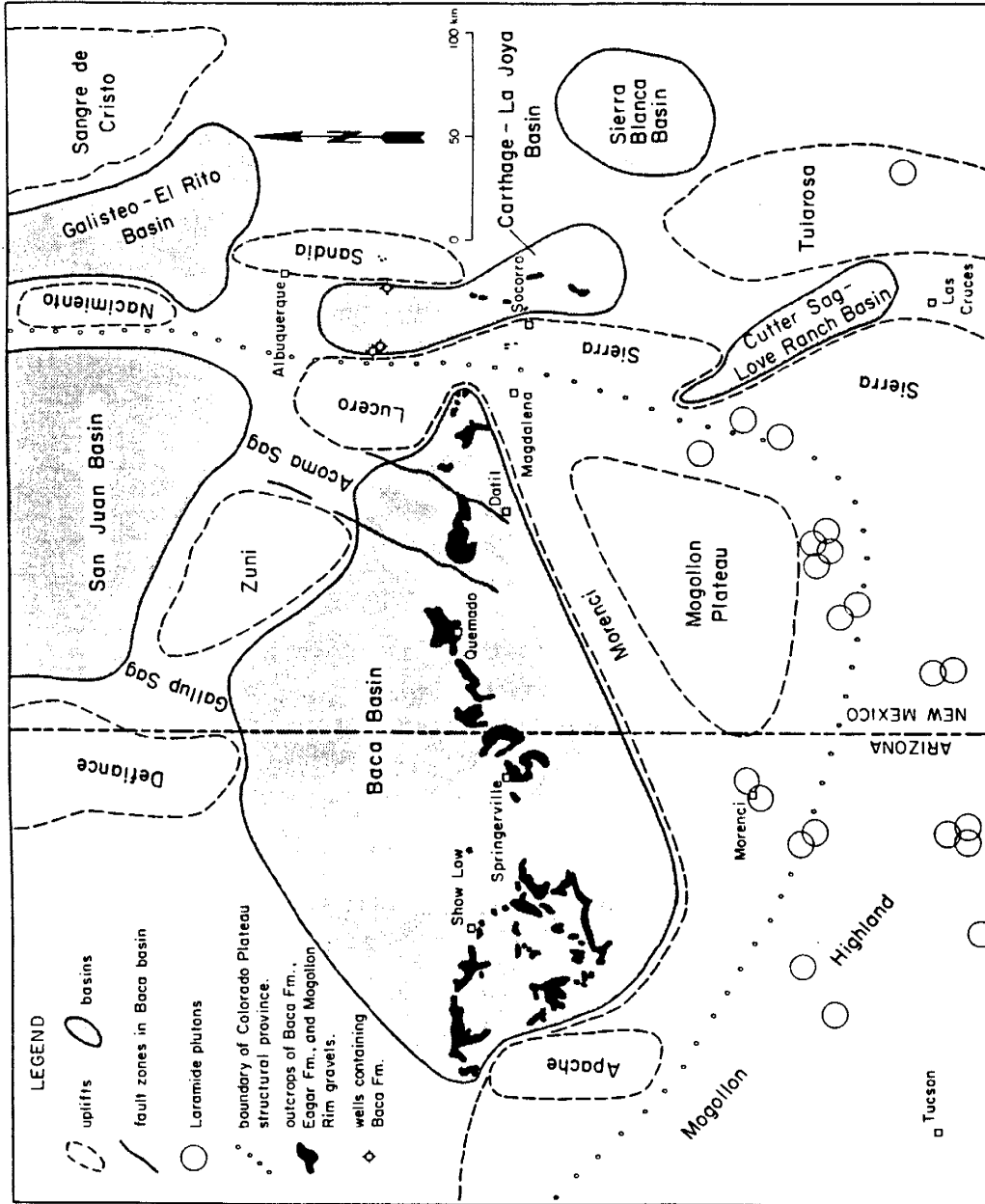


Figure 9. Map showing distribution of Eocene uplifts and basins in western New Mexico and eastern Arizona. Modified from Cather and Johnson (1984).

late Cretaceous-early Tertiary geomorphology of the Morenci district. Cather and Johnson (1984) state, "The existence of a Morenci uplift (Laramide positive area) would also explain the increased abundance of volcanic clasts in the western part of the Baca basin. Laramide volcanic rocks in the vicinity of Morenci, Arizona, would not have been isolated by the postulated drainage divide and may have supplied detritus to the western part of the Baca basin."

The character of the supergene processes responsible for the formation of most of the ore-grade mineralization in the Morenci district further supports an active erosional regime from approximately 56 Ma to the onset of middle Tertiary volcanism. It has already been established that some type of Laramide volcanic rocks must have overlain the Morenci district during the time of formation of the mineralizing hypabyssal intrusions (Preece, 1986). Further, mass-balance considerations pertaining to the supergene ore-forming processes require a larger volume of low-grade source rock than can be accounted for by the existing rock units in the district (North & Preece, 1993). Leaching of copper from these rocks would have begun as soon as they were exposed to oxygenated water. The leaching/enrichment front just above the water table appears to have descended at a rate equal to erosion, resulting in widespread chalcocite mineralization on pyrite and chalcopyrite with copper grades of 0.3 to 0.6%. Thus, an active erosional regime has been postulated to have attended formation of a first-generation chalcocite blanket. The onset of middle Tertiary volcanism and associated extensive volcanic cover temporarily halted the leaching and enrichment processes in the Morenci mining district (Moolick & Durek, 1966).

Middle Tertiary Tectonism

Beginning in the late Eocene to early Oligocene, a new tectonic regime began to emerge throughout the southwestern United States and Mexico. By the late Oligocene to early Miocene, magmatism and lithospheric extension was regionally widespread. Both extension and magmatism can be related to the evolving plate tectonic setting of the continental margin of western North America (Atwater, 1970; Zoback & Zoback, 1980; Dickinson, 1981)

Space-time patterns of middle Tertiary magmatism reflect a westward sweep of magmatism, attributed to an increase in dip of the subducted slab that shallowed, during the Laramide orogeny (Coney, 1976; Coney & Reynolds, 1977; Dickinson & Snyder, 1978; Dickinson, 1981). The resurgence of magmatism was regionally time-transgressive (Coney & Reynolds, 1977; Dickinson, 1989; Shafiquallah & others, 1980; Reynolds & others, 1986; Spencer & Reynolds, 1989). Approximately 40 m.y. ago, intermediate-silicic volcanic activity began in south-central Colorado (Lipman and others, 1972 & 1978; Lipman, 1981). The Mogollon-Datil volcanic field of New Mexico, dominated by andesites, basaltic andesites, silicic ash-flow tuffs and associated volcanoclastics, has early dates ranging from 36-32 Ma (Elston & others, 1973; Ratte & others, 1984; McIntosh & others, 1990, 1991 & 1992; Cather, 1990). By 30-29 Ma, calc-alkaline volcanism crossed the New Mexico-Arizona border and had swept southwestward across Arizona by 25 Ma (Damon & others, 1981; Reynolds & others, 1986; Nealey & Sheridan, 1989).

Silicic to intermediate volcanic flows, pyroclastic rocks and wide-spread ash-flow tuffs,

which characterize the bulk of post-Eocene volcanism, cover enormous areas immediately surrounding the mountains containing the porphyry copper deposits of the Morenci district (Ratte & others, 1969 & 1984; Strangway & others, 1976; Reynolds & others, 1986; Marvin & others, 1987; McIntosh & others, 1990, 1991 & 1992; Wahl, 1980). Figure 10 and Table 3 illustrate important units and time correlations pertinent to this region.

Predominantly synchronous with middle Tertiary magmatism was the onset of an extensive regime of continental extension. The initiation of extension along the subducting continental margin occurred around 29 Ma when the Pacific-Farallon ridge first began to encounter the Farallon-American trench near the latitude of the Mexican border (Atwater, 1970; Zoback & Zoback, 1980; Dickinson, 1981).

In the southern Basin and Range province, large-magnitude lithospheric extension was accommodated at upper crustal levels primarily by formation of and movement on regional, low-angle normal faults (e.g., Spencer & Reynolds, 1989). In southern Colorado and New Mexico, extensional tectonism resulted in the development of a continental rift system (e.g., Chapin, 1979 & 1988; Aldrich & others, 1986; Elston & Bornhorst, 1979). Due to the location of the Morenci mining district (Figure 1), it is important to discuss extensional tectonism with regards to structural styles documented in the southern Basin and Range province and the Rio Grande rift province. The characteristics of extensional tectonism in the regions surrounding the southeastern edge of the Colorado Plateau are of particular importance.

The Morenci mining district is located on the southeastern edge of the Transition zone

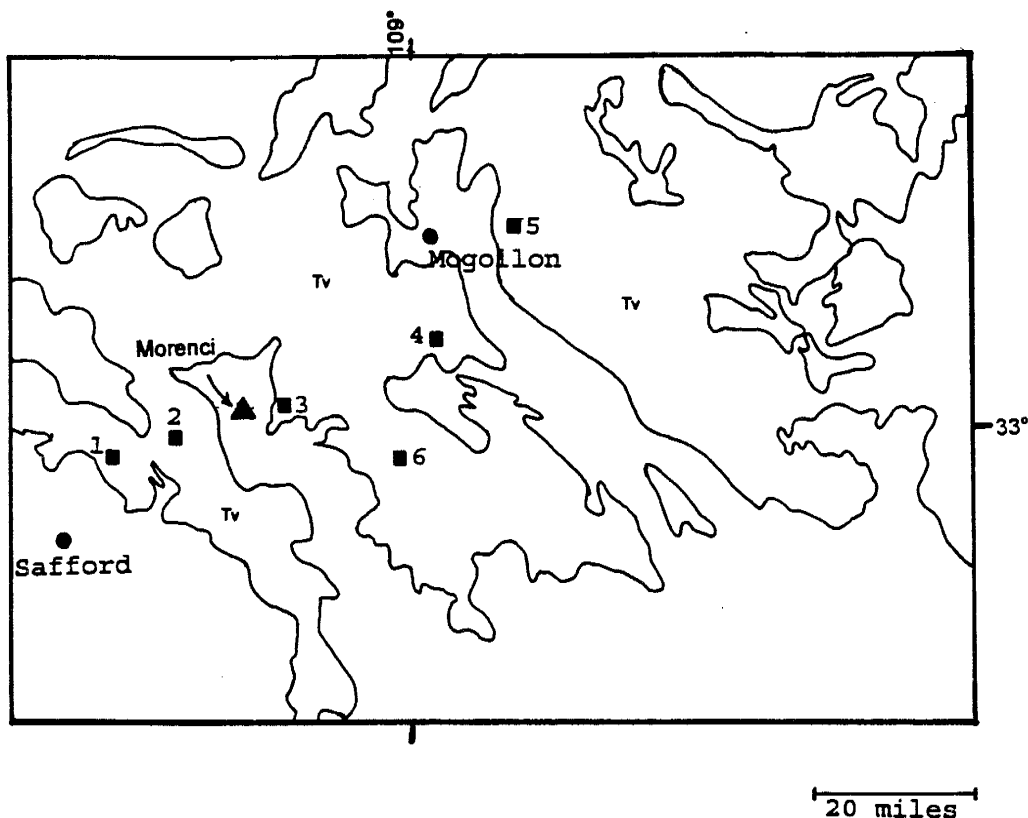


Figure 10. Middle Tertiary volcanic rocks near the Morenci mining district. Numbers correspond with Table 3.

LOCATION	AGE (Ma)	REFERENCE
1: Bear Springs Dacite & Rhyolite	24.5±0.6 K-Ar biotite	Houser & others, 1985
	26.5±0.6 K-Ar plagioclase	
2: Turtle Mountains	23.6±0.5 K-Ar plagioclase	Houser & others, 1985
3: Bloodgood Canyon Tuff Cooney Tuff Clifton Tuff	28.1±0.1 Ar-Ar sanidine	McIntosh & others, 1991 Ratte & others, 1984
	Approx. 34.0 correlation	Ratte & others, 1984 McIntosh & others, 1991
	32.70±4.9 FT zircon	Wahl, 1980
4: Davis Canyon Tuff	29.0±0.1 Ar-Ar sanidine	McIntosh & others, 1991 Ratte & others, 1984
5: Shelly Peak Tuff	28.7±0.08 Ar-Ar sanidine	McIntosh & others, 1991 Ratte & others, 1984
	28.5±0.09 Ar-Ar sanidine	
6: Steep Rock Tuff	36-35 correlation	McIntosh & others, 1991

Table 3. Radiometric age determinations for middle Tertiary volcanic rocks near the Morenci mining district. Numbers on table correspond with the numbered locations on Figure 10.

physiographic province of Arizona. The Transition zone is a broad physiographic boundary that lies between the relatively structurally intact Colorado Plateau and the highly extended terrain of the southern Basin and Range province. The southern margin of the Colorado Plateau in Arizona is defined by the Mogollon Rim (Figure 11), a zone where north-dipping Permian strata terminate southward (Peirce & others, 1979). This portion of the southern Colorado Plateau margin is thought to have formed in Neogene time during extensional unloading in the Arizona Transition zone (Pierce, 1985).

Latest Oligocene to middle Miocene extension in the southern Basin and Range province is characterized by the development of metamorphic core complexes. Metamorphic core complexes record ductile to brittle deformation which is superimposed on rocks and structures that range in age from Proterozoic to early Tertiary (Keith & others, 1980; Haxel & others, 1984; Reynolds, 1985; Reynolds & others, 1986). They are distinguished by the spatial association of extensive mylonite zones with the low-angle normal or detachment faults (e.g., Davis, 1980; Rehrig, 1986; Reynolds & others, 1988; Lister & others, 1986; Spencer & Reynolds, 1989). Mylonitic lineations throughout most of the southern Arizona metamorphic core complexes trend $060^{\circ} \pm 10^{\circ}$ (Davis, 1981) and are generally parallel to the direction of displacement along the detachment faults.

The hanging walls of major detachment faults are generally composed of a series of uniformly dipping high-angle normal faults between which strata are uniformly tilted in one direction over large regions (Wernicke & Burchfiel, 1982; Faulds & others, 1990). Regional structural domains of hanging wall rocks referred to as tilt-block domains occur throughout the

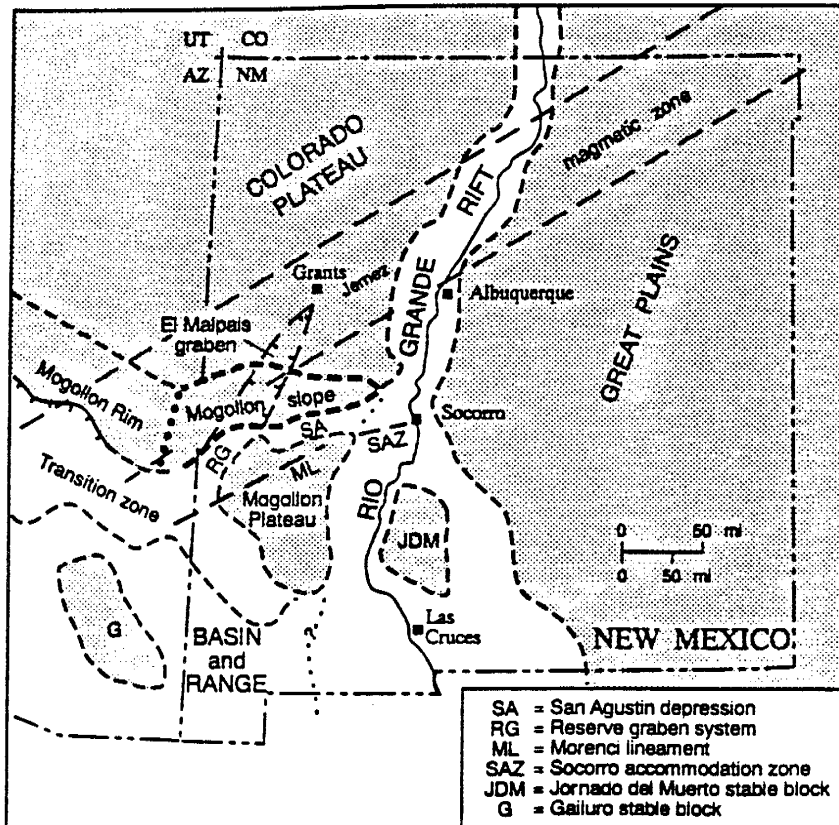


Figure 11. Generalized tectonic map of New Mexico and eastern Arizona showing the relationship of the Mogollon Rim and Mogollon slope to regional structural elements. Provinces and domains of moderate Cenozoic extension are shown in white. Crustal provinces and blocks that have generally resisted Cenozoic extension are shaded grey. From Chamberlain and Cather (1994).

southwest. These domains are known or inferred to be representative of extension above a detachment fault or several faults that dip regionally in the same direction (Spencer & Reynolds, 1989).

Evidence for metamorphic core complex-type deformation occurs within 25 km southwest of the Morenci mining district. In the Pinaleno-Santa Teresa Mountains, two exposures of a single detachment fault are exposed: the Eagle Pass fault and the Black Rock fault (Figures 12 and 12.1). This detachment displaces late Oligocene through early Miocene volcanic and sedimentary rocks and all the strata within the hanging wall dip moderately to steeply to the southwest (Rehrig & Reynolds, 1980; Davis & Hardy, 1981). A 27 km long, 0.5 km thick mylonite zone overprints the northeast flank of the Pinaleno Mountain range. This mylonite zone trends to the northwest and dips moderately to the northeast. A top-to-the-northeast sense of shear was determined by macroscopic shear-zone geometry and S-C structures. The principle extension direction, indicated by the orientation of the mylonitic lineation and the long axis of the finite strain ellipsoid, is oriented northeast (Naruk, 1986; Spencer & Reynolds, 1989). This orientation is parallel to the direction of slip determined for the Eagle Pass-Black Rock detachment fault. This correlation strongly suggests that the Pinaleno mylonite zone is kinematically related to the Eagle Pass-Black Rock detachment fault (Davis & Hardy, 1981). Spencer and Reynolds (1989) project the detachment fault beneath the Gila Valley and relate the overall southwest dip of Proterozoic and Paleozoic strata in the San Carlos area to large northeast-dipping faults that are structurally continuous along the Santa Teresa Mountains. Figure 12 shows the location of the Morenci mining district and

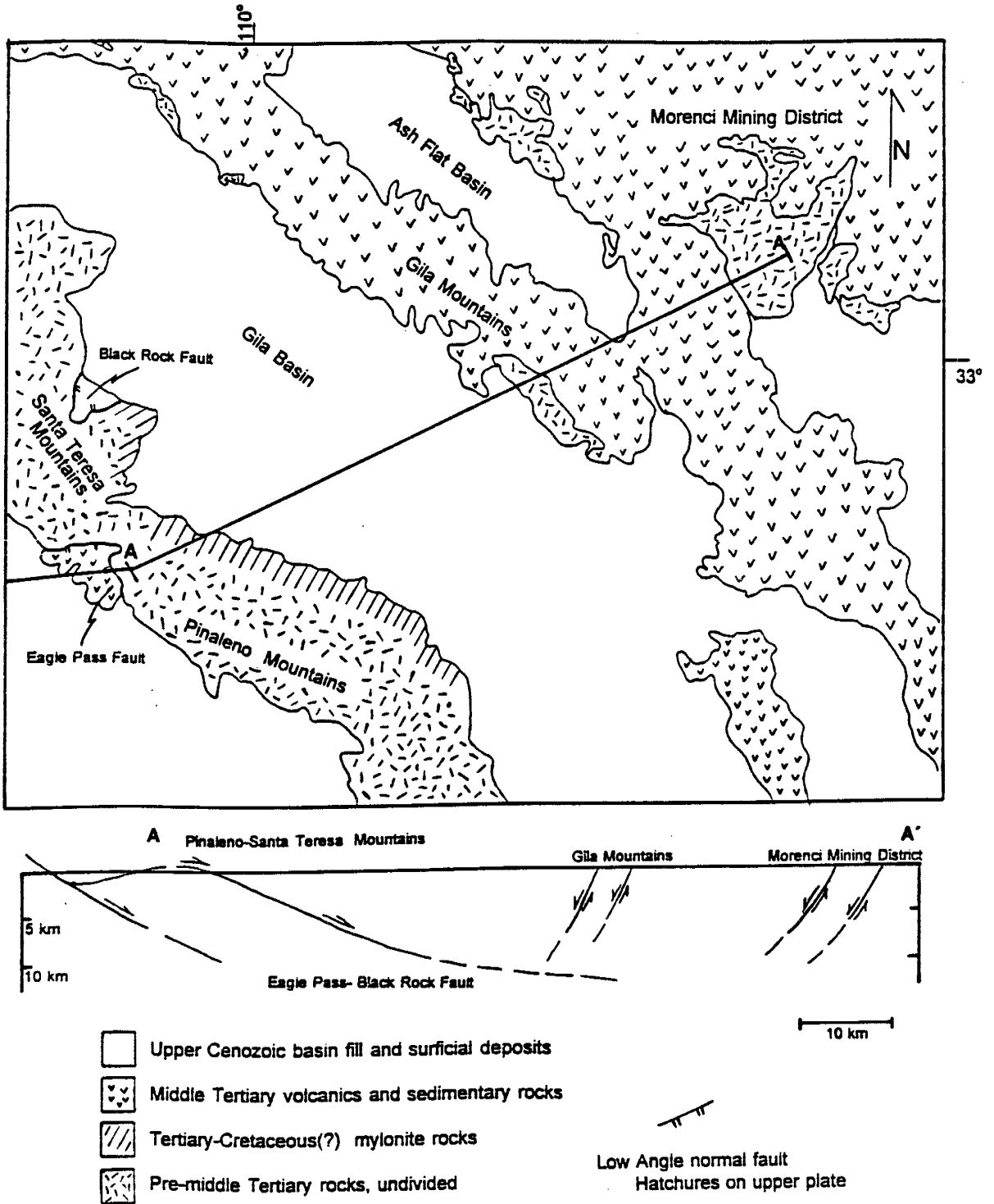


Figure 12. Map and cross section showing major middle Tertiary tectonic features in part of southeastern Arizona. See text for details. Map and cross section modified from Spencer and Reynolds (1989).

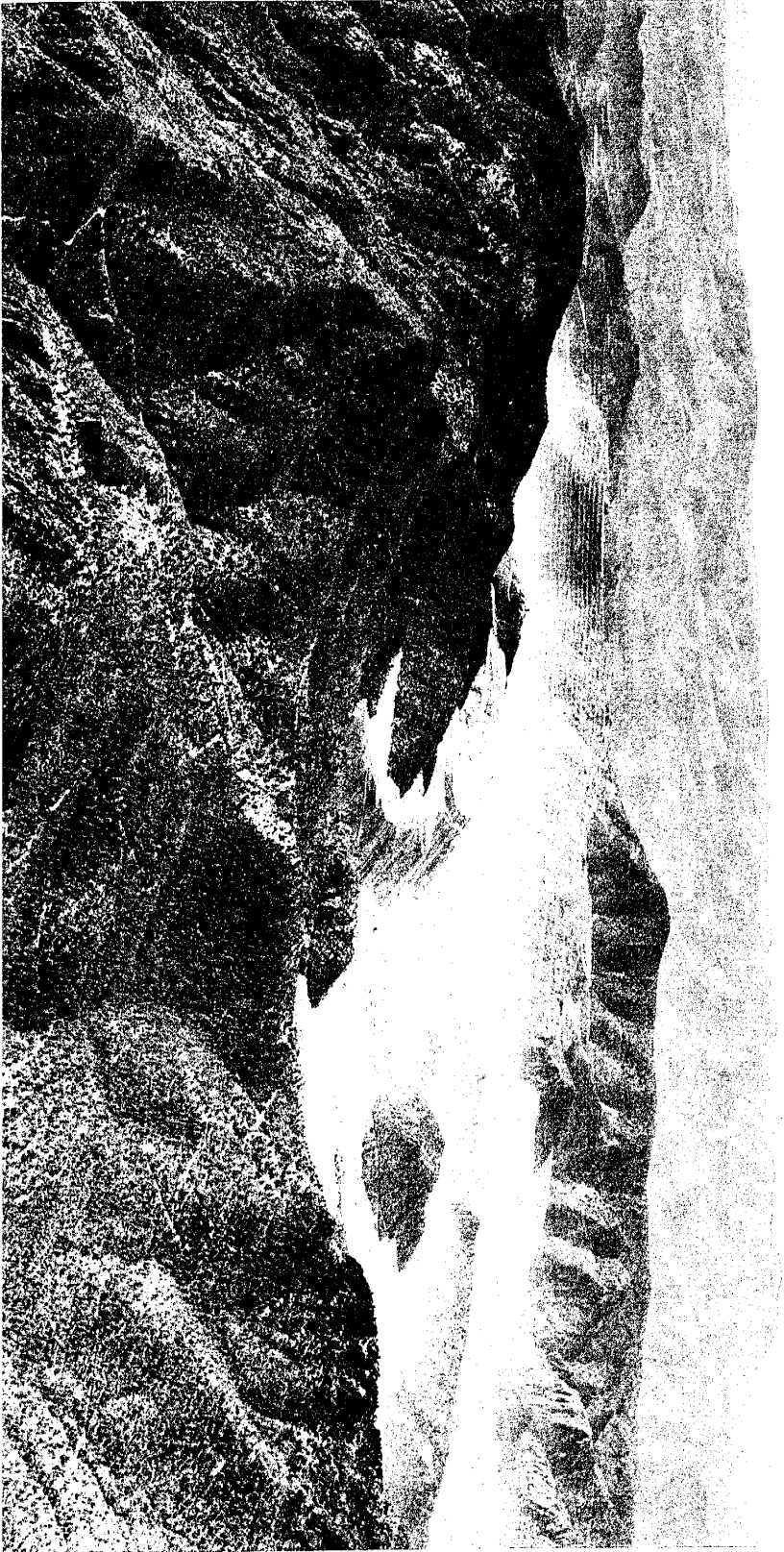


Figure 12.1. Aerial view looking southwest, the Morenci mining district in the foreground and the Pinaleno Mountains on the horizon. The intervening mountains are composed of middle Tertiary volcanic flows that dip gently toward the northeast.

relates the southwest-dipping Paleozoic and Cretaceous strata and northwest-striking faults in this district to the middle Tertiary extensional tectonics proposed for this area.

Near the Arizona-New Mexico border, the extreme southeastern edge of the Colorado Plateau is covered by volcanics of the Mogollon-Datil volcanic field. In this area, the north-dipping strata on the Mogollon Rim grade into the south-dipping strata of the Mogollon slope. (Chamberlin & Cather, 1994). The Mogollon slope is primarily defined by gently south dipping ($2-10^\circ$) Eocene to Oligocene orogenic and volcanogenic strata, approximately 1.3 to 2.1 km thick, that generally parallel the classic (physiographic) southeastern margin of the Colorado Plateau (Chamberlin & Cather, 1994) (Figure 11). The Mogollon slope is thought to represent downwarping of the southeastern margin of the Colorado Plateau during Eocene to Oligocene time (Chamberlin & Cather, 1994). The southern margin of the Mogollon slope is defined by the moderate to strongly extended domains along the San Agustin arm of the Rio Grande rift.

Structural and stratigraphic data indicate that extension began about 35-36 Ma along the Rio Grande rift. By late Oligocene, the rift was a north-trending zone of longitudinally linked extensional basins and related fault zones extending from central Colorado through New Mexico and southeastward along the Texas-Mexico border (Chapin, 1971; Cordell, 1978; Chapin, 1979; Elston & Bornhorst, 1979; Aldrich & others, 1986; Cather, 1990 & 1992). Complex transverse structural zones or accommodation zones formed where the north-trending Rio Grande rift broke across preexisting northeast-trending lineaments (Chapin & Cather, 1994). These older structural zones were oriented approximately parallel to small

circles of rotation between the Colorado Plateau and the stable craton during northeast to east-northeast directed Miocene extension (Chapin & Cather, 1994). The Socorro accommodation zone (Chapin & others, 1978; Chapin, 1979) is one of the best documented of these structures. It is near the Socorro accommodation zone that the Rio Grande rift widens and bifurcates into a weaker arm (the San Agustin rift) which extends southward into Arizona along the Morenci lineament (Chapin, 1971; Chapin and others, 1978; Chapin & Cather, 1994). The moderately to strongly extended domains of the San Agustin basin form a regional west-southwest trending topographic low and mark the southeastern boundary of the Colorado Plateau in west-central New Mexico. The western portion of the 060°-trending domain of the San Agustin basin is connected with the 040° to 030°-trending Morenci-Reserve fault zone by a narrow, topographically low, distended zone northeast of the Reserve graben (Ratte & others, 1991; Chamberlin & Cather, 1994).

Ratte (1989) describes the Morenci-Reserve fault zone as a complex graben system that trends 040° - 030° and is 40 to 50 km wide. This fault zone lies between the southeastern edge of the Colorado Plateau and the northwestern rim of the Mogollon Plateau and is part of a series of northeast-trending structural zones that define the southeastern edge of the Colorado Plateau. The Morenci-Reserve fault zone has accommodated moderate to strong crustal extension, forming a chain of narrow middle Miocene to younger grabens (Ratte, 1989; Crews, 1994; Houser, 1994). The Reserve graben (Ratte, 1989; Crews, 1994) which extends northeast through west-central Catron County, New Mexico, is part of the Morenci-Reserve fault zone (Figure 13). The Reserve graben is comprised of a series of distinct half-graben sub-

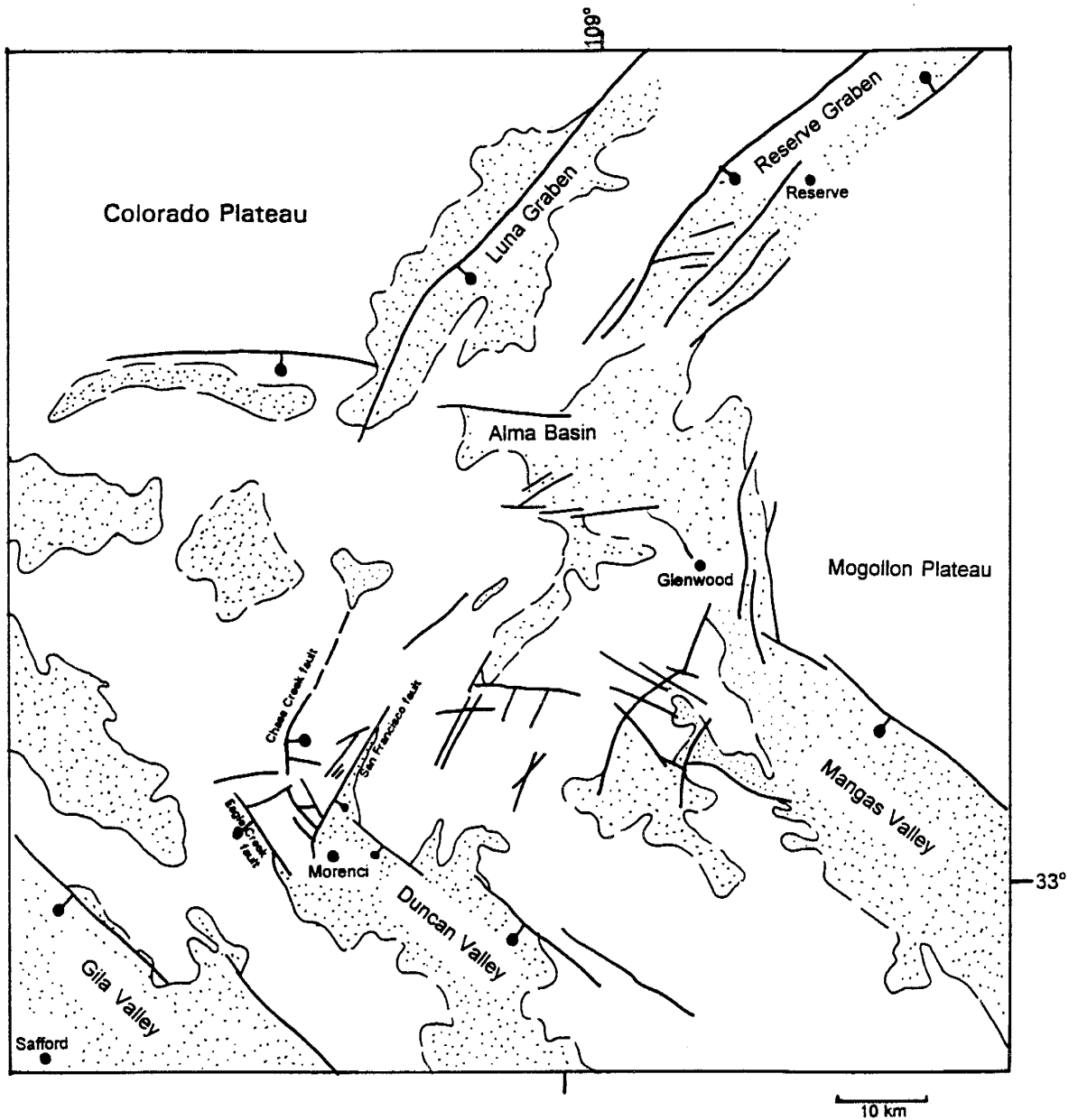


Figure 13. Simplified map placing the major faults in the Morenci mining district in context with northeast-striking faults that are part of the Morenci-Reserve fault zone, the northwest-trending basins of the southern Basin and Range province, and the southeastern edge of the Colorado Plateau. Stippled pattern indicates late Cenozoic basins. Faults are shown by heavy lines, ball on the down-dropped side. Compiled from Ratte (1994), Houser (1994), Simons (1964), and unpublished maps obtained from Phelps Dodge Morenci, Inc.

basins and is filled with alluvial deposits of the Gila Group (Crews, 1994). The sedimentary units of the Gila Group (Gilbert, 1875) are characterized by thick conglomeratic sequences. The conglomerates are of local origin, most commonly derived from the mountains that flank the deposits. In this graben, Gila group sediments were clearly deposited in the context of the same fault blocks that define current topography. They overlie pre-faulting 27-23 Ma Bearwallow Mountain Andesite, and are interbedded with basalt flows having ages ranging from 21 to 1 Ma (Crews, 1994). Principal faults strike north-northeast, and nearly all dip southeasterly (Figure 13). The San Francisco Mountains fault zone, which extends in strike over 9 km, defines the northwest margin of the graben and appears to be the main bounding fault zone of the basin (Crews, 1994). Transverse faults that strike east-west are associated with mountainous zones at the end of each basin, separating the Reserve graben from neighboring basins (Crews, 1994).

The Alma basin, which lies approximately 20 km southwest of the Reserve graben, crossing the New Mexico-Arizona border, is described as an irregularly shaped late Cenozoic basin located at the intersection of the Morenci-Reserve fault zone and the Mangas valley (Figure 13) (Houser, 1994). The Mangas valley is a northwest-trending basin that formed during Basin and Range extension. This northwest-trending basin is one of several basins along the southeastern margin of the Colorado Plateau (Houser, 1994). The Mangas Valley is bound near the Alma basin by the 040° to 030°-trending faults of the Morenci-Reserve fault zone. Although late Cenozoic uplift and subsidence has been controlled by interaction between both the northwest and northeast structural trends, the Alma basin is described as a fairly

simple asymmetric graben composed of about six unrotated blocks, stepped down on the east side adjacent to the Mogollon Plateau (Houser, 1994). Nearly all of these faults are high-angle normal faults that dip 70 to 85° to the southeast or east with the overall sense of displacement being down to the southeast (Houser, 1994). The basin is filled with predominantly Gila Group sediments, which record episodic basin subsidence beginning around 23 Ma and ending when Quaternary stream erosion began to exhume the basin (Houser, 1994).

Houser (1994) suggests that the northwest-trending extensional structures of the Arizona Transition zone appear to give way to the northeast-trending structures of the San Agustin arm of the rift near Alma, New Mexico (Figure 13). The en echelon pattern of the Reserve graben system and the San Agustin depression has been attributed to sinistral transtension associated with Neogene clockwise rotation of the Colorado Plateau as it pulled away from the batholithically rooted Mogollon Plateau (Chapin, 1971; Chamberlin & Cather, 1994).

Middle to Late Miocene Extension

A distinctive suite of characteristics permits differentiation of Basin and Range deformation from the earlier middle Tertiary extensional tectonism in the southwest. Regional studies in the southern Basin and Range indicate that major faulting began between 13 and 10 Ma, probably continued up until about 6 Ma and should be considered a "late-stage" episode of extensional tectonism (Menges & Pearthree, 1989). Near-surface extension was accommodated primarily by moderately to steeply dipping normal faults which form the

structural boundaries of grabens or tilted half-grabens and fault-block ranges. In southeastern Arizona, the basins and ranges have a fairly consistent north-northwest orientation. Structural relief indicates large normal separation. Estimates of cumulative regional post-15 Ma horizontal extension vary from 5 to 20 percent, depending on the fault geometries. (Scarborough & Peirce, 1978; Shafiqullah & others, 1978, 1980; Davis, 1980; Zoback & others, 1981; Anderson & others, 1983; Seager & others, 1984; Keith & Wilt, 1985; Menges & Pearthree, 1989).

Second Generation of Supergene Enrichment in the Morenci District

Recently obtained radiometric age determinations suggest that an episode of supergene sulfide enrichment in the Morenci district occurred between 30 and 10 Ma (North & Preece, 1993; Cook, 1994). A K-Ar age of 30.0 ± 0.7 Ma (Table 1) (Cook, 1994), was obtained from a trachyte dike exposed in upper benches along the extreme southeastern edge of the Metcalf open-pit. The dike had been locally argillized by supergene solutions and veined by chalcocite. Alunite from veinlets that cut chalcocite has been dated at 9.88 ± 0.26 Ma (Table 1) (Cook, 1994), indicating that supergene processes had ceased by this time. Alunite cutting chalcocite collected near the Northwest Extension open-pit gave a K-Ar age of 7.19 ± 0.27 Ma (Table 1) (Cook, 1994), again indicating that most enrichment had ceased, in this area, by that time.

During this period of supergene enrichment, the first-generation blanket was exposed to oxygenated water and the pyrite content became the most important factor in determining what supergene processes occurred (North & Preece, 1993). Where pyrite content was high,

chalcocite and pyrite were leached, leaving behind a hematitic leached capping. Where pyrite content was low, copper was oxidized in place, resulting in the formation of copper oxide minerals such as chrysocolla, malachite and azurite. Lateral transport of copper-bearing solutions along major structures was also important in determining the distribution of the enrichment blanket in the Morenci and Metcalf open-pit areas (North & Preece, 1993).

STRUCTURAL DESCRIPTION AND ANALYSIS OF THE MORENCI MINING DISTRICT

Introduction

Lindgren (1905) stated that the most accurate description of this region would be the "broken down edge of the plateau", and suggested that " a glance at the (district) map shows the multitude and importance of faults." He described the precipitous granite ridges north of the district that rise to elevations greater than 2,195 m and the wide conglomerate-filled valley, with rolling hills and deeply incised canyons that extend south and southwest from the district. Lindgren also noted..."faulting movement, which was practically confined to one epoch falling between the intrusion of the porphyry (latest Cretaceous to earliest Tertiary) and the eruptions of the lavas (late Tertiary)".

Although our knowledge of the tectonic events that have dominated this region from latest Cretaceous to late Tertiary time has greatly expanded since 1905, it is still quite right to say that the most profound faulting events in this district began in the latest Cretaceous and extended into the late Tertiary. The previous discussion of Precambrian through late

Cretaceous stratigraphy of the Morenci mining district has shown that relative stability prevailed, in this district, during most of the Paleozoic through the late Cretaceous. The first marked disturbance of the stratified formations occurred at the time of the Laramide porphyry intrusions.

The district map (Plate 1) and a simplified map showing the major faults of the district (Figure 14) show several structural trends. The most prominent structural trend is demonstrated by the 040° to 020° -striking Laramide veins, dikes and stocks (Figure 5). Similar strikes are also exhibited by many of the faults in the district. E-striking faults are notable, particularly in the northwestern portion of the district. In general both the NE-striking and the E-striking faults are cut by a series of NW-striking faults. An exception is the San Francisco fault, which bounds the district to the southeast and cuts all other faults to the north and northwest. The district is bound to the southwest by the NW-striking Eagle Creek fault. The N-striking Chase Creek fault is associated with the mountainous region to the north of the district. The WNW-striking Garfield fault also occurs in the northern portion of the district. The significance of each of these fault trends will be discussed in the following sections.

Terminology

Both major and minor faults, in the Morenci mining district are mesoscopic surfaces marked by fault breccia or gouge, fault slickenside surfaces, and/or lithologic discontinuities. Following Sibson (1977), incohesive cataclastic rocks are subdivided into fault breccia and fault gouge. In fault breccia, visible fragments of the parent rock comprise at least 30% of the

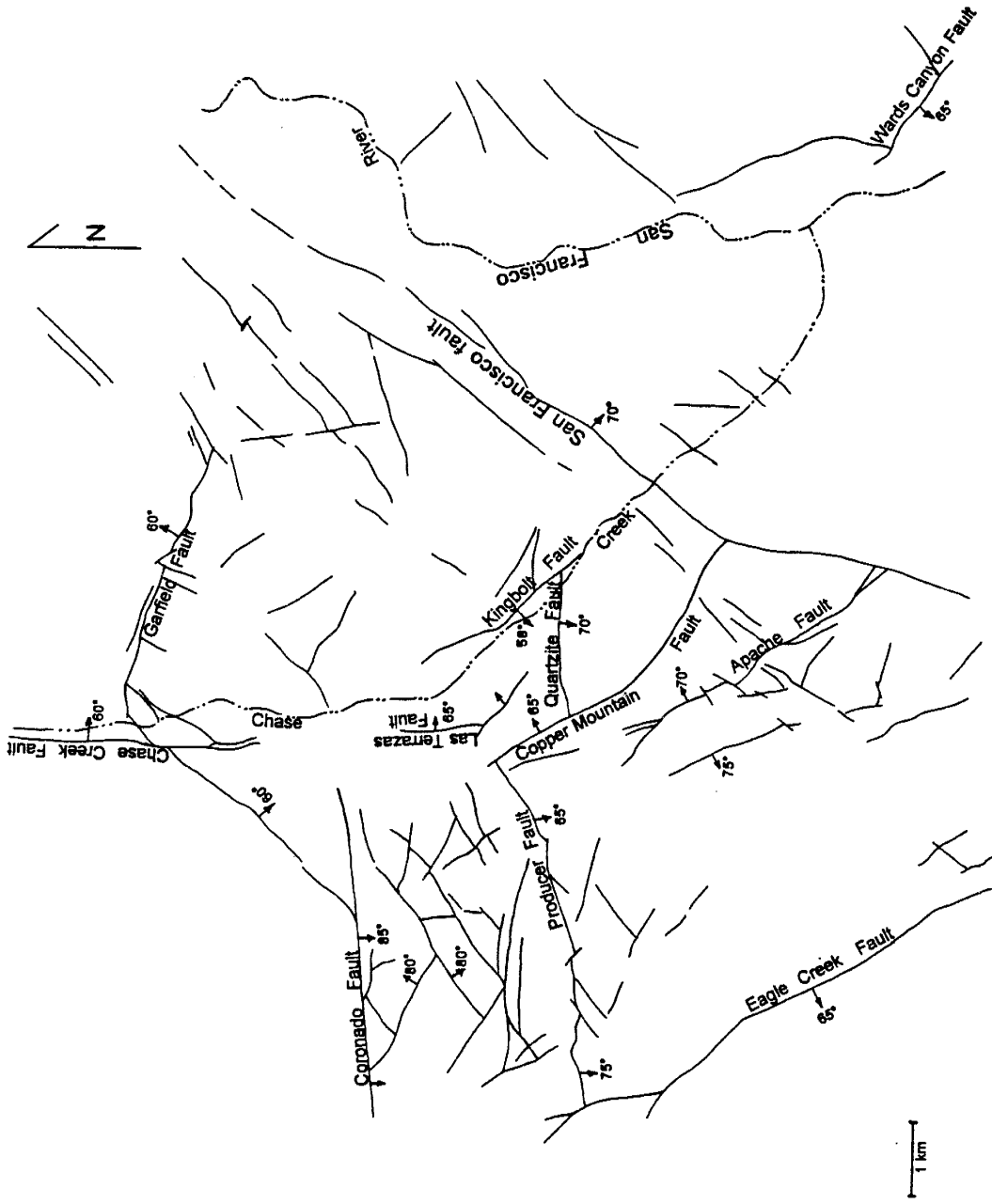


Figure 14. Major faults of the Morenci mining district. Arrows point in the direction of dip, numbers indicate average dip angle.

rock mass, whereas fault gouge contains less than 30% visible fragments. Fault gouge, where observed, commonly occurs in the most intensely deformed portion of a fault zone, and is seen to anastomose around lenses of somewhat less-deformed material. Fault slickensides are defined following Fleuty (1975), as polished and commonly striated brittle shear surfaces. Slickenside striae are linear structures on a slickenside that form by friction parallel to the direction of movement. Faults with similar attitudes, crosscutting relationships, and movement histories are collectively referred to as fault systems. Nomenclature that is accepted and entrenched in the historic literature of the Morenci mining district is maintained and defined where appropriate.

Evidence of Laramide-age faulting

The importance of the 040°-020°-striking Laramide extensional features has been discussed previously. Many faults of similar orientation are spatially associated with the Laramide dike swarm. These faults are commonly mineralized breccia zones and are presumed to be Laramide in age. However, there are several other structural trends associated with Laramide deformation. These include E-striking faults (locally associated with NE-striking faults) and at least one NW-striking fault. Evidence for sense and timing of movement on these faults is presented below.

The east-striking Coronado fault (Figures 14 & 15), bounds the district on the northwest. The fault can be traced along strike for nearly 5 km from where it is covered by middle to late Tertiary basaltic rocks on the west to where it terminates on the east into the

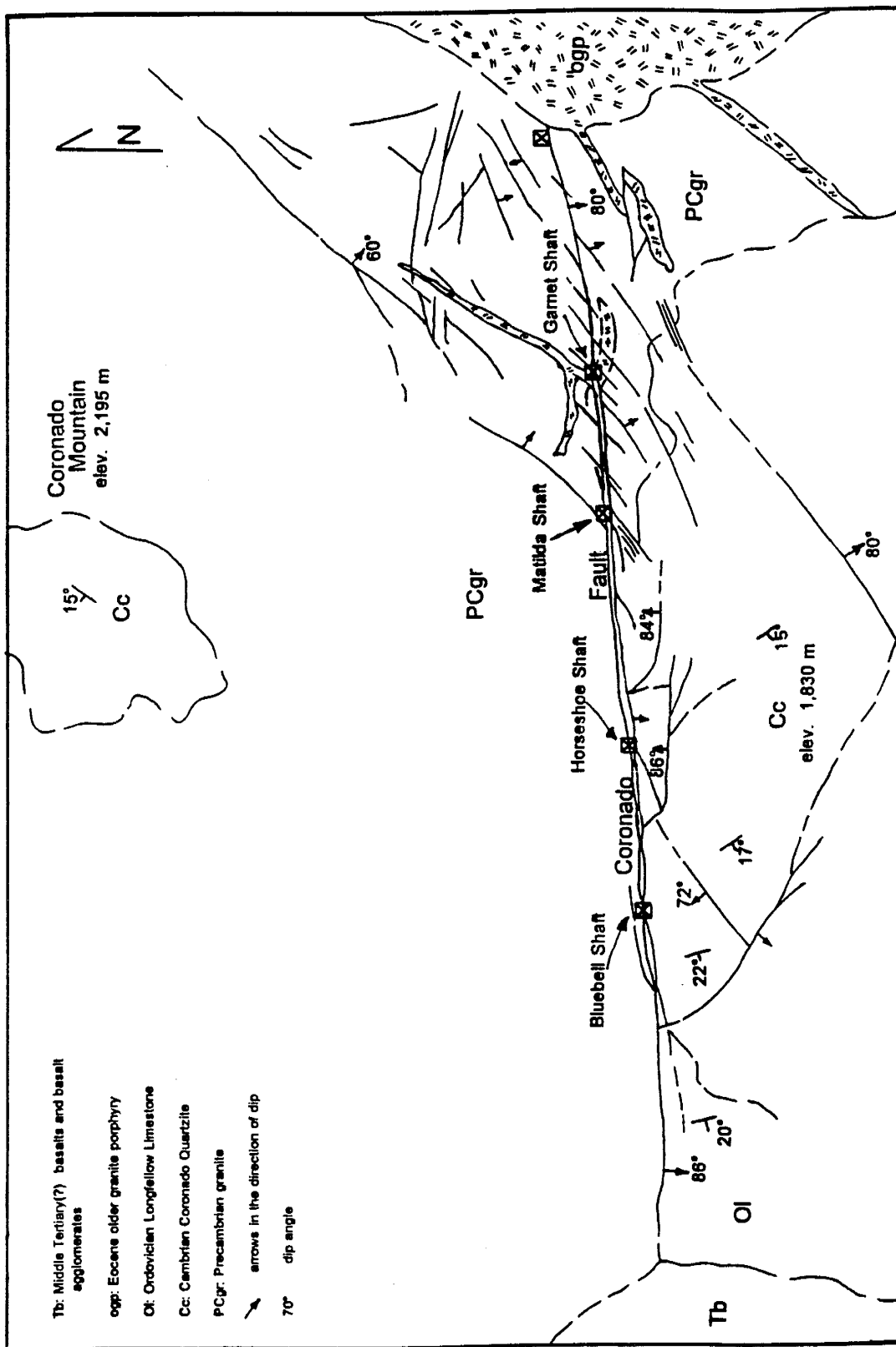


Figure 15. The Coronado fault and surrounding geologic relationships.

northern portion of the Older Granite Porphyry stock. North of the fault is the high ridge of Coronado Mountain. Here, approximately 65 m of Cambrian quartzite overlie Precambrian granite at an elevation of 2,195 m. The sedimentary rocks have an average strike of 020° and dip of $10-25^{\circ}$ NW (Figure 15). South of the fault, Precambrian granite is overlain by lower Paleozoic strata and intruded by the Older Granite Porphyry stock and cogenetic dikes. The Cambrian quartzite occurs at an elevation of approximately 1,830 meters, has an average strike of 330° and dips consistently to the WSW at $10-25^{\circ}$ (Figure 15). The fault maintains a remarkably straight trace of 080° . The dip is also fairly uniform, averaging $80-85^{\circ}$ to the south. The fault zone varies in width from 4 to 46 m, averaging approximately 20 m, and is marked by a strongly silicified brecciated zone that forms a resistant rib exposed along most of its strike length (Figures 16 & 16.1). The breccia is typically matrix-supported with clasts of Precambrian granite, Cambrian quartzite and vein quartz that range in size from less than 2 cm to more than 61 cm. The clasts are angular to sub-rounded and commonly appear highly fractured and brecciated (Figures 17 & 17.1). Pervasive quartz \pm sericite \pm pyrite \pm hematite alteration is a common feature in breccia samples taken along most of the strike length of the fault zone (Figure 18). Fractures in the clasts have been healed by quartz and in many instances original textures are partially obliterated by alteration. Pyrite, now completely oxidized, occurred as subhedral to euhedral grains and aggregates associated with quartz in the matrix and in quartz veins that cut across fragments (Figure 19).

The Coronado fault is an important ore-controlling feature. The Coronado Lode follows the fault zone for most of its strike length. Extensive underground workings along this



Figure 16. View looking east from the Matilda shaft. Strongly silicified brecciated zone of the Coronado fault in foreground, fault zone shown is approximately 25m wide. Metcalf open-pit in background.



Figure 16.1. View looking west from the Matilda shaft. Arrows point to exposures of the silicified breccia zone that forms resistant ribs along strike of the Coronado fault. Middle Tertiary volcanic rocks form hills in background, overlie the Coronado fault, and lie approximately three kilometers west from the fault zone in foreground.



Figure 17. Coronado fault breccia. Highly fractured, angular to sub-rounded clasts of Cambrian quartzite and Precambrian granite.

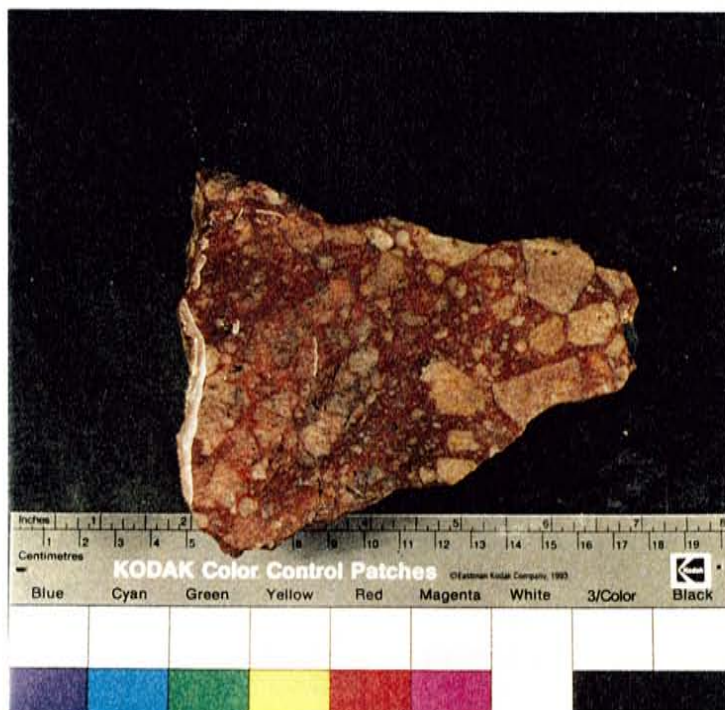


Figure 17.1. Slab from the Coronado fault showing breccia clasts within a breccia.



Figure 18. Slabs of Coronado fault breccia showing pervasive quartz \pm sericite \pm pyrite \pm hematite alteration.

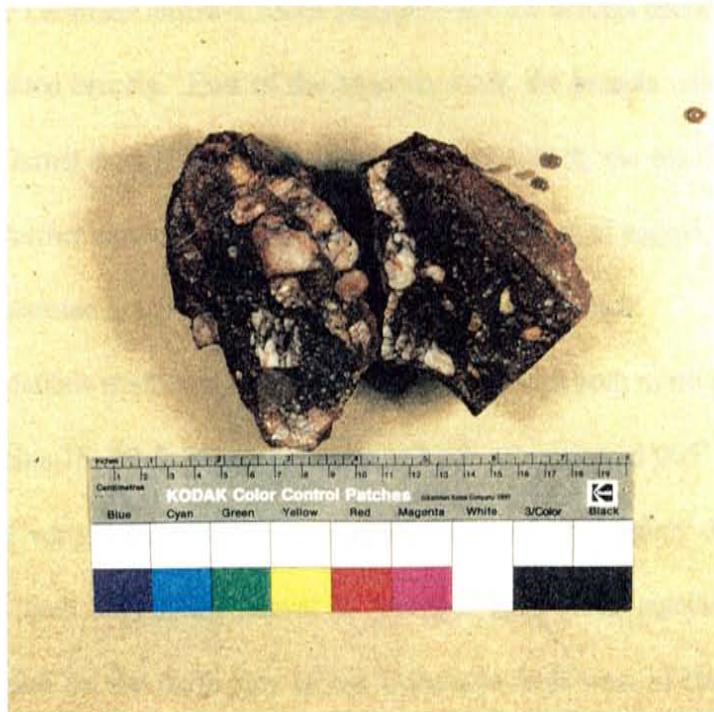
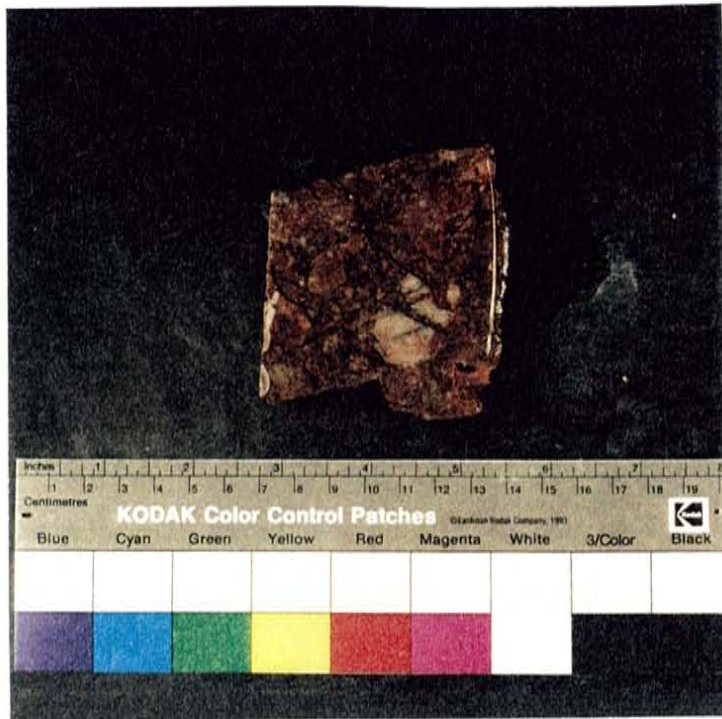


Figure 19. Slabs of Coronado fault breccia showing oxidized pyrite with quartz in matrix and in quartz veins that cut across fragments.

mineralized fault zone were some of the first in this district and date back to the 1800's. The Coronado vein is described in records from these old underground mining ventures: "The Coronado Lode is a clearly defined fissure characterized by a wide breccia zone that varies in width considerably.....The ores of the vein consist of partly oxidized minerals such as chrysocolla and malachite, partly of glance averaging up to 25 % Cu grade, and partly of pyrite and chalcopyrite.....The footwall is sharply defined and most of the crushed vein matter extends between fresh granite on the north and fresh quartzite on the south" (Lindgren, 1905). The mineralized breccia zone is readily traced by its conspicuous outcrop, from the Matilida shaft westward to the Bluebell shaft (Figures 15 & 16.1). Between these two points the breccia lies between quartzite and granite and Laramide diabase intruded along the strike of the fault. The diabase is typically highly argillized and intrudes along the footwall side of the fault. West of the Bluebell shaft, the Laramide intrusive rocks disappear and the breccia becomes a hard, iron-stained, quartz-cemented breccia. East of the Matilida shaft, the breccia continues as a well defined zone to the Garnet shaft (Figure 15). From the Garnet shaft, the silicified breccia zone is difficult to follow further eastward, but an almost continuous row of jagged, irregular, highly fractured, weakly brecciated granite outcrops marks the trace of the fault.

East of the Matilida shaft, faults that strike NE are present both north and south of the Coronado fault (Figures 15, 20 & 21). The faults strike in sets oriented 065° or 045° and dip within 10 degrees of vertical NW or SE respectively. These faults slightly displace or splay from the Coronado fault suggesting coeval to younger ages. No significant faulting or fracturing can be found on the north side of the Coronado fault west of the Matilida shaft,



Figure 20. Well developed northeast-striking faults and fractures north of the Coronado fault. View looking southwest.



Figure 21. Northeast-striking faults that are splays to the Coronado fault. View looking north.

where competent Precambrian granite appears to have been unaffected by the deformation associated with movement along the Coronado fault. West of the Matilida shaft NE-striking faults are not found (Figure 15). The most notable structural features south of the fault are several large faults that roughly parallel the Coronado fault. These faults strike ESE and are typically nearly vertical. Near the Coronado fault zone they turn markedly and intersect it. These faults are marked by weakly silicified, iron-oxide stained zones that become prominent brecciated zones near the Coronado fault. The Coronado fault zone appears to bulge at the intersection of these faults.

The amount and direction of movement accommodated by the Coronado fault is difficult to determine with certainty. The Paleozoic sedimentary rocks form the only reliable datum that can be used to determine separation. As mentioned earlier, Cambrian quartzite crops out on either side of the fault but the northern exposures are nearly 0.6 km away from the fault plane. Further, the sediments strike and dip in different directions north and south of the fault (Figure 15). The vertical component of separation can only be estimated by the stratigraphic offset of approximately 275 to 305 m (Plate 3, cross section C-C'). Slickenside striations, while not very common, have been found in widely separated areas along the fault zone. The striations are almost always coated and accentuated by hematite staining (Figure 22). The lineations record strike-slip, oblique-slip and dip-slip movement (Figure 23). The striations that indicate oblique-slip trend consistently 080° and plunge $12-28^{\circ}$ to the east. The striations commonly overprint each other with the only recurring relationship observed being that of oblique-slip striations overprinted by dip-slip striations. Also, slickenside surfaces are



Figure 22. Slickenside striations coated and accentuated by hematite staining from the Coronado fault.

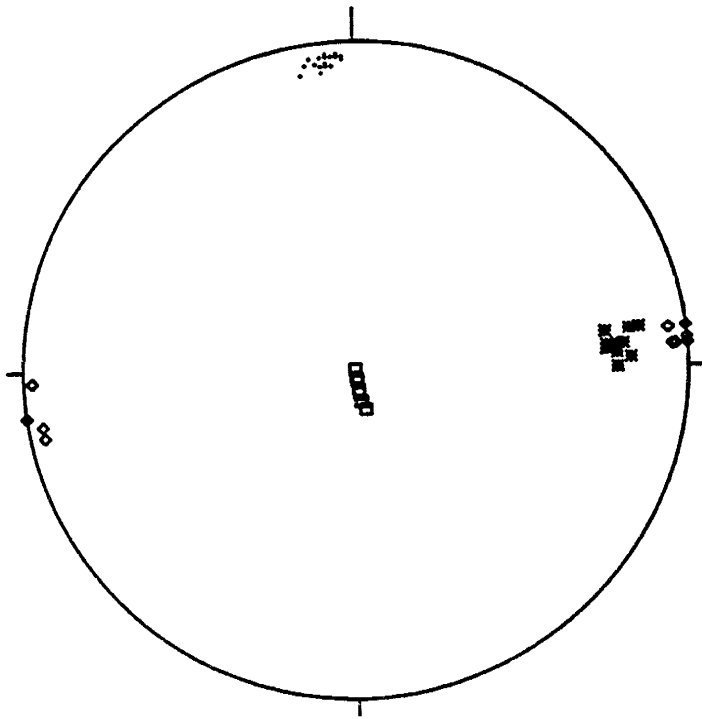


Figure 23. Lower hemisphere, equal-area plot. Poles to the Coronado fault are indicated by points (n=28). Strike-slip slickenside striae are indicated by diamonds (n=11); oblique-slip slickenside striae are indicated by stars (n=12); dip-slip slickenside striae are indicated by squares (n=9).

found on the individual clasts of the brecciated zone. In the absence of piercing points, the magnitude of the horizontal component of movement is impossible to determine.

Despite complications in understanding the timing and character of movement along the Coronado fault, there are several clear relationships: 1) movement occurred before the middle Tertiary volcanic rocks were erupted, 2) the Older Granite Porphyry stock appears to have cut and/or truncated the fault, 3) the fault acted as a conduit for hydrothermal fluids during the main mineralizing event in the district, 4) Laramide diabase was intruded along the fault. These are clear timing constraints that suggests that faulting along the Coronado fault was coeval with the Laramide intrusive/mineralizing event.

The NE-striking faults that intersect the main trace of the Coronado fault are interpreted in terms of Riedel shear geometries. These faults are properly oriented for slip as synthetic left-lateral Riedel shears during left-lateral movement on the Coronado fault (Figure 24). Further, NE-SW to NNE-SSW shortening during the Laramide orogeny would have favored left-lateral strike-slip and/or left-lateral transpressional movement on east-west oriented faults (Figure 25).

The overprinting of dip-slip striae over oblique-slip striae can be interpreted in two ways. The Coronado fault may have moved in an oblique sense with a reverse component (left-lateral transpressional) during Laramide deformation. In this case the dip-slip indicators could be recording reverse movement along this trend. Conversely, the dip-slip striae could indicate a component of dip-slip movement that occurred subsequent to movement during Laramide deformation. This reactivation could have occurred as the extensional orogenic

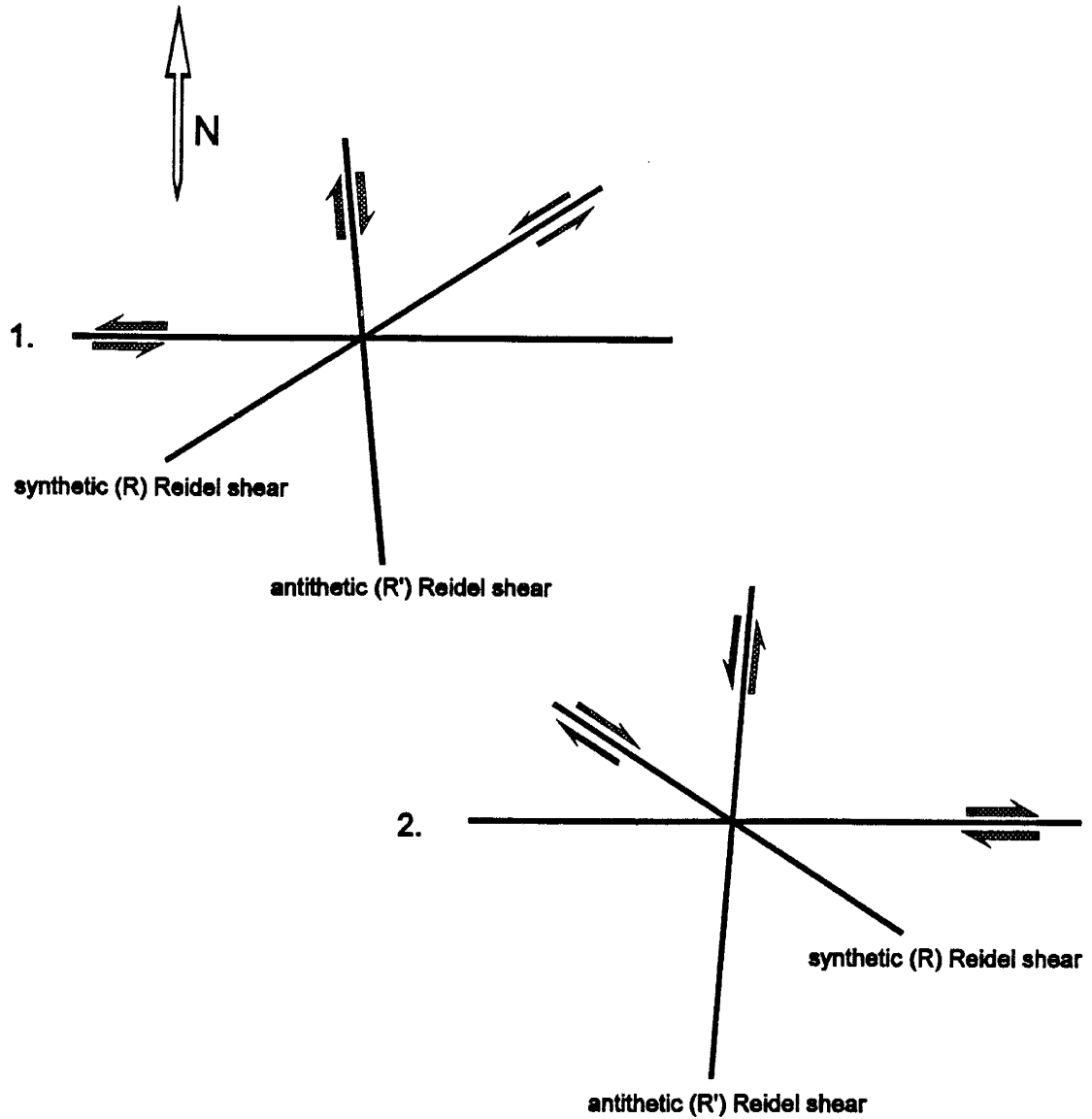


Figure 24. Anticipated Riedel shear geometries. 1. Left-lateral motion on the Coronado fault. 2. Existing geometries along the Coronado fault are not consistent with right-lateral movement.

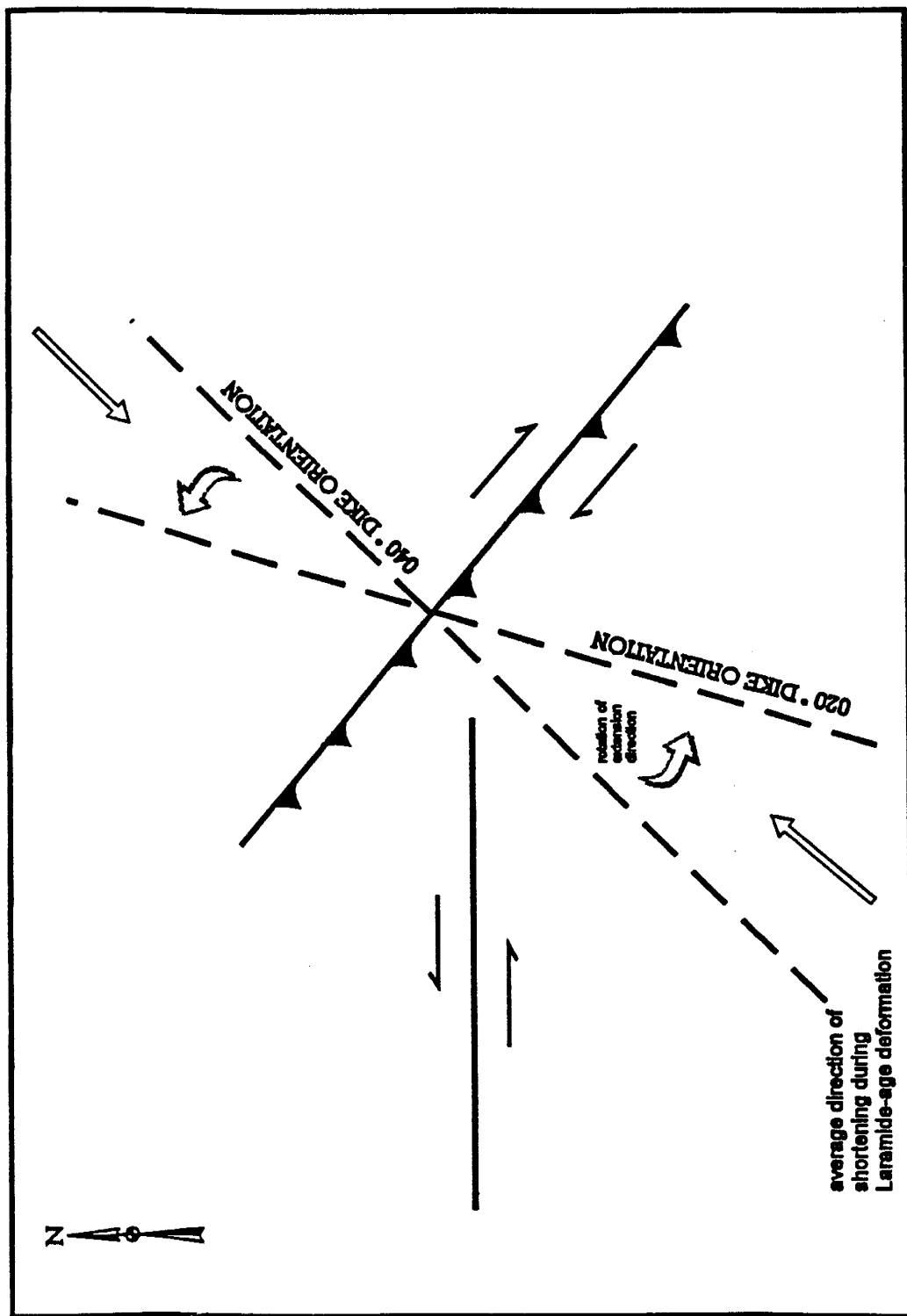


Figure 25. Anticipated behavior of faults during the Laramide orogeny based on the orientations of the faults in the Morenci mining district and the known extension and shortening directions. Average direction of shortening during Laramide deformation is indicated by straight arrows. NW-striking faults are expected to be reverse (040° dike orientation) or right-lateral transpressional (020° dike orientation) faults. East-striking faults are expected to be left-lateral and/or left-lateral transpressional faults. NE-striking faults (not shown) are expected to be normal faults.

regime of the southwest became dominant. Evidence for post-Laramide extension in this district is discussed in following sections.

There are two other major east-striking faults in the district. The timing of movement along these faults is well constrained, however no evidence of slip directions was observed. These east-west faults are considered to be similar in character to the Coronado fault.

The Producer fault (Figure 14) can be traced for approximately 6 km from west to east. It is cut off by the Eagle Creek fault at its western end and by the Copper Mountain fault at its eastern end. Its strike changes from 080° to 075° to 060° from west to east. The fault has an average dip of 65° toward the SSE. The fault zone includes a weakly mineralized silicified breccia, similar to the Coronado fault, in some exposures. Replacement of hypogene sulfides by hematite along the center of the breccia and a quartz-sericite altered halo at the margins of the breccia are common features in some exposures (Figure 26). Limited historic mining occurred in areas where the mineralized breccia outcrops, with mines targeting high-grade copper oxides and minor occurrences of gold. The breccia zone is not continuous and in many instances the fault is marked only by the contact between offset Paleozoic sediments.

In its western exposures, the Producer fault cuts and offsets Laramide dikes but Laramide diabase is intruded along its strike. Toward the eastern-most limit of the fault exposure, the fault appears to be the boundary between the monzonite porphyry stock in the hangingwall and Precambrian granite in the footwall. Precambrian granite and granodiorite are also brought into contact along the eastern portion of the fault. Dip separation can be determined by offset Paleozoic strata and ranges from approximately 150 meters to 90 meters,



Figure 26 . Photos showing the mineralized breccia of the Producer fault. Note the quartz-sericite halo surrounding the leached center. The bottom photograph is an enlargement of the area outlined in top photograph.

decreasing westward.

The fault is cut and/or offset by two populations of minor faults. One population strikes predominantly 050° and dips nearly vertically. The second population of minor faults strike 320° and dip $55-65^{\circ}$ to the SW. The crosscutting relationships between the minor faults are not clear, however the strike and dip of each population of minor faults is consistent with district-wide orientations. No sense-of-slip indicators were observed along the Producer fault zone or recorded in historic mining records.

The timing of faulting along the Producer fault can be constrained by crosscutting relationships. The most obvious crosscutting relationship is the fact that the fault is truncated to the west and to the east by faulting that occurred post-Laramide deformation (see following sections), clearly indicating that movement along the Producer fault occurred before this time. The occurrence of a mineralized breccia suggests that this fault was open to fluid flow during the time of mineralization. Further, the fault cuts Laramide dikes but is intruded by Laramide diabase. Plate 3, cross-section C-C', shows the spatial relationships between the Coronado fault and the Producer fault.

The Quartzite fault, located in the center of the district (Figures 14 & 27), strikes east and dips $65^{\circ}-70^{\circ}$ south. The fault crops out for approximately 2 km, cuts the monzonite porphyry stock, is cut by the Copper Mountain fault and appears to be cut and offset by the Kingbolt fault. The fault places Cambrian quartzite, which overlies Precambrian granodiorite on the south, next to Precambrian granite to the north. Stratigraphic offset indicates that the southern block has been dropped at least 90 m. The Quartzite fault is the southern boundary of

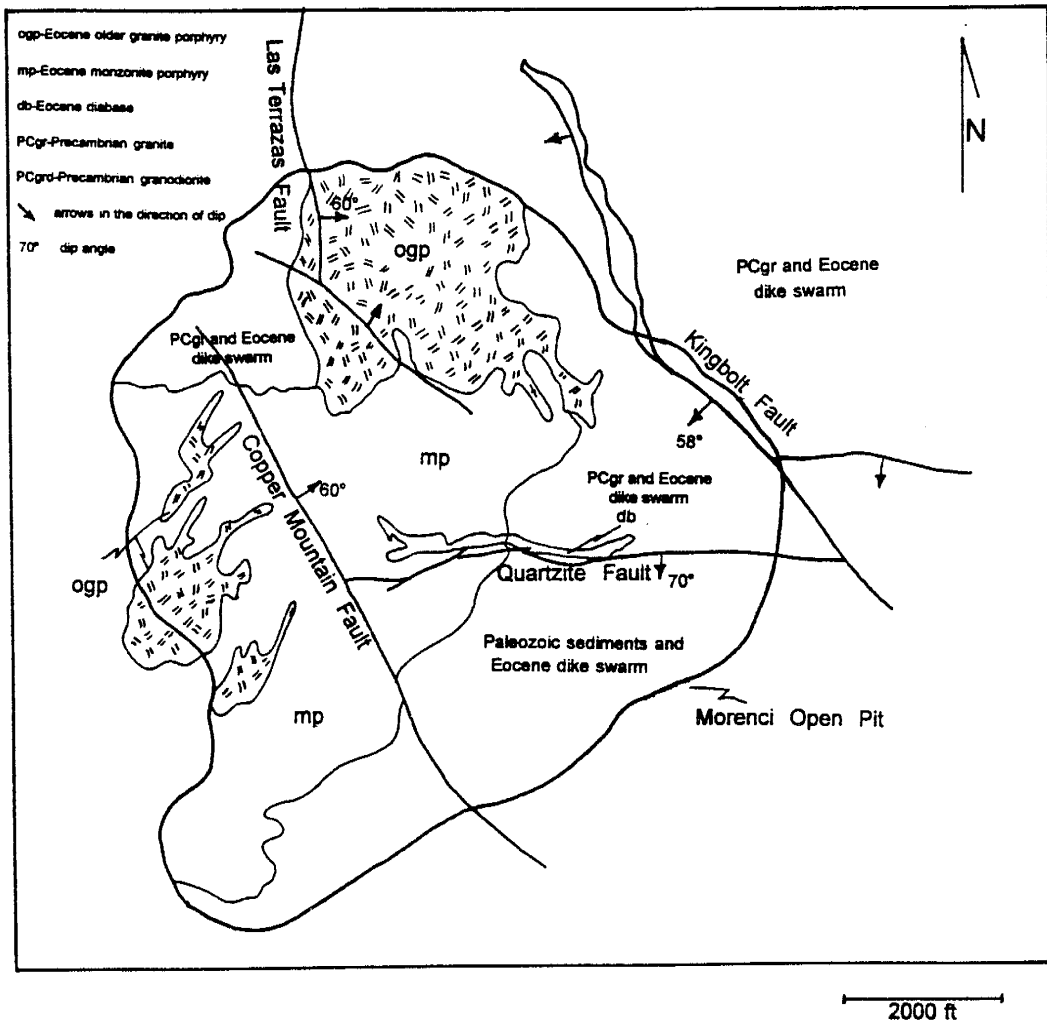


Figure 27. Simplified geology of the Morenci open-pit. Modified from Preece and others (1984).

major hypogene mineralization in the main Morenci open-pit and it also limits the distribution of supergene enrichment in this area. Consequently, the fault marks the southern boundary of mining in the Morenci open-pit and deep mining activity along the trace of the fault has obliterated most of the fault plane. Mining has exposed large volumes of diabase that intruded along the strike of the Quartzite fault (Figure 28). Historic records contain no evidence of sense-of-slip indicators and this information cannot be observed at present exposures.

Timing of movement along the Quartzite fault can be constrained by the following observations: 1) The fault limited the distribution of hypogene mineralization (57-55 Ma) (Table 1), 2) Laramide diabase intruded along its strike, 3) the fault controlled the distribution of supergene enrichment (approximately 56 Ma to 10 Ma) and, 4) the fault is cut by NW-striking faults that record post-Laramide movement (see following sections).

The east-striking faults in the Morenci district are herein collectively called the Coronado fault system. Fault-zone deformation features, cross-cutting relationships, sense-of-slip indicators and the character of ore distribution with respect to this system of faults suggest that it is a Laramide fault system. The orientation of this system of faults and Riedel shears associated with the Coronado fault are consistent with left-lateral strike-slip movement or left-lateral transpressional movement that would have been favored during NE-SW to NNE-SSW directed shortening that was operative in the district during the Laramide orogeny (Figure 25).

The Kingbolt fault is a prominent NW-striking fault that marks the eastern limit of mining in the Morenci open-pit (Figure 14). To the east of this fault are high (approximately 1,950 m) Precambrian granite ridges that are cut by Laramide dike swarms. To the west of the



Figure 28. Deep mining in the Morenci open-pit has exposed large volumes of Laramide-age diabase that intruded along the strike of the Quartzite fault. Diabase is the dark grey rock exposed on the wall of the open-pit. Trace of the fault indicated on photo. The view is looking south. Paleozoic sedimentary rocks are exposed in the benches above the diabase.

fault is the main monzonite porphyry stock (Figure 27). At its northern known limit, the fault cuts through the southern portion of the older granite stock and the younger granite porphyry. From this point, the fault can be traced SSE along a 160° strike until it enters the monzonite porphyry stock where it appears to turn and strike $130\text{-}140^\circ$ for several kilometers. The fault cannot be traced south along the Chase Creek drainage (Figure 14) and the point of its southern termination is not clear. Mining along the eastern side of the Morenci open-pit has exposed the fault zone to a depth of approximately 1,160 m. Here, the fault plane is a smooth and polished surface and the dip averages $60^\circ\text{-}65^\circ$ toward the WSW. A zone of fracturing, brecciation and pervasive argillic alteration marks the fault within the pit. Surface exposures of the fault are also marked by a brecciated zone with strongly fractured rocks that are parallel to the steep slopes to the east of the fault. The fault zone has been intercepted in many deep drill holes and in most instances is greater than 90 m wide.

There is evidence for multiple episodes of movement on the Kingbolt fault. Both syn-mineralization and post-mineralization relationships are observed in the Kingbolt fault breccia. The monzonite porphyry intrudes the breccia, locally forming the matrix and wrapping around clasts that range in size from less than 1 mm to greater than 12 cm (Figure 29). Flow banding textures are locally present in the monzonite porphyry. Subhedral to euhedral pyrite and accompanying chalcopyrite are also present in the matrix. Veins cut both clasts and matrix with only minor offsets. Quartz + molybdenite veins are often observed as stringers that wrap around clasts and fill void spaces in the matrix. Supergene chalcocite veins exhibit similar characteristics and are abundant in the matrix (Figure 30). These same veinlets also appear

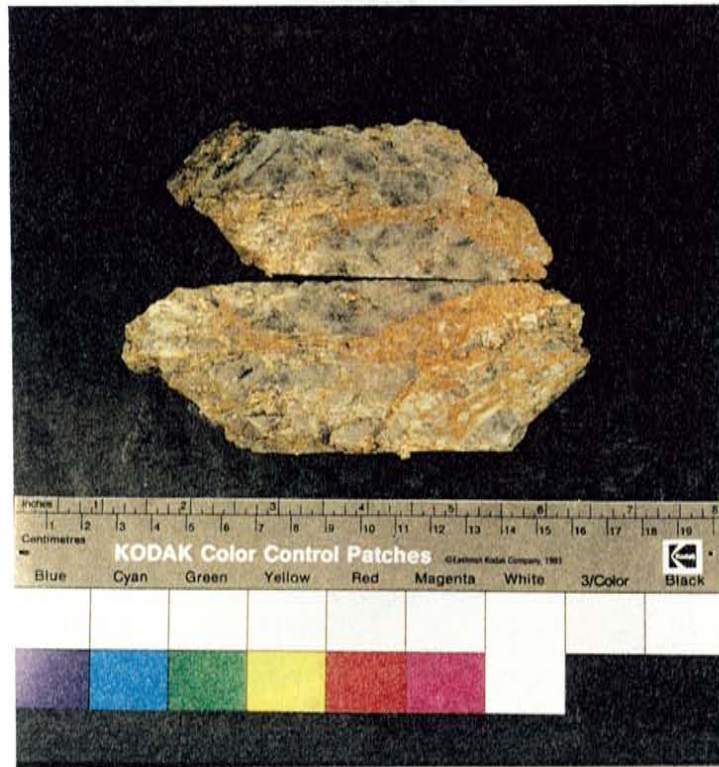


Figure 29. Slab showing monzonite porphyry forming matrix around clasts of Precambrian granite in the Kingbolt fault breccia..

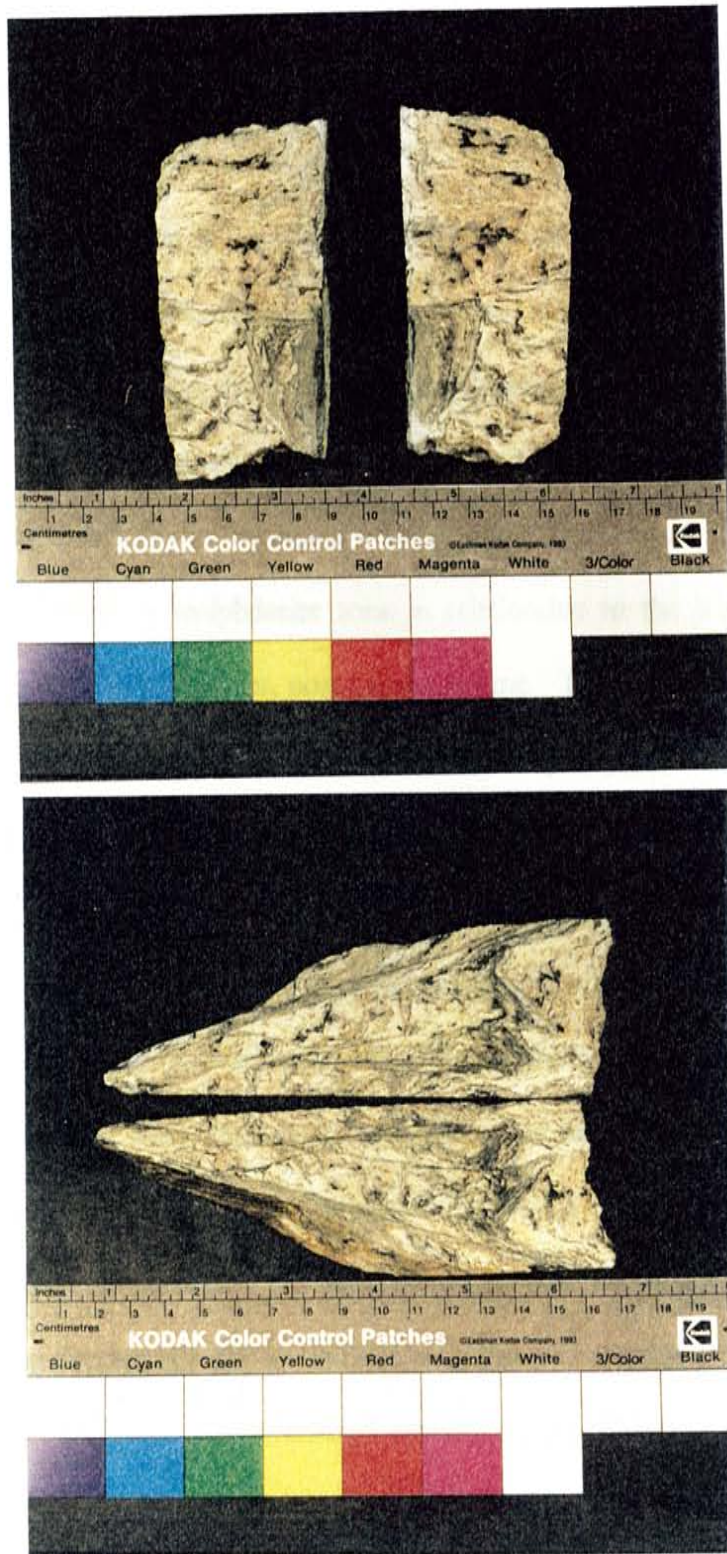


Figure 30. Slabs from Kingbolt fault showing stringers of quartz-molybdenite and pyrite-chalcopyrite \pm chalcocite veins wrapping around clasts and filling void spaces in the matrix.

bent, offset, brecciated and occur as clasts. Clasts of monzonite porphyry are also common (Figure 31). Surface exposures of the breccia zone often appear to be pervasively altered by hydrothermal fluids.

Evidence for reactivation of the Kingbolt fault is also recorded. Slickenside striations are prominent on quartz + molybdenite veins and supergene chalcocite veins within exposures of the fault plane (Figure 32). The striations are predominantly oriented in the direction of dip (Figure 33). This evidence suggests that dip-slip movement occurred post-mineralization. Although the original distribution of hypogene mineralization is not known, the distribution of the high-grade chalcopyrite \pm molybdenite zone in relationship to the Kingbolt fault may provide evidence for normal movement, post-Laramide time. The present distribution of the high-grade hypogene zone is apparently controlled by the Kingbolt fault. This zone occurs at approximately 350 m along the hanging wall side of the fault. Deep drilling (+ 650 m) in the Morenci open-pit indicates that high-grade hypogene mineralization is absent where the footwall rocks of the Kingbolt fault are intercepted. Conversely, a high-grade hypogene zone is intercepted at shallow levels (approximately 150 m) on the footwall side of the fault.

The Kingbolt fault zone appears to be a brecciated breccia with evidence of pre-intrusion, syn-mineralization and post-Laramide movement. Pre-intrusion and syn-mineralization evidence suggest that the Kingbolt fault was active during the Laramide orogeny. Shortening directed NE-SW to NNE-SSW during the Laramide orogeny would have favored reverse to right-lateral transpressional motion on the NW-striking Kingbolt fault (Figure 25), though any evidence of slip sense has been erased by more recent deformation.

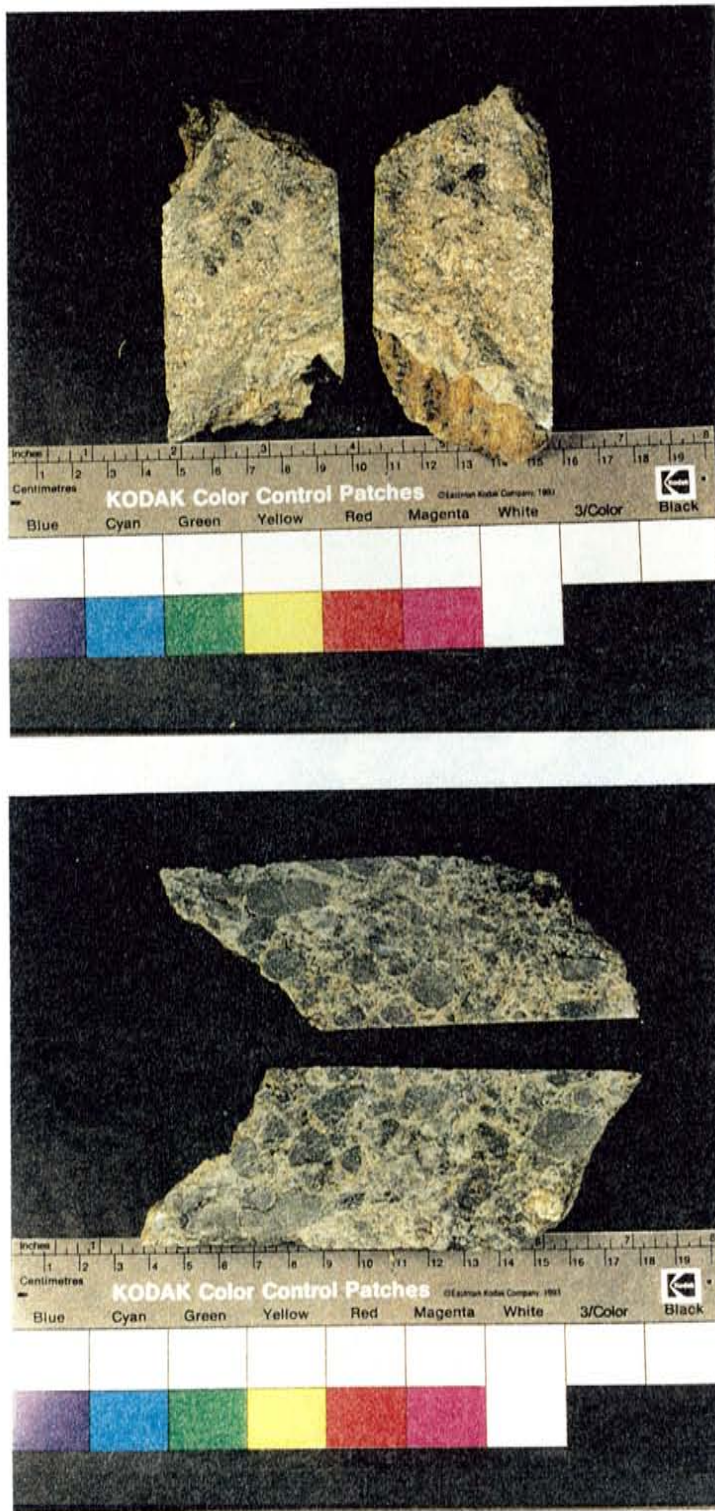


Figure 31. Slabs from Kingbolt fault showing clasts of monzonite porphyry, clasts of Precambrian granite, and clasts of veins. The clasts range in size from <1mm to >2 cm. The matrix includes stringers of pyrite-chalcopyrite \pm chalcocite veins and monzonite porphyry.

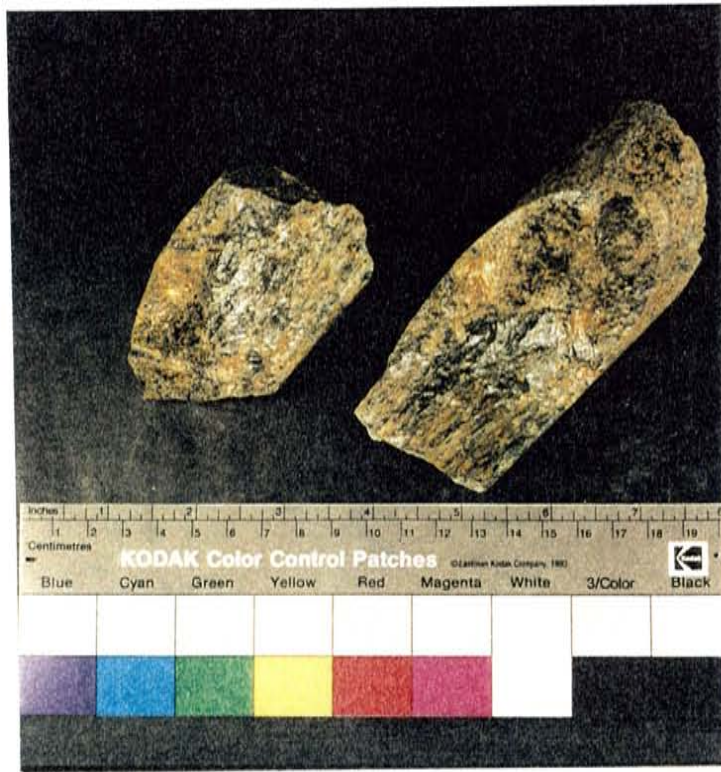


Figure 32. Striated quartz-molybdenite and pyrite-chalcopyrite \pm chalcocite veins typical of striated surfaces along the Kingbolt fault.

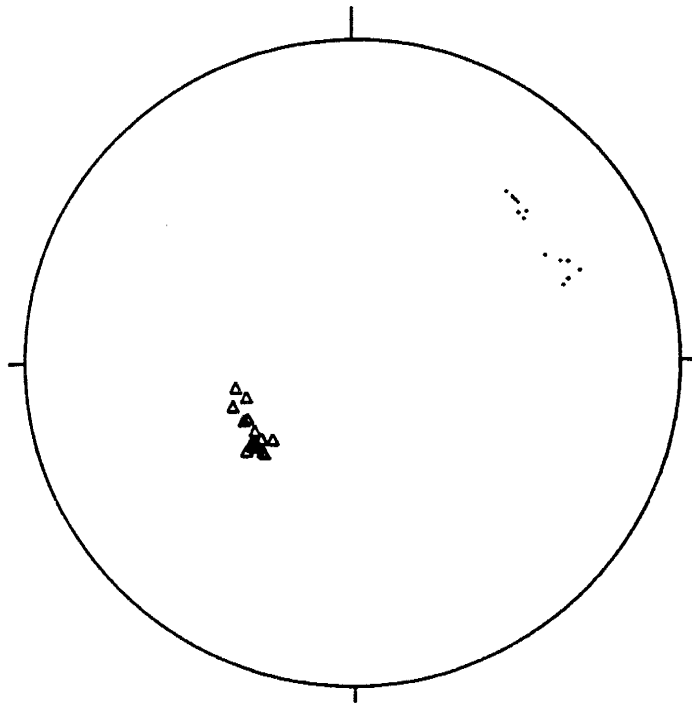


Figure 33. Lower hemisphere, equal-area plot. Poles to the Kingbolt fault are indicated by points (n=15). Dip-slip slickenside striae are indicated by triangles (n=10).

Reactivation in a normal sense along the Kingbolt fault is also favorable when viewed in the context of regional tectonism. Further, a component of normal movement along other NW-striking faults in the district has been documented (see following sections).

Northwest-Striking Faults

The district is bounded on the southwest by the Eagle Creek fault (Figure 14), which can be traced for more than 8 km, striking 305° . All of the Precambrian through early Tertiary rocks of the district are truncated along its trace. The fault disappears into Gila Group sedimentary deposits at its southeastern limit and terminates into a 1-km splay that trends approximately 330° at its northwestern limit. The trace of the fault is marked by a zone in which Cretaceous sediments and Laramide dikes, present to the northeast, are juxtaposed against middle Tertiary volcanic rocks and conglomerates on the southwest. In several isolated exposures, the fault plane dips 65° toward the southwest and deformation is characterized by a zone nearly 7 m wide in which the rocks are highly fractured and weakly brecciated. A 31 m zone of fracturing and brecciation marks the fault zone where it splays near its northwestern termination. This breccia is composed of angular to sub-angular clasts of immature feldspathic sandstone ranging from 15 cm to sub-cm in size (Figure 34). The matrix is composed of fragments similar in composition to the sediment fragments. Very fine, angular, sometimes elongate quartz clasts, mixed with coarser rounded to subrounded quartz clasts also characterize the breccia matrix.

A drill hole (SW-1), located in the hanging wall side of the Eagle Creek fault, provides



Figure 34. Slab of brecciated zone exposed along the splay of the Eagle Creek fault. Clasts are of immature, feldspathic sandstone; matrix is composed of fragments similar to the clasts.

important geological information (Plate 3, cross-section B-B'). The hole was drilled to a total depth of 1,397 meters. An average of 1,160 meters of conglomerates and volcanic were intercepted below which the Cretaceous Pinkard Formation was encountered. The formation includes weakly altered and poorly mineralized sandstones, shales and coal seams. A relatively thick diorite porphyry sill was encountered at a depth of 1,230 m. The hole was terminated in Cretaceous sediments at 1,397 m. The projected depth of the top of the Paleozoic section is approximately 1,646 m. At least 1,160 m of vertical separation along the Eagle Creek fault is thereby indicated.

A second drill hole, located southwest of the 330° striking splay of the Eagle Creek fault, was drilled to a depth of 860 m. The Cretaceous Pinkard Formation was encountered at 460 m, beneath basalts and basalt agglomerates. Drilling continued through the Cretaceous and Paleozoic strata into the Precambrian granodiorite. This relationship indicates a vertical separation of about 610 m near the northwestern termination of the Eagle Creek fault.

Gila Group conglomerate is present along the extreme southeastern portions of the Eagle Creek fault. A reconnaissance examination indicates that these conglomerates typically contain clast-supported units that exhibit poor sorting and bedding. The clasts are angular to sub-rounded and range from pebble to large boulder in size. The conglomerate is moderately to well cemented with clasts primarily of andesitic and basaltic composition. Locally the conglomerate may be interbedded with pyroclastic deposits and andesite flows that make the contact between the conglomerate and the underlying volcanic units difficult to identify. A major drainage in this region located approximately 1,000 meters southwest of the Eagle Creek

fault has exhumed units that are primarily volcanic rocks (Plate 2). A traverse along this drainage indicates that the terrain to the north becomes dominated by volcanic units that are similar to those described along the northwestern portion of the Eagle Creek fault. Within 2,450 m of the trace of the Eagle Creek fault, high mountains of andesitic volcanic flows are present that dip gently toward the northeast.

Some movement may have occurred along the Eagle Creek fault after deposition of the conglomerate and volcanic units. Close to the fault contact, these units are often fractured and exhibit varying dips. This is most evident along the northwestern portion of the fault where beds of the basalt agglomerates that are near the fault contact dip nearly 45° to the northwest.

Northeast of the Eagle Creek fault, the Cretaceous sediments and diorite porphyry constitute the predominant rock types. The sedimentary rocks generally strike NW and dip fairly uniformly averaging $20\text{-}25^{\circ}$ toward the WSW. Several faults oriented subparallel to the Eagle Creek fault strike 300° and dip approximately $65^{\circ}\text{-}75^{\circ}$ toward the SW (Figure 14). These faults have strike lengths of less than 2 km and juxtapose the Cretaceous Pinkard formation against the Ordovician Longfellow limestone, with an average of 175 m of stratigraphic separation (Plate 2).

The Apache fault (Figure 14), strikes 300° and can be traced along strike for approximately 5 km, to a point where it is cut by the San Francisco fault. It has an average dip of 70° NE. The trace of the fault is marked by a 15 to 30 m wide zone of brecciation that is cemented with clay in some areas and by quartz in other areas. A dip-separation of approximately 240 m is evident along the fault's southern exposures where Cretaceous shales

on the east are juxtaposed against Ordovician limestone on the west (Plate 2). Eocene monzonite porphyry dikes and associated veins are truncated by the Apache fault (Figures 35 & 36). Surface exposures of this contact show porphyry in the hanging wall and quartzite in the footwall of the Apache fault. The fault continues northwest where it juxtaposes Ordovician limestone against Cambrian quartzite. Here a dip separation of approximately 90 m is evident from this offset. Where the fault splays at its northwestern termination, faulting with minor dip-slip displacement toward the NE is evident.

The Copper Mountain fault (Figure 14), extends through the district for nearly 5 km. The fault can be traced from approximately its intersection with the Producer fault, southeast through the monzonite porphyry stock and Paleozoic sedimentary rocks to a point where it is terminated by the San Francisco fault. The Copper Mountain fault strikes approximately 300° where it cuts the Paleozoic formations, but changes to a 330° strike where it enters the monzonite porphyry. The fault dips $60-65^{\circ}$ toward the ENE. The rocks are brecciated near the fault and often there are two or three parallel slip planes within a few feet (Figure 37). The fault is defined by a zone of deformation, including a 5-10 m wide zone of brecciation (10-20 % fault gouge and 80-90 % rock fragments) and a 0.5-1.5 m wide zone of fault gouge (70-80 % fine matrix and 20-30 % rock fragments) (Figure 38). The brecciated zone is moderately cemented with clay and/or quartz where it cuts the Paleozoic sediments. Approximately 62 to 78 m of vertical down-to-the NE separation is evidenced where the fault cuts the Paleozoic section. The sediments along the footwall side of the fault dip gently to the southwest an average of 15° .



Figure 35. View looking south along the plane of the Apache fault. Highly argillized monzonite porphyry dike (left side of photos) is cut off by the fault.

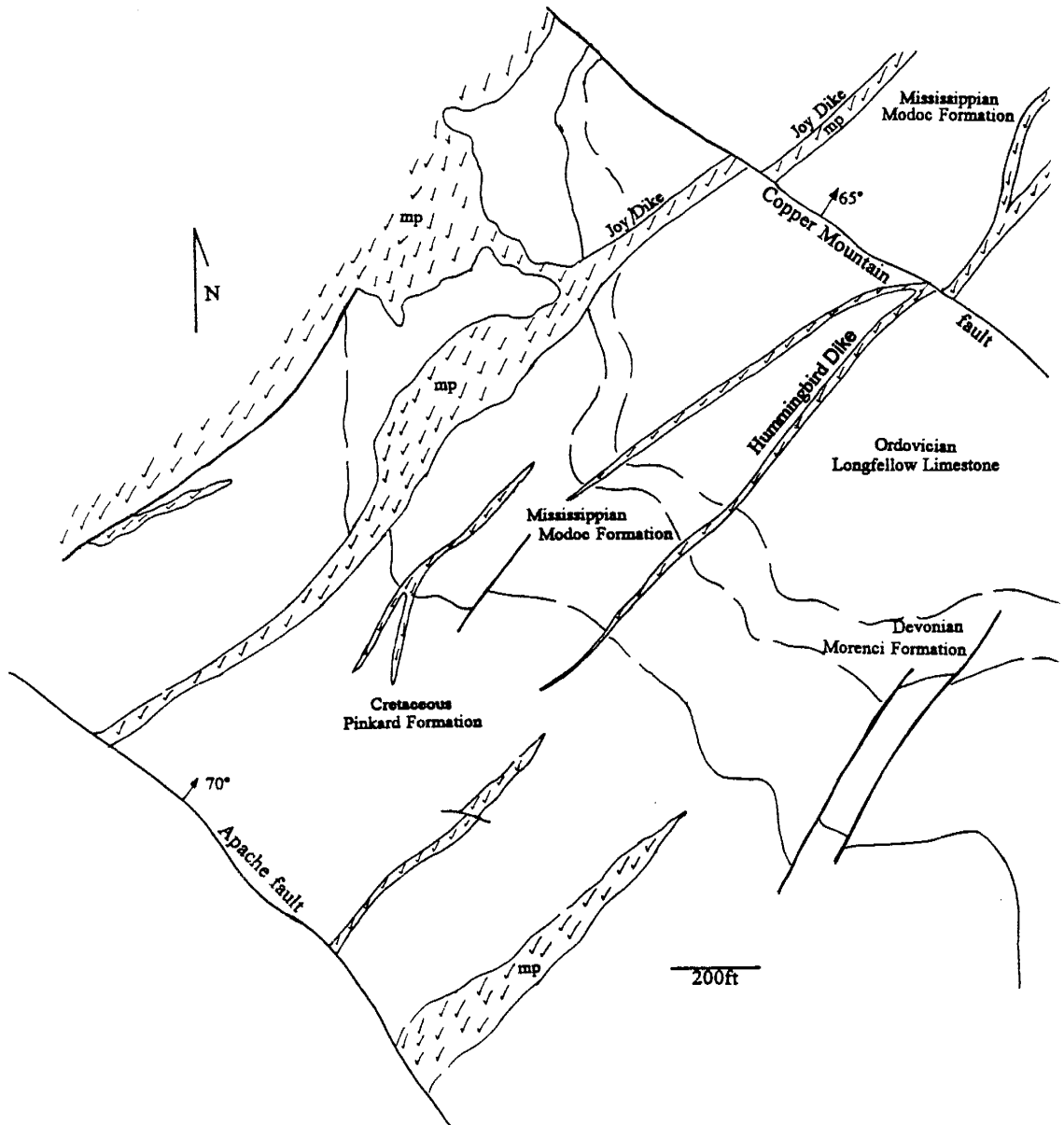


Figure 36. Simplified geology map showing the Copper Mountain fault and the Apache fault near the southern edge of the Morenci open-pit. Faults are shown by bold lines, contacts are shown by light or dashed lines, monzonite porphyry dikes (mp) indicated by check marks, arrows are in the direction of dip with the dip angle indicated by numbers. From recent mapping by author and unpublished maps obtained from Phelps Dodge Morenci, Inc.



Figure 37. Two parallel slip-planes along the trace of the Copper Mountain fault.



Figure 38. Breccia zone along the Copper Mountain fault. Clasts of mineralized and hydrothermally altered Paleozoic sedimentary rocks and monzonite porphyry in a moderately cemented matrix of clay.

There is ample evidence to bracket the timing and character of movement on the Copper Mountain fault. Major sulfide-bearing fissure veins accompany dikes that cut the sedimentary formations to the southeast of the monzonite porphyry stock. Many of these veins were exploited by early underground mining in the district and old records from some of these operations describe the Copper Mountain fault with regards to its control on the porphyry dikes and related lode deposits of the veins. The following descriptions were derived from these historic records: the Joy mine, the Detroit mine and the Humbolt mine: Arizona Copper Company (1882-1921); the Manganese Blue mine and the Arizona Central mine: Detroit Copper Company (early 1870's-1921), and Lindgren (1905). Zones of brecciated porphyry and sedimentary rocks that include fragments of chalcocite ore from the main lode veins mark the Copper Mountain fault in many of these underground workings. Large, steeply dipping monzonite porphyry dikes and associated fissure veins were cut and offset by the Copper Mountain fault (Figure 36). The Joy dike and the Hummingbird dike display approximately 70 m of vertical separation. The Arizona Central vein followed the near vertical southeast contact of another large NE-striking dike with Paleozoic formations. This contact was characterized as a fault-vein and could be traced continuously for a distance of 430 m where it was cut off by the Copper Mountain fault. The sediment-porphry contact could be followed across the fault, displaced vertically approximately 60 m and horizontally 22 m toward the southeast. This evidence indicates that movement along the Copper Mountain fault occurred later than the development of the dikes and the primary bodies of sulfide ore and that a small component of dextral movement may have accompanied normal displacement.

In the western portion of the Morenci open-pit, drilling and mining have shown that the Copper Mountain fault exerted an important control on the distribution of the supergene enrichment blanket (Preece, 1983). The blanket on the footwall side of the fault is characterized by partial to almost complete destruction, has an average thickness of only 30 to 46 m and underlies a leached capping zone 120 to 155 m thick. Pods of residual, highly-enriched sulfides occur locally within the leached capping zone. The deeper zone of enrichment is a result of post-faulting enrichment after destruction of the original blanket (Preece, 1983). In contrast, the leached zone on the hanging-wall side of the fault is 61 to 150 m thick and reflects only a limited response to the original topography. The highly-enriched chalcocite blanket occurs below the leached zone and is 98 to 197 m thick, dipping gently toward Chase Creek. This evidence suggests that a well developed supergene blanket was present in the western portion of the Morenci open-pit prior to movement along the Copper Mountain fault (Preece, 1983). In addition, the high-grade chalcocite blanket of the Morenci open-pit lies in a small graben that formed between the Copper Mountain fault to the west and the Kingbolt fault to the east.

The NW-striking faults in the Morenci district are herein collectively called the Eagle Creek fault system. Documented movement of Laramide age followed by reactivation of the NW-striking Kingbolt fault as a normal fault could suggest that deformation on all of the NW-striking faults may have been initiated during the Laramide orogeny. As discussed earlier, these faults are oriented favorably for reverse to right-lateral transpressional movement during the Laramide orogeny. Constraints on timing of movement along the Eagle Creek, Apache and

Copper Mountain faults, however suggest that movement occurred after Laramide tectonism (latest Cretaceous to early Eocene), subsequent to the first generation of erosion and enrichment (approximately 56-35 Ma) and closely following the deposition of the middle Tertiary volcanic units in this region (32-28 Ma). Although pure dip-slip movement cannot be documented for all faults within this system, a component of post-Laramide normal movement can be documented along all of the NW-striking faults. Further, the Eagle Creek fault accommodated a large magnitude of apparent down-dip displacement (Plate 3, cross section B-B'). Using slickenside evidence for dip-slip motion on the Kingbolt fault, the general orientation of extension on the Eagle Creek fault system was probably ENE-WSW. This extension direction is consistent with previously discussed extension throughout the southern Basin and Range province beginning around early Oligocene time.

The large, range-bounding, high-angle faulting associated with Basin and Range extension is not typical of the Eagle Creek fault system. The typical horst and graben or half-graben structural pattern commonly associated with normal faulting is not well developed, and antithetic sets of faults are absent along this trend (Plate 3, Cross section B to B'). Rather, the Eagle Creek system appears as a series of moderate to high-angle conjugate faults that dip, toward the SW and NE. The uniform southwest dip of the Laramide and older rocks in this district, despite multiple episodes of deformation, may suggest large-scale fault-block rotation. As previously discussed, the distinguishing features of middle Miocene extension in southern Arizona are block-tilting and attendant displacement on planar and listric normal faults. Regional tilt-block domains are known or inferred to be representative of extension above

detachment faults that dip regionally in one direction (Davis & Hardy, 1981; Spencer & Reynolds, 1989). Extension along the Eagle Creek fault system may be kinematically related to the low-angle detachment fault that is documented in the Pinaleno-Santa Teresa Mountains, southwest of the Morenci district (Figure 12). Spencer and Reynolds (1989) hypothesize that the Pinaleno-Santa Teresa Mountains detachment fault dips under the Gila Valley and use southwest dipping Paleozoic strata that crop out northwest of the Morenci mining district to support the hypothesis. They draw a line of section from the detachment surface exposed in the Pinaleno-Santa Teresa Mountains, 040° toward the southwest-dipping Paleozoic sediments. The cross-section on Figure 12 is modified from this interpretation by drawing a line of section 050° , or parallel to the mylonitic lineations, toward the uniformly southwest dipping Paleozoic and Cretaceous strata in this portion of the Morenci mining district. The relationship shown in this figure would suggest that extension documented along the NW-striking Eagle Creek fault system could have been associated with low-angle normal faulting that was active from the latest Oligocene through early Miocene.

The Garfield fault zone is included in this section, however, it is not interpreted as part of the Eagle Creek system. The fault zone strikes $285-295^{\circ}$, dips $55^{\circ}-60^{\circ}$ NNE and comprises a series of fault strands that cut through the Paleozoic section as well as the Laramide intrusives (Plate 1 & Figure 14). At the extreme northwestern end, the fault places Paleozoic sedimentary rocks next to middle Tertiary volcanic rocks, but as the fault zone is traversed toward the southeast, Paleozoic sedimentary rocks and Laramide porphyry dikes outcrop on both sides of the zone. The fault zone truncates NE-striking Laramide-age faults that are

present along the footwall side. Field relationships suggest that movement along the Garfield fault occurred post-Laramide time. However, the nature of the movement cannot be constrained.

Northeast-Striking Faults

As previously discussed, there are numerous NE-striking faults that are thought to have formed during the Laramide orogeny (Richard Preece, pers. comm., 1995). However, younger faulting occurred along the NE-striking San Francisco fault (Figure 14). This steeply dipping (averaging 70°) fault bounds the southeastern portion of the district and juxtaposes Gila Group conglomerate against Precambrian granite and granodiorite. The fault can be traced for approximately 10 km along an average strike of 210 - 220° to a point where the strike direction abruptly changes to 190 - 195° . From here, the fault can be traced southward another 4 km until it disappears into the conglomerate-filled valley that extends south of the district. The fault can be seen to cut all other faults that are present toward the north-northwest (Plate 1). Surface geology and drill hole data indicate that the San Francisco fault system is the structural boundary of a half-graben. The simple half-graben geometry is illustrated in Plate 3, cross section A to A'. The San Francisco fault is the major bounding fault of the half-graben. The middle Tertiary volcanic rocks and the underlying Paleozoic strata dip homoclinally west at 20 - 30° (Figure 39). Several drill-hole intercepts near the fault zone indicate apparent dip-slip separation in excess of 915 m. No sense-of-slip indicators are evident along the trace of the fault.



Figure 39. Aerial view looking NNW toward the half-graben formed by the San Francisco fault. Precambrian granite is exposed in the mountains along the footwall side of the fault. Gila Group conglomerates fill the valley that is occupied by the San Francisco river in the center of the photo. Beds of gently dipping middle Tertiary volcanic rocks crop out in the foreground.

The basin into which the Gila Group conglomerates were deposited parallels the strike of the San Francisco fault. The syntectonic basin sediments (Frostick & Reid, 1987; Leeder & Gawthorpe, 1987; Mack & Seager, 1990; Leeder & Jackson, 1993) reach thicknesses of greater than 460 m and consist almost exclusively of weakly stratified coarse subangular gravels. Within this basin, two facies of the Gila Group conglomerate have been identified (Preece & Menzer, 1982). The two facies are readily distinguished both in color aerial photographs and on the ground. The Chase Creek facies occurs in the southwestern portion of the basin, is reddish-brown in color and is composed primarily of intrusive and altered sedimentary rock fragments from the Morenci mining district. The San Francisco facies occurs in the northeastern portion of the basin, is grey-brown in color and is primarily composed of middle Tertiary volcanic rock fragments (Preece & Menzer, 1982). The conglomerates rest unconformably on middle Tertiary volcanic and volcanoclastic rocks that are thought to be derived from the Mogollon-Datil volcanic field (Wahl, 1980; Ratte & others, 1984; McIntosh & others, 1991). This relationship constrains the age of deposition to post-28 Ma (Table 3). Further, the Gila Group is interbedded with basaltic flows with ages ranging from 20-18 Ma (Wahl, 1980). Syntectonic basin filling probably occurred episodically until Quaternary stream erosion began to exhume the basin.

The half-graben asymmetry controlled by displacement along the San Francisco fault is similar to that of many extensional basins: an abruptly faulted, high-relief margin on one side, contrasted with a hinged opposing margin with proportionally lower relief (Mohr, 1982; Burke, 1980; Rosendhal, 1987). Although pure dip-slip normal movement cannot be

documented along the San Francisco fault it is clear that a component of normal movement accommodated extension along this fault. The style of extension along the San Francisco fault conforms with regional extensional styles documented in the southern Basin and Range province and the Rio Grande rift province. However, the strike direction is nearly perpendicular to regional north-northwest trends observed in the southern Basin and Range. In addition the timing of movement (post-28 Ma) suggests that extension along the San Francisco fault is more appropriately explained in the context of the previously discussed northeast-trending structural corridor of the Morenci-Reserve fault zone (Ratte, 1989) and/or the Morenci lineament (Mayo, 1958; Chapin & others, 1978).

The half-graben formed by the NE-striking San Francisco fault in the Morenci mining district lies approximately 30 km south-southwest of the Alma Basin (Figure 13). South and southwestward of the Morenci district, the common northwesterly trends of the southern Basin and Range province become the dominant structural feature. The northwest trending Duncan valley is bounded, on the northwest, similarly to the Mangas valley, by the NE-striking San Francisco fault system (Figure 13). Correlating the most recent episode of faulting recorded in the Morenci district with extension and faulting associated with the basins that lie between the Colorado Plateau and the Mogollon Plateau aids in constraining the timing and nature of deformation along the San Francisco fault. Evidence from this district combined with evidence from other basins along the Morenci-Reserve fault zone suggest that extension began in the late Oligocene or early Miocene, 28 to 23 Ma and probably continued episodically until the late Miocene (Ratte, 1989; Crews, 1994; Houser, 1994). Further, extension along this NE-

trending structural corridor has been kinematically related to Neogene structural adjustments along the southeastern edge of the Colorado Plateau (Chapin & Cather, 1994; Chamberlin & Cather, 1994; Crews, 1994; Houser, 1994). As discussed earlier, Chamberlin & Cather (1994) and Houser (1994) suggest that the northwest-trending extensional structures of the Arizona Transition zone appear to give way to the northeast-trending structures of the San Agustin arm of the Rio Grande rift near Alma, New Mexico. The previous correlations suggest that the northwest-trending extensional structures in this region may, however, give way to the northeast-striking structures near the Morenci mining district. Further, it is postulated that the distinct northeast strike of the Morenci-Reserve structural zone may reflect reactivation of an older, perhaps Laramide-age, fault system.

North-Striking Faults

The Chase Creek fault bounds the east side of Coronado Mountain and can be traced due north along strike for nearly 8 km (Figure 14) to a point where it turns and strikes 060° (Plate 2). The fault appears to terminate to the south within the Older Granite Porphyry stock and cannot be traced through or south of the Candelaria breccia (Figure 40). For most of its strike length, the Chase Creek fault is marked by the contact between middle Tertiary volcanic rocks on the east and Precambrian granite to the west. The volcanic units east of the fault dip gently, approximately $10-15^{\circ}$ toward the west-northwest, into the fault (Figures 41 & 42). South of the Garfield fault, the fault is marked by the contact between Precambrian granite to the west and Paleozoic sedimentary rocks to the east (Figure 40). The fault plane can be

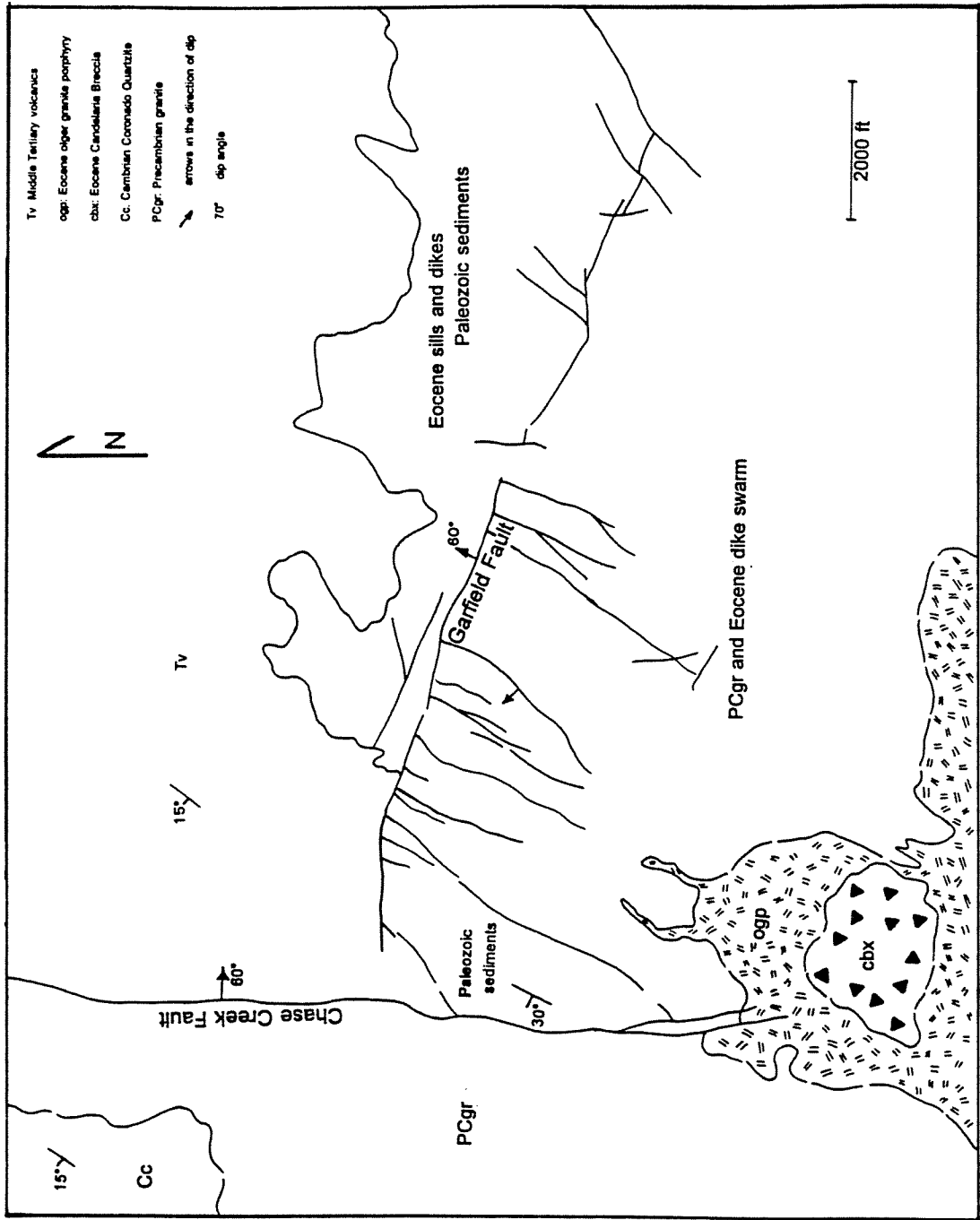


Figure 40. The Chase Creek fault, Garfield fault, and the surrounding geological relationships

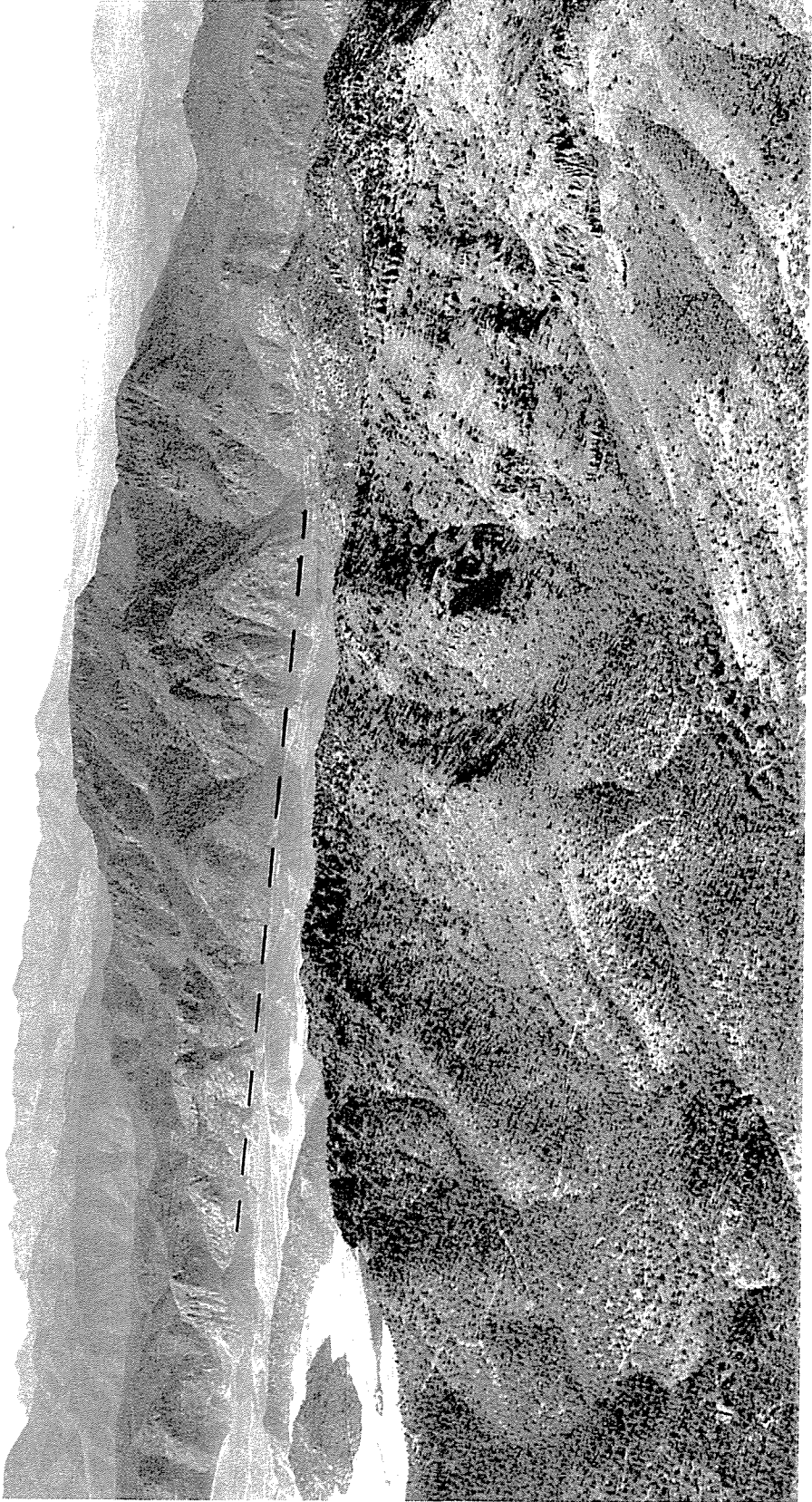


Figure 41. Aerial view looking west. Middle Tertiary volcanics in the foreground. Cambrian Coronado Quartzite capping Coronado Mountain forms the distinctive ridge, top center. Precambrian granite crops out west of the Chase Creek fault. The fault strikes north in the center of the photo. Trace of the fault indicated by dashed line. The Northwest Extension open-pit mine is visible in the left center of the photo.



Figure 42. View looking north from the southern boundary of the Morenci open-pit. The middle Tertiary volcanic rocks, located east and on the horizon, dip $10-15^{\circ}$ WNW into the Chase Creek fault. The fault is obscured by dumps in the left-center of the photo.

observed in only a few areas. At these locations, the fault dips 50-60° toward the east and the plane of the fault is a smooth and polished surface with slickenside striae that are clearly parallel to the dip direction (Figure 43). Deformation along the fault zone in these exposures is characterized by a 3-4 m zone of fault gouge surrounded by a zone of brecciation (Figure 44). Several drill holes, located south of the Garfield fault, have penetrated the fault from the hangingwall through to the footwall. The fault zone in these drill holes is a 32 m wide breccia containing clasts of Precambrian granite and Paleozoic sediments in a matrix of clay which is commonly heavily stained with iron oxides. Directly south of the Garfield fault, preliminary investigations suggest that there is no mineralization in the footwall side of the fault, however, these relationships are not clear in drill hole intercepts to the south. It appears that the fault terminates into several splays as it enters the Older Granite Porphyry stock with mineralization occurring both on the hanging wall and footwall sides of these splays. The magnitude of displacement cannot be determined with certainty, however, a stratigraphic offset of nearly 310 m can be determined from the elevation of the base of the Cambrian quartzite on either side of the fault (Figure 40).

Several north-south striking faults are also located near the center of the district. The Las Terrazas fault (Figure 14) strikes 350-010°, dips approximately 60° toward the east, and is defined by a narrow, matrix-supported breccia to clay gouge zone. Clasts of Older Granite Porphyry and Precambrian granite within the breccia are typically angular to sub-rounded and range from sub-centimeter to greater than 10 cm in size. The matrix is locally composed of copper oxide minerals such as chrysocolla, malachite and azurite (Figure 45). Commonly, very

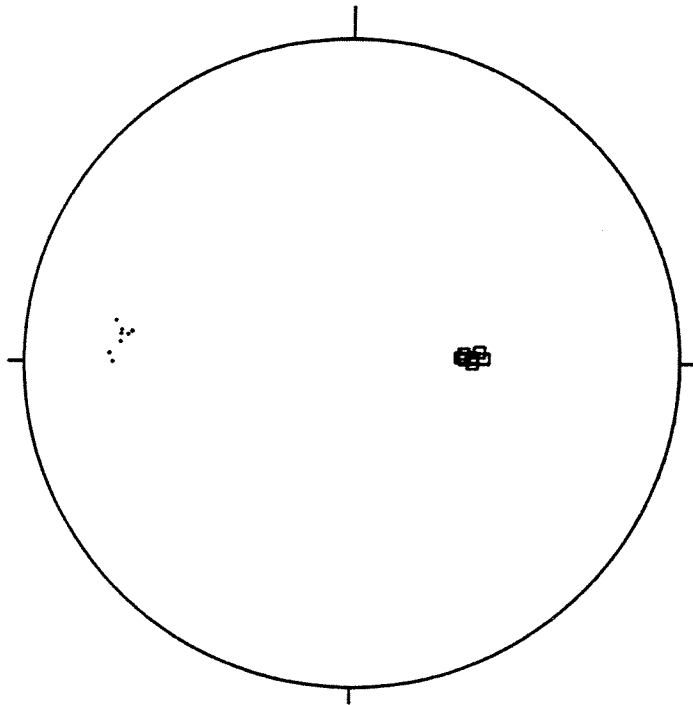


Figure 43. Lower hemisphere, equal-area plot. Poles to the Chase Creek fault are indicated by points ($n=8$). Dip-slip slickenside striae are indicated by squares ($n=8$).

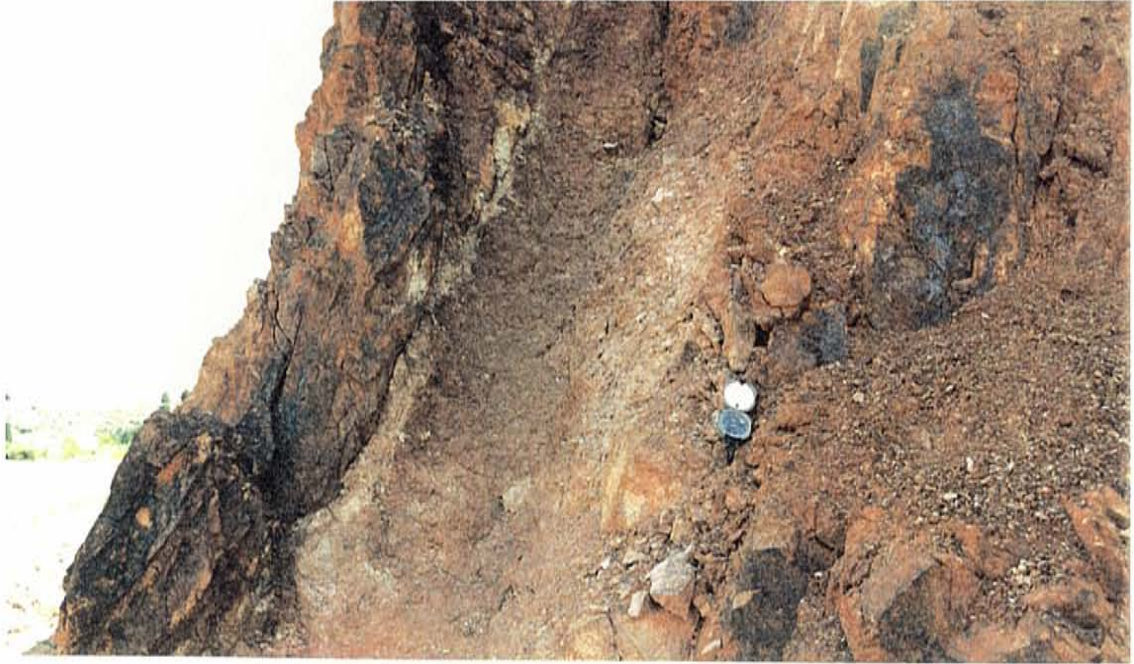


Figure 44. Gouge and breccia zones of the Chase Creek fault.

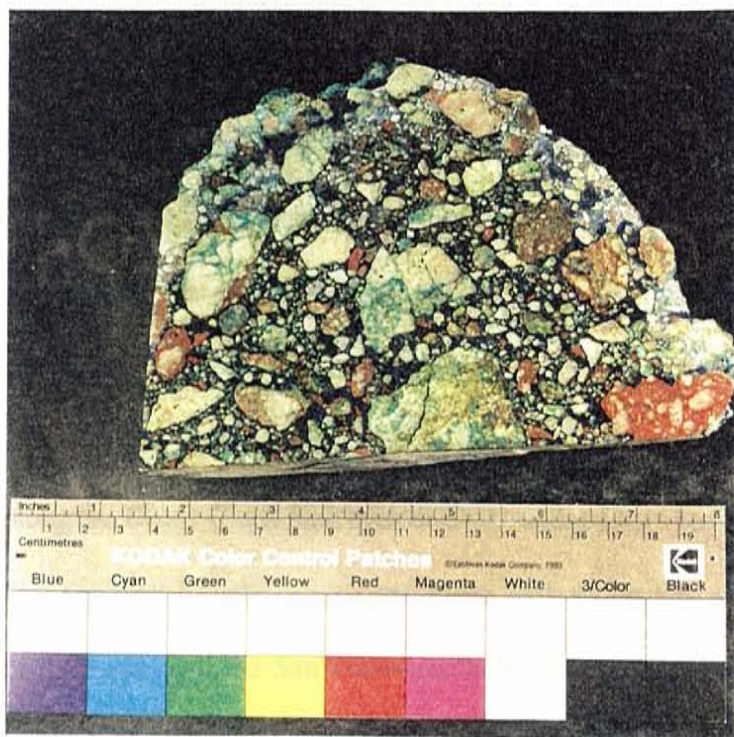


Figure 45. Slabs of the matrix-supported breccia zone of the Las Terrazas fault. The matrix is predominantly azurite, malachite and chrysocolla. Very fine, sharp edged azurite crystals line vugs within the matrix. Note breccia clasts in the breccia, which indicates multiple episodes of brecciation.

fine, sharp edged azurite crystals, pseudomorphs after malachite line vugs within gouge zones. Delicate crystals such as these must have developed after fault movement. Timing constraints previously suggested for the second generation supergene cycle would indicate that faulting occurred before approximately 10 Ma. The War Eagle fault (not shown) is another north-striking fault, located in the Metcalf open-pit. This fault also exhibits similar timing relationships in that the breccia zone is locally cemented with alunite that is presumed to be nearly the same age as alunite collected and dated in the vicinity of the fault (Table 2).

Timing relationships can be constrained along the faults that strike north, herein collectively called the Chase Creek fault system. The Chase Creek fault places Precambrian granite adjacent to middle Tertiary volcanic rocks. This clearly indicates that normal faulting occurred subsequent to deposition of the volcanic rocks at 32 Ma to 28 Ma (Table 3). Further, evidence which brackets the second generation supergene cycle suggests that movement along several north-striking faults occurred prior to 10 Ma. Therefore, assuming that all N-striking faults are related, these faults were active approximately between 28 Ma and 10 Ma.

Each of the previously described faults and fault systems in the Morenci mining district have been discussed in relation to regional tectonism. It is more difficult to discuss regional correlations for normal faulting along the north-striking Chase Creek fault system. The timing of movement along the Chase Creek fault system is constrained between approximately 28 Ma and 10 Ma. This timing is broadly contemporaneous with movement along the Eagle Creek fault system (post-28 Ma) and the San Francisco fault (post-28 Ma). In addition, extension directions are constrained along the Eagle Creek fault system (ENE-WSW) and although

difficult to constrain along the San Francisco fault the extension direction can be suggested to have been oriented approximately NW-SE. Pure dip-slip movement documented along the Chase Creek fault constrains the direction of extension along this trend to an orientation of east-west. Further, distinct kinematic controls have been suggested for faulting along the Eagle Creek fault system and the San Francisco fault. These correlations suggest that a very complex interaction of extensional tectonism was occurring in the Morenci mining district beginning in late Oligocene time. If extension accommodated along the Eagle Creek fault system and the San Francisco fault occurred broadly coeval, they could accommodate regional E-W extension (Figure 46). This would be consistent with normal faulting on the north-striking Chase Creek fault system. Figure 13 shows the relationship between structures in the transition zone between the Colorado Plateau and the northwest-striking basins of the southern Basin and Range in this area. It is interesting to note the orientation of the Chase Creek fault with regard to the other structural trends that occur north of the Morenci mining district. These relationships suggest that extension along the Chase Creek fault occurred in response to the structural adjustments within the transition zone between the highly extended terrain of the southern Basin and Range and the stable Colorado Plateau.

Summary and Discussion

The complex faulting relationships observed in this district have been described by examining major and minor faults in the Morenci mining district. Fault zone deformation features, crosscutting relationships, relative timing with respect to intrusion and mineralization

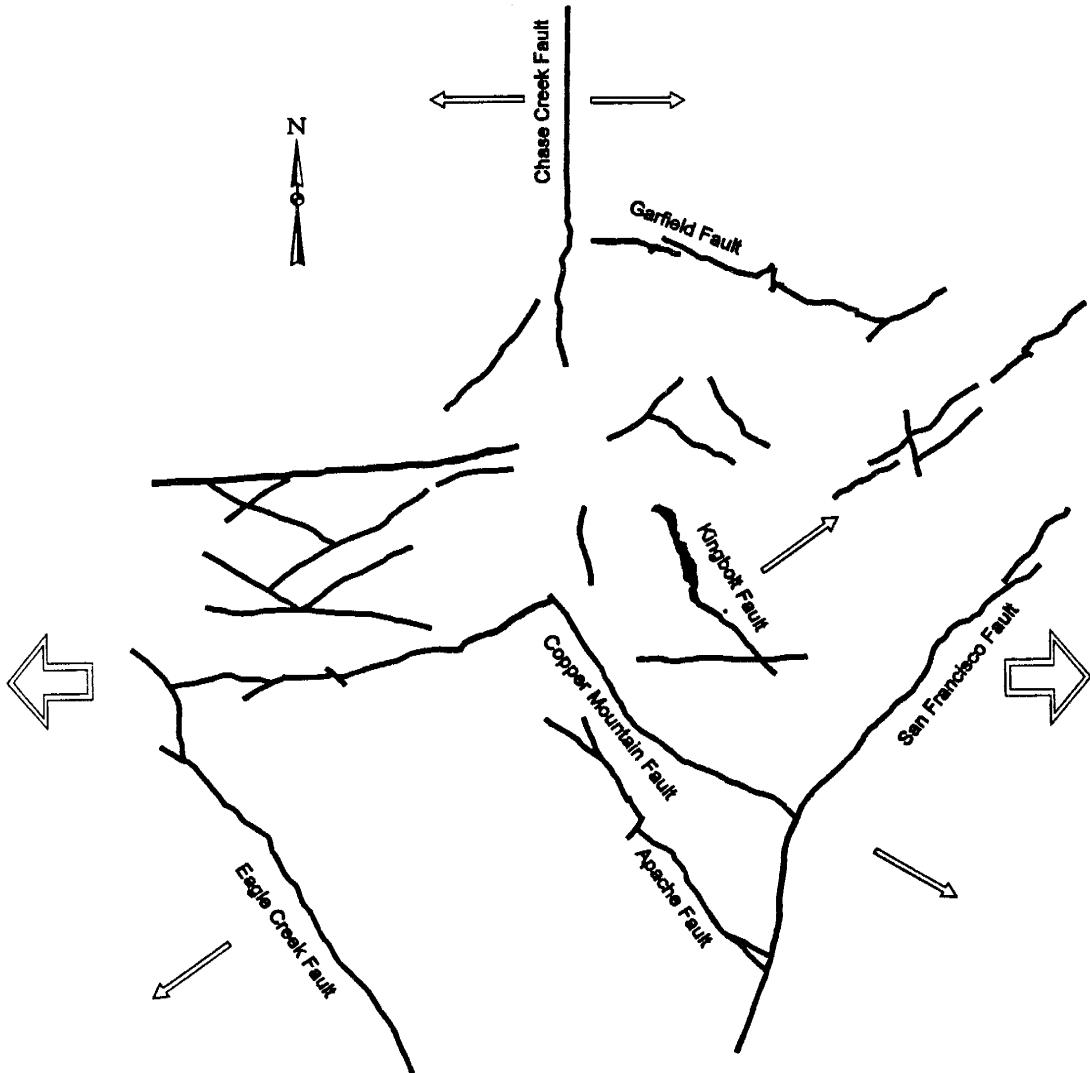


Figure 46. Major faults in the Morenci mining district. Approximate direction of extension for each of the fault systems that record movement beginning around latest Oligocene time is indicated by small arrows. Overall extension accommodated by NE-striking, NW-striking, and N-striking faults is indicated by large arrows.

and constraints on sense of movement were documented. The nature and timing of faulting was evaluated with regard to regional structural trends. Several episodes of faulting are delineated in the previous synthesis. Laramide tectonism is reflected in NE-striking porphyry intrusions, dikes, faults and veins. The east-striking Coronado fault system and the NW-striking Kingbolt fault also contain evidence of Laramide movement. The next episode of faulting in this district probably occurred during the first episode of extensional tectonism which was active throughout the southern Basin and Range beginning in the early Oligocene and may be associated with the Pinaleno metamorphic core complex. This is reflected in the NW-striking Eagle Creek fault system. This was closely followed by or synchronous with movement along the NE-striking San Francisco fault. Normal faulting along the Chase Creek fault is thought to be related to complex structural adjustments within the transition zone between the Colorado Plateau and the highly extended terrain of the southern Basin and Range. East of the Morenci district, extension was dominantly NW-SE. West of the Morenci district, extension was dominantly NE-SW. In the Morenci district, these opposing extensional regimes appear to have been accommodated by E-W extension along fault systems of three different orientations (Figure 46).

As stated earlier, the Paleozoic and Cretaceous strata in the Morenci mining district appeared to have remained undisturbed until the onset of Laramide tectonism. Thus, the previous discussion has focused, locally and regionally, on tectonism and deformation beginning with the Laramide orogeny. The Precambrian history of this region is notably absent. However, a significant portion of the rocks exposed in this district are of Precambrian

origin which suggests that the Precambrian geology of this region should not be ignored.

Three fundamentally different major tectonic assemblages make up the early Proterozoic crust of Arizona (Anderson, 1989). These tectonic assemblages are divided into lithotectonic blocks by northeast- and north-trending shear zones (Karlstrom & Bowering, 1988). The Morenci mining district lies in the Southeast Schist Belt (Figure 47) (Anderson, 1989) or the Pinal block (Karlstrom & Bowering, 1988). The Southeast Schist Belt is a terrain of immature, silicic, micaceous, metasedimentary rocks derived from quartz wacke protoliths; these rocks are known as Pinal Shist (Ransome, 1903) and are lithologically distinct from all other terrains in the Arizona Proterozoic belts (Anderson, 1989). The sediments that make up the Pinal Shist are thought to have been deposited into a large northeast trending interarc basin from approximately 1720 Ma to approximately 1675 Ma (Anderson, 1989, Conway & Silver, 1989). The early Proterozoic period of principal continental growth was followed by widespread intrusion of epizonal, potassium-rich granites into the upper crust (Anderson, 1989). The most profound period of igneous activity was from 1.41 to 1.49 Ga with over 60 complexes forming a NE-striking transcontinental belt over 1,000 km wide (Figure 48) (Anderson, 1983). The Precambrian granite and granodiotite that is exposed throughout the Morenci mining district is correlated with the 1.41 to 1.49 Ga granites that occur within this transcontinental belt (Preece & Menzer, 1992). The Proterozoic structural trends within and immediately adjacent to the Morenci mining district have not been thoroughly examined and thus, are not well constrained.

The idea that regional structures control the location of porphyry copper districts began

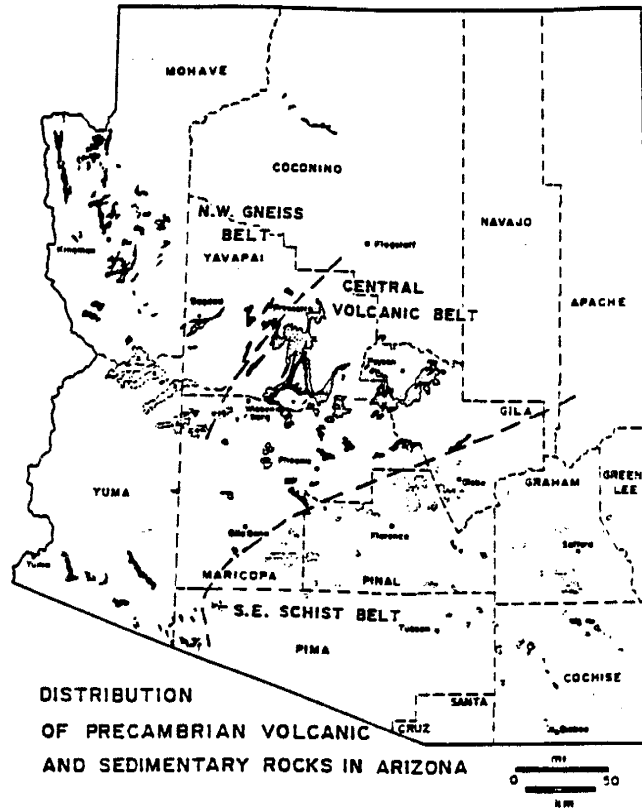


Figure 47. Distribution of Precambrian volcanic and sedimentary rocks in Arizona in relation to the three major lithologic belts - Northwest Gneiss Belt, Central Volcanic Belt, and Southeast Schist Belt- that make up the Proterozoic crust. Rocks of dominantly sedimentary origin are shown in black, rocks of volcanic origin are stippled, rocks of mainly volcanosedimentary origin in the Southeast Schist Belt are shown in dotted outlines, the Mazatzal Group is vertically ruled, and terranes remobilized by younger events are denoted "R". From P. Anderson, 1989.

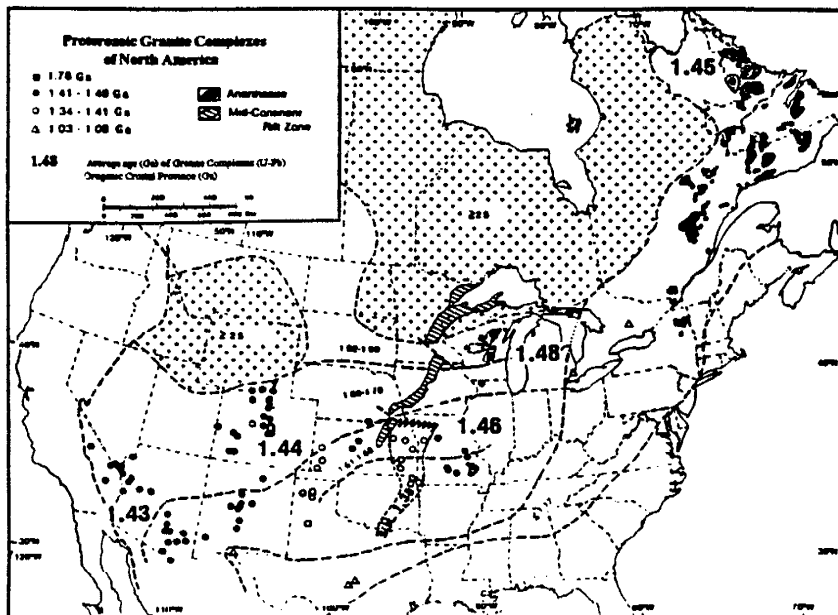


Figure 48. Distribution of Proterozoic granite complexes of North America. Modified from J. L. Anderson, 1989.

with early workers such as Billingsley and Locke (1935, 1941), Mayo (1958) and Schmitt (1966). A recurring topic of several decades of geological studies into the structural setting of porphyry copper deposits is the concept of lineament control of ore districts. The basic premise has been that many ore districts may be localized at the intersection of major regional structures or lineaments that are associated with major tectonic belts. Two major regional trends commonly discussed in the literature surrounding structural interpretations of southwestern North America are northwest-oriented structural trends (e.g., Dickinson, 1981; Titley, 1976; Davis, 1979; Dickinson & others, 1989) and northeast-oriented structural trends (e.g., Aldrich & Laughlin, 1984; Chapin & others, 1978; Karlstrom & Bowring, 1988; Anderson, 1989).

The most obvious regional northwest-striking structural zone in the vicinity of the Morenci mining district is the southern edge of the Colorado Plateau. Although the structural evolution of this zone is inherently complicated, it appears that in a regional context, northwest-striking structural trends have been predominant in this portion of Arizona since the middle to late Mesozoic (e.g., Dickinson, 1981, 1989). A northeast-trending regional lineament that may have influenced the structural character of the Morenci porphyry copper deposit has been considered by Chapin & others (1978) and Chapin and Cather (1994). As previously discussed, Chapin and Cather (1994) describe the Socorro accommodation zone as one of several complex structural zones that developed where the Rio Grande rift broke across NE-trending lineaments of probable Precambrian ancestry. These accommodation zones were oriented approximately parallel to small circles of rotation between the Colorado Plateau and

the stable craton during Miocene extension. Chapin and Cather (1994) locate the Euler pole of Miocene rotation of the Colorado Plateau relative to the stable craton in northeastern Utah and estimate 1.0 to 1.5° of clockwise rotation of the Colorado Plateau from late Oligocene to at least late Miocene (Figure 49). This small amount of rotation could have provided the space needed to accommodate the moderate to strong crustal extension documented along the San Francisco fault and the Morenci-Reserve fault zone.

Northeast and northwest-oriented structural trends are conspicuously prevalent in the Morenci mining district. Further, the northeast-striking and the northwest-striking structures in this district were active during Laramide deformation. It is tempting to speculate that, with further study, these local relationships considered in context with regional structural associations may be interpreted as evidence that the Morenci mining district is localized at the intersection of two major long-lived regional structural trends.

CONCLUSION

The Morenci mining district has been affected by several regional deformational events since late Cretaceous time. Evidence that mountain building occurred in this region during the Laramide orogeny is recorded in Eocene basins that lie to the north of this district. During the second stage of the Laramide orogeny, regional tectonism exerted a strong control on the distribution of the late Paleocene to Eocene hypabyssal intrusives that crop out in this district for nearly 13 km in an arcuate NE-NNE trend. The Eocene dikes, faults, veins, and elongate stocks are the most obvious indicators of extension during this time period. Strong evidence

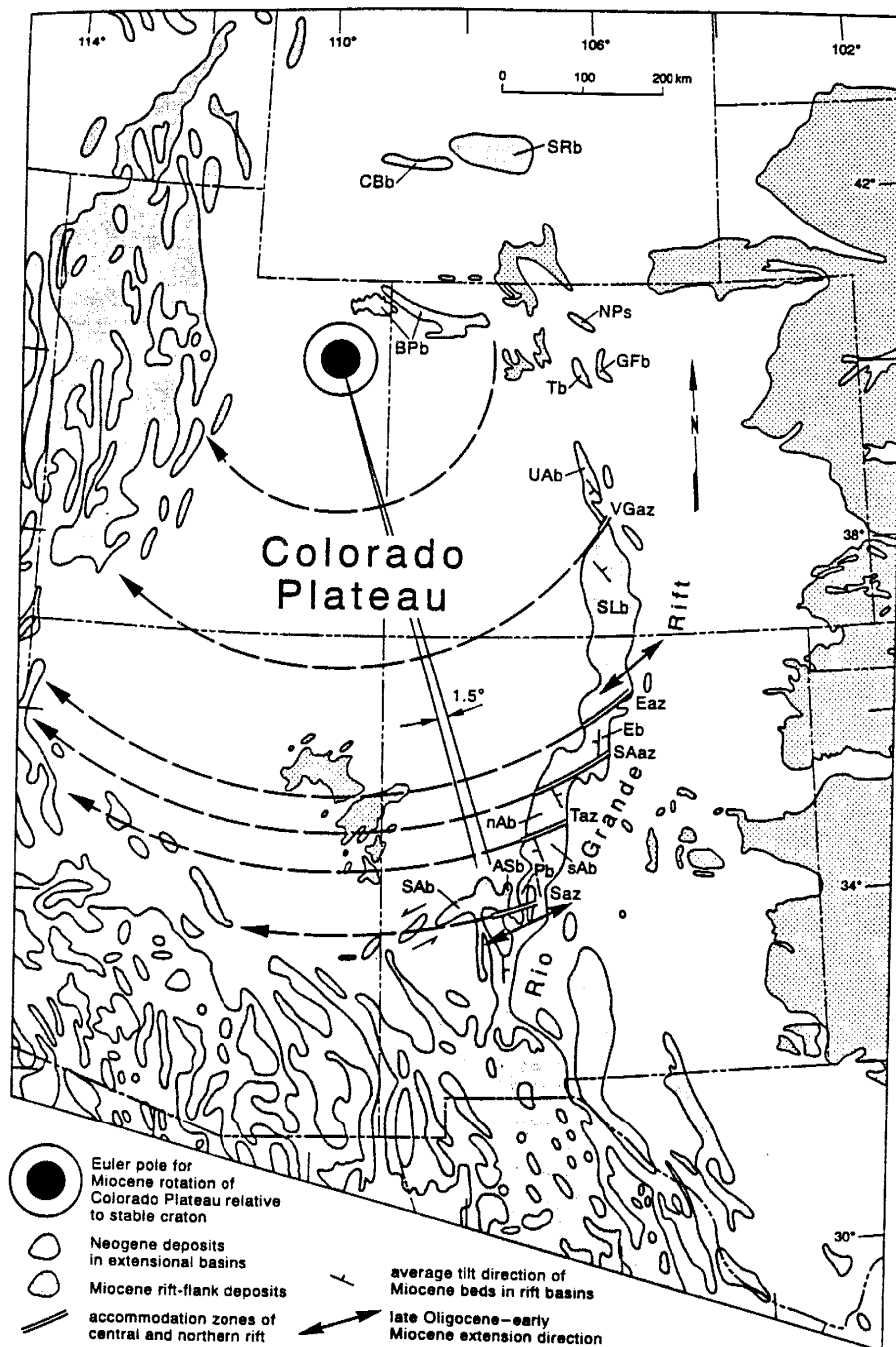


Figure 49. Map showing distribution of Neogene basin-fill and rift-flank deposits and selected structural features. Abbreviations for the basins (from north to south) are CBB, Circle Bar Basin; SRb, Split Rock Basin; BPb, Browns Park Basin; NPs, North Park syncline; Tb, Troublesome Basin; Gfb, Granby-Fraser basin; UAb, Upper Arkansas Basin; SLb, San Luis Basin; Eb, Espanola Basin; nAb, northern Albuquerque Basin; sAb, southern Albuquerque Basin; Pb, Poptosa basin; ASb, Abbe Springs Basin. Abbreviations for accommodation zones are VGaz, Villa Grove; Eaz, Embudo; SAaz, Santa Ana; Taz, Tijeras; Saz, Socorro. From Chapin and Cather, 1994

suggests that NNE-SSW shortening accompanied NNW-SSE extension in this district around 57-55 Ma. The east-striking Laramide Coronado fault system records evidence of left-lateral strike-slip movement. The NW-striking Kingbolt fault also records Laramide-age movement and is oriented favorably for reverse to right-lateral transpressional movement during this time, though the sense of movement during the Laramide orogeny cannot be determined.

A period of quiescence during which erosion beveled the region and the important supergene process began was followed by renewed magmatism and tectonism. Beginning in the late Oligocene, widespread alkalic-calcic volcanism and faulting associated with regional extension dominated the tectonic regime. Subsidence associated with extension began to shape the region and dramatic structural modifications took place. The Colorado Plateau was established as a positive area relative to surrounding regions and the Morenci mining district, located along the southeastern edge of this area accommodated complex structural readjustments. Broadly coeval extension occurred along several different fault systems.

The NW-striking Eagle Creek fault system, located in southwestern portion of the district, accommodated approximately ENE-WSW extension. At least 1,160 m of apparent down-dip displacement occurred along the Eagle Creek fault, which bounds the district to the southwest. Minor extension and accompanying displacement is evidenced along the other NW-striking faults in the district. This extensional regime caused a small graben to form between the Copper Mountain fault and the Kingbolt fault. Within this graben a rich chalcocite enrichment blanket formed, which has supported mining in the Morenci mining district for the past 60 years. Regional tectonism that was active in the southern Basin and Range province

from latest Oligocene through early Miocene is characterized by the formation of metamorphic core complexes. Evidence for this type of deformation lies within 25 km southwest of this district. It is hypothesized that the extension accommodated along the NW-striking faults of Morenci is kinematically related to the Pinaleno metamorphic core complex.

Faulting along the NE-striking San Francisco fault, which bounds the district to the southeast, resulted in the formation of a half-graben southeast of the fault. Middle Tertiary volcanic rocks, Cretaceous through Paleozoic strata and Precambrian basement rocks dip gently into the San Francisco fault. The half-graben is filled with the syntectonic basin deposits of the Gila Group. Extension accommodated along this fault is believed to be related to the northeast-trending structural corridor of the Morenci-Reserve fault zone. The Morenci-Reserve fault zone is part of a series of northeast-trending structural zones that accommodated moderate to strong crustal extension and define the southeastern edge of the Colorado Plateau. The northwest-trending extensional structures of this region of the southern Basin and Range appear to give way to the northeast-trending structures of the San Agustin arm of the Rio Grande rift, which includes the Morenci-Reserve fault zone, near the Morenci mining district. It can be postulated that the distinct northeast strike of this zone may reflect reactivation of an older, perhaps Laramide or older fault zone.

The north-striking Chase Creek fault occurs north of the district. The Chase Creek fault places Precambrian granite against middle Tertiary volcanic rocks and records normal movement that accommodated E-W extension. This extension direction is accounted for by the interaction between ENE-WSW extension to the west, reflected by the Eagle Creek fault

system, and NW-SE extension to the east along the Morenci-Reserve structural corridor. The Chase Creek fault is therefore interpreted to have formed in response to structural adjustments that occurred within the transition zone between the highly extended terrain of the southern Basin and Range and the stable Colorado Plateau.

The late Cenozoic structural character of the Morenci mining district suggests that it is located near the intersection of several major regional structural trends. It is perhaps no coincidence that one of the world's largest copper deposits occurs in such a location.

REFERENCES

- Aldrich, M. J., and Laughlin, A. W., 1984, A model for the tectonic development of the southeastern Colorado Plateau boundary: *Journal of Geophysical Research*, v. 89, p. 10207-10218.
- Aldrich, M. J., Chapin, C. E., and Laughlin, A. W., 1986, Stress history and tectonic development of the Rio Grande rift, New Mexico: *Journal of Geophysical Research*, v.91, no.B6, p.6199-6211.
- Anderson, J. A., 1982, Characteristics of leached capping and techniques of appraisal, *in*, Titley, S.R., ed., *Advances in geology of the porphyry copper deposits, southwestern North America*: Tucson, University of Arizona Press, p.275-296.
- Anderson, J. L., 1983, Proterozoic anorogenic granite plutonism of North America, *in*, Medaris, L.G., Mickelson, D.M., Byers, C.W., Shanks, W.C., eds., *Proterozoic Geology*: Geological Society of America Memoir 161, p.133-154.
- _____, 1989, Proterozoic anorogenic granites of the southwestern United States, *in* Jenny, J.P., and Reynolds, S.R., eds., *Geologic evolution of Arizona*: Tucson, Arizona Geological Society Digest 17, p.211-259.
- Anderson, P., 1989, Proterozoic plate tectonic evolution of Arizona, *in* Jenney, J.P., and Reynolds, S.R., eds., *Geologic evolution of Arizona*: Tucson, Arizona Geological Society Digest 17, p.17-57.
- Anderson, R. E., Zoback, M. L., and Thompson, G. A., 1983, Implications of selected subsurface data on the structural form and evolution of some basins in the northern Basin and Range province, Nevada and Utah: *Geological Society of America Bulletin*, v.96, p.347-361.
- Atwater, T., 1970, Implications of plate tectonics for the Cenozoic tectonic evolution of eastern North America: *Geological Society of America Bulletin*, v.81, p.3513-3536.
- Arizona Copper Company, Anonymous, 1921, Estimate of ore reserves, Coronado Division: unpublished report on file in Phelps Dodge Morenci, Inc., geology office.
- _____, 1919, Earling, R. B., Report on low-grade oxidized ores of the Arizona Copper Co.: unpublished report on file in Phelps Dodge Morenci, Inc., geology office.
- _____, 1915, Earling, R. B., Report on Wright's Keystone group; Metcalf Arizona: unpublished report on file in Phelps Dodge Morenci, geology office.

- _____, 1915, Earling, R. B., Report on the Abbie B.-Keystone mine of the Arizona Copper Co., Ltd.: unpublished report on file in Phelps Dodge Morenci, Inc., geology office.
- _____, 1915, Earling, R. B., Report on the Coronado mine: unpublished report on file in Phelps Dodge Morenci, Inc., geology office.
- Armstrong, R. L., 1974, Magmatism, orogenic timing, and orogenic diachronism in the Cordillera from Mexico to Canada: *Nature*, v. 247, p. 348-351.
- Armstrong, A. K., and Mamet, B. L., 1978, The Mississippian System of Southwestern New Mexico and Southeastern New Mexico, *in* Callender, J.F., Wilt, J.C., Clemons, R.E., & James, H.L., ed., *Land of Cochise Southeastern Arizona: New Mexico Geological Society, 29th Field Conference*, p.183-193.
- Bennett, K. C., 1975, Geology and origin of the breccias in the Morenci-Metcalf district Greenlee Co., Arizona: unpublished M.S. Thesis, Univ. of Arizona, 153 p.
- Beus, S. S., 1989, Devonian and Mississippian geology of Arizona, *in* Jenny, J.P., and Reynolds, S.J., ed., *Geologic evolution of Arizona: Tuscon, Arizona Geological Society Digest 17*, p.287-313.
- Billingsley, P., and Locke, A., 1935, Tectonic position of ore districts in the Rocky Mountain region: *Transactions of the American Institute of Mining and Metallurgical Engineers*, v. 115, p.59-68
- _____, 1941, Structure of ore districts in the continental framework: *Transactions of the American Institute of Mining and Metallurgical Engineers*, v. 144, p.9-64
- Bird, P., 1984, Laramide crustal thickening event in the Rocky Mountain foreland and Great Plains: *Tectonics*, v. 3, no. 7, p. 741-758.
- Blackstone, D. L., 1983, Laramide compressional tectonics, southwestern Wyoming: *Contributions to Geology, Univ. of Wyoming*, v. 22, no. 1, p.1-38.
- Burke, K., 1980, Intracontinental rifts and aulacogens, *in* *Continental tectonics: Washington, D.C., National Academy of Sciences*, p.42-49.
- Cather, S. M., 1992, Suggested revisions to the Tertiary tectonic history of north-central New Mexico, *in* Lucas, S.G., Kues, B.S., Williamson, T.E., and Hunt, A.P., eds., *San Juan Basin IV: Socorro, New Mexico Geological Society Guidebook 43*, p.109-122.

- _____. 1990, Stress and volcanism in the northern Mogollon-Datil volcanic field, New Mexico: Effects of the post- Laramide tectonic transition: Geological Society of America Bulletin, v.102, p.1447-1458.
- _____. 1980, Petrology, diagenesis, and genetic stratigraphy of the Eocene Baca Formation, Alamo Navajo Reservation and vicinity, Socorro County, New Mexico: M.S. Thesis, The University of Texas at Austin.
- Cather, S. M., and Chapin, C. E., 1990, Paleogeographic and paleotectonic setting of Laramide sedimentary basins in the central Rocky Mountain region, Alternative interpretation: Geological Society of America Bulletin, v.102, p.256-260.
- Cather, S. M., and Johnson, B. D., 1984, Eocene tectonics and depositional setting of west-central New Mexico and eastern Arizona: Socorro, New Mexico Bureau of Mines and Mineral Resources, Circular 192.
- Chamberlin R. M., and Cather, S. M., 1994, Definition of the Mogollon Slope, west-central New Mexico, *in* Chamberlin, R.M., Kues, B.S., Cather, S.M., Barker, J.M., and McIntosh, W.C., eds., Mogollon Slope: west-central New Mexico and east-central Arizona: Socorro, New Mexico Geological Society Guidebook 45, p.5-6.
- Chapin, C. E., 1971, The Rio Grande rift, Part I; Modifications and additions: Socorro, New Mexico Geological Society Guidebook 22, p.191-201.
- Chapin, C. E., 1979, Evolution of the Rio Grande rift: A summary, *in* Riecker, R.E., ed., Rio Grande rift: tectonics and magmatism: Washington, D.C., American Geophysical Union, p.1-15.
- Chapin, C. E., 1988, Axial basins of the northern and central Rio Grande rift, *in* Sloss, L.L., ed., Sedimentary cover North American craton: United States Geological Society of America, The Geology of North America, v. D-2, p.165- 170.
- Chapin, C. E., and Cather, S. M., 1981, Eocene tectonics and sedimentation in the Colorado Plateau - Rocky Mountain area, *in* Dickinson, W.R., & Payne, W.D., ed., Relations of tectonics to ore deposits in the southern Cordillera: Arizona Geological Society Digest, v. 14, p.173-198.
- Chapin, C. E., and Cather, S. M., 1994, Tectonic setting of the axial basins of the northern and central Rio Grande rift, *in* Keller, G.R., and Cather, S.M., eds., Basins of the Rio Grande rift: Structure, stratigraphy, and tectonic setting: Boulder, Colorado, Geological Society of America Special Paper 291, p.5-25.

- Chapin, C. E., Chamberlin, R. M., Osburn, G. R., White, D. W., and Sanford, A. R., 1978, Exploration framework of the Socorro geothermal area, New Mexico: New Mexico Geological Society, Special Publication 7, p.115-129.
- Cobban, W. A., and Hook, S. C., 1984, Mid-Cretaceous molluscan biostratigraphy and paleogeography of the southwestern part of the Western Interior, United States, *in*, Westermann, G.E.G., ed., Jurassic-Cretaceous Biochronology and Paleogeography of North America: Geological Association of Canada Special Paper 27, p.257-271.
- Condie, K. C., 1982, Plate tectonics model for Proterozoic continental accretion in the southwestern U.S.: *Geology* v. 10, p. 37-42.
- Coney, P. J., 1971, Cordilleran tectonic transitions and motions of the North American plate: *Nature*, v. 233, p. 462-465.
- _____, 1972, Cordilleran tectonics and North American plate motion: *Amer. Jour. Sci.*, v.272, p.603-628.
- _____, 1976, Plate Tectonics of the Laramide orogeny, *in* Woodward, L. A., and Northrop, S. A., eds., Tectonics and mineral resources of southwestern North America: New Mexico Geological Society Special Publication 6, p.5-10.
- Coney, P. J., and Reynolds, S. J., 1977, Cordilleran Benioff zones: *Nature*, v. 270, p.403-406.
- Conway, M. C., and Silver, L. T., 1989, Early Proterozoic rocks (1710-1615 Ma) in central to southeastern Arizona, *in*, Jenney, J.P., and Reynolds, S.J., Geologic evolution of Arizona: Tucson, Arizona Geological Society Digest 17, p.165-186.
- Cook, S. S., 1994, The geologic history of supergene enrichment in the porphyry copper deposits of southwestern North America: unpublished Ph.D. dissertation, Tucson, University of Arizona, 163 p.
- Cordell, L., 1978, Regional geophysical setting of the Rio Grande rift: *Geological Society of America Bulletin*, v.89, p.1073-1090.
- Crews, S. G., 1994, Tectonic control of synrift sedimentation patterns, Reserve graben, Southwest New Mexico, *in* Chamberlin, R.M., Kues, B.S., Cather, S.M., Barker, J.M., and McIntosh, W.C., eds., Mogollon Slope, west-central New Mexico and east-central Arizona: New Mexico Geological Society Guidebook, 45th Annual Field Conference, p.125-134.

- Cross, T. A., 1986, Tectonic controls on foreland basin subsidence and Laramide style deformation, western United States: International Association of Sedimentologists Special Publication 28, p.15-39.
- Damon, P. E., Shafiqullah, M., and Clark, K. F., 1981, Age trends of igneous activity in relation to metallogenesis in the Southern Cordillera, *in* Dickinson, W.R., and Payne, W.D., eds., Relations of tectonics to ore deposits in the southern Cordillera: Tucson, Arizona Geological Society Digest 14, p.137-154.
- Damon, P. E., 1971, The relationship between late Cenozoic volcanism and tectonism and orogenic-epirogenic periodicity, *in* Turekain, K.K., ed., Conference on late Cenozoic glacial ages: New York, John Wiley and Sons, p.15-35.
- Davis, G. H., 1978, Monocline fold pattern of the Colorado Plateau, *in* Matthews, V., ed., Laramide folding associated with basement block faulting in the western United States: Geological Society America Memoir 151, p.215-233.
- _____, 1979, Laramide folding and faulting in southeastern Arizona: American Journal of Science, v. 279, p.543-569.
- _____, 1980, Structural characteristics of metamorphic core complexes, southern Arizona, *in* Crittenden, M.D., Coney, P. J., and Davis, G.H., eds., Cordilleran metamorphic complexes: Geological Society of America Memoir 153, p.35-78.
- _____, 1981, Regional strain analysis of the superposed deformations in southeastern Arizona and the eastern Great Basin, *in* Dickinson, W.R., and Payne, W.D., eds., Relations of tectonics to ore deposits in the Southern Cordillera: Tucson, Arizona Geological Digest 14, p. 155- 172.
- Davis, G. H., and Hardy, J. J., 1981, The Eagle Pass detachment, southwestern Arizona: Product of mid-Miocene listric(?) normal faulting in the southern Basin and Range: Geological Society of America Bulletin, Part 1, v.92, p.749-762.
- Detroit Copper Company, 1913, Boutwell, J. M., Prospects on the Detroit property, Morenci Arizona: unpublished report on file in Phelps Dodge Morenci, Inc. geology office
- _____, 1910, Devel, D. C., Report on general development, Detroit Copper Company: unpublished report on file in Phelps Dodge Morenci, Inc. geology office.
- _____, 1916, Porri, W., Pyramid mine new ore body: unpublished report on file in Phelps Dodge Morenci, Inc. geology office.

- Dewey, J. F., 1988, Extensional collapse of orogens: *Tectonics*, v.7, p.1123-1139.
- Dickinson, W. R., 1981, Plate tectonic evolution of the southern cordillera: *in* Dickinson, W.R., & Payne, W.D., ed., *Relations of tectonics to ore deposits in the southern Cordillera: Arizona Geology Society Digest*, v. 14, p.113-135.
- _____ 1989, Tectonic setting of Arizona through geologic time, *in* Jenny, J.P., and Reynolds, S.J. ed., *Geologic evolution of Arizona: Tucson, Arizona Geological Society Digest* 17, p.1-16.
- Dickinson, W. R. and Snyder, W. S., 1978, Plate Tectonics of the Laramide Orogeny: *in* Matthews, V., ed., *Laramide Folding Associated with Basement Block Faulting in the Western United States*, Geological Society America Memoir 151, p.355-365.
- Drews, Harald, 1981, Tectonics of southern Arizona: United States Geological Survey Professional Paper 1144, p.96.
- _____ 1978, The Cordilleran orogenic belt between Nevada and Chihuahua: *Geological Society America Bulletin*, v.89, p.641-657.
- Eaton, G. P., 1982, The Basin and Range province: Origin of tectonic significance: *Annual Review of Earth and Planetary Sciences*, v.10, p.409-440.
- Elston, W. E., Damon, P. E., Coney, P. J., Rhodes, R. C., Smith, E. I., and Bikerman, M., 1973, Tertiary volcanic rocks, Mogollon-Datil province, New Mexico, and surrounding region: K-Ar dates, patterns of eruption, and periods of mineralization: *Geological Society of America Bulletin*, v.84, p.2259-2274.
- Elston, W. E., and Bornhorst, T. J., 1979, The Rio Grande rift in context of regional post-40 m.y. volcanic and tectonic events, *in* Riecker, R.E., ed., *Rio Grande rift: Tectonics and magmatism: Washington D.C., American Geophysical Union*, p.416-438.
- Epis, C. R., and Chapin, C. E., 1975, Geomorphic and tectonic implications of the post-Laramide, late-Eocene erosional surface in the Southern Rocky Mountains: *in* Curtis, B.F., ed., *Cenozoic History of the Southern Rocky Mountains: Geological Society America Memoir* 144, p.45-73.
- Faulds, J. E., Geissman, J. W., and Mawer, C. K., 1990, Structural development of a major accommodation zone in the Basin and Range Province, northwestern Arizona and southern Nevada; Implications for kinematic models of crustal extension, *in* Wernicke, B.P. ed., *Basin and Range extensional tectonics near the*

- latitude of Las Vegas, Nevada: Geological Society of America Memoir 176, p.37-76.
- Fleuty, W. L., 1975., Slickensides and slickensides: Geological Magazine, v. 112, no.3, p.319-322.
- Foster, D. A., Harrison, T. M., Miller, C. F., and Howard, K. A., 1990, The $^{40}\text{Ar}/^{39}\text{Ar}$ thermochronology of the eastern Mojave Desert, California, and adjacent western Arizona with implications for the evolution of Metamorphic core complexes: Journal of Geophysical Research, v.5, p.20,005-20,024.
- Frostric, L.E., and Reid, I., 1987, Tectonic control of desert sediments in rift basins ancient and modern, *in* Frostric, L.E., and Reid, I., eds., Desert sediments: ancient and modern: Geological Society of London, Special Publication 35, p.53-68.
- Frazier, W. J., and Schwimmer, D. R., 1987, Regional stratigraphy of North America: Plenum Press, New York.
- Gilbert, G. K., 1875, Geology of portions of New Mexico and Arizona, explored and surveyed in 1873, *in* Wheeler, G.M., Report on geographical and geological exploration and surveys west of the 100th meridian, v.3, part 5: Washington, Government Printing Office, p.507-567.
- Goodwin, L. B., and Haxel, G. B., 1990, Structural evolution of the southern Baboquivari Mountains, south-central Arizona and north-central Sonora: Tectonics, v.9, no.5, p.1077-1095.
- Griffin, J. B., Ring, J. A., and Lowery, R. E., 1993, Laramide intrusive complex of the Morenci District, Greenlee County, Arizona: Arizona Conference A.M.I.E., Geology Division Spring Field Trip, Morenci, Arizona, unpublished Phelps Dodge Corp. report.
- Hamilton, W. B., 1981, Plate-tectonic mechanisms of Laramide deformation, *in* Boyd, D.W., and Lillegraven, J.A., eds., Rocky Mountain foreland basement tectonics: Laramie, University of Wyoming Contributions to Geology, v.19, p.87-92.
- _____ 1988, Laramide crustal shortening: Geological Society of America Memoir 171, p.27-39.
- Haxel, G. B., Tosdal, R. M., May, D.J., and Wright, J.E., 1984, Latest Cretaceous and early Tertiary orogenesis in south-central Arizona: Thrust faulting, regional metamorphism, and granitic plutonism: Geological Society of America Bulletin 95, p.631-653.

- Hayes, P. T., 1970, Cretaceous paleogeography of southeastern Arizona and adjacent areas: United States Geological Survey Professional Paper 658-B, p.1-34.
- Hayes, P. T., 1978, Cambrian and Ordovician Rocks of Southeastern Arizona and Southwestern New Mexico, *in* Callender, J.F., Wilt, J.C., Clemons, R.E., & James, H.L., ed., Land of Cochise Southeastern Arizona: New Mexico Geological Society, 29th Field Conference, p.165-175.
- Hayes, P. T., and Drews, H., 1978, Mesozoic Depositional History of Southeastern Arizona: *in* Callender, J.F., Wilt, J.C., Clemons, R.E., & James, H.L., ed., Land of Cochise Southeastern Arizona: New Mexico Geological Society, 29th Field Conference, p.201-209.
- Heidrick, T. L., and Titley, S.R., 1982, Fracture and dike patterns in Laramide plutons and their structural implications, *in* Titley, S. R., ed., Advances in geology of the porphyry copper deposits, southwestern North America: Tucson, University of Arizona Press, p.73-91.
- Houser, B. B., 1994, Geology of the late Cenozoic Alma Basin, New Mexico and Arizona, *in* Chamberlin, R.M., Kues, B.S., Cather, S.M., Barker, J.M., and McIntosh, W.C., eds., Mogollon Slope, west-central New Mexico and east-central Arizona: New Mexico Geological Society Guidebook, 45th Annual Field Conference, p.121-124.
- Houser, B. B., Richter, D. H., and Shafiqullah, M., 1985, Geologic map of the Safford Quadrangle, Graham County, Arizona: U.S. Geological Survey Misc. Investigations Series, Map MI-1617.
- Jones, R. W., 1966, Differential vertical uplift-A major factor in the structural evolution of southeastern Arizona: Arizona Geological Society Digest, v.8, p.97-124.
- Jordan, T. E., Isacks, B. L., Allemendinger, R. W., Brewer, J. A., Ramos, V. A., Ando, C. J., 1983, Andean tectonics related to geometry of subducted Nazca plate: Geological Society America Bulletin v. 94, p.341-361.
- Karlstrom, K. E., and Bowering, S. A., 1988, Early proterozoic assembly of tectonostratigraphic terranes in southwestern North America: Journal of Geology, v. 96, p. 561-576.
- Keith, S. B., and Wilt, J. C., 1985, Late Cretaceous and Cenozoic orogenesis of Arizona and adjacent regions: A stratotectonic approach, *in* Flores, R.M., and Kaplan, S.S., eds., Cenozoic paleogeography of west-central United States: Denver,

Colorado, Rocky Mountain Section, Society of Economic Paleontologists and Mineralogists, p.403-437.

- Keith, S. B., Reynolds, S. J., Damon, P. E., Shafiqullah, M., Livingston, D. E., and Pushkar, P.D., 1980, Evidence for multiple intrusions and deformation within the Santa Catalina-Rincon-Tortolita crystalline complex, southeastern Arizona, in Crittenden, M., Coney, P.J., and Davis, G.H., eds., Cordilleran metamorphic core complexes: Geological Society of America Memoir 153, p.217-267.
- Keith, S. B., 1978, Paleosubduction geometries inferred from Cretaceous and Tertiary magmatic patterns in southwestern North America: *Geology*, v. 6, pp. 516-521.
- Knapp, R. B., and Norton, D. L., 1981, Preliminary numerical analysis of processes related to magma crystallization and stress evaluation in cooling pluton environments: *American Journal of Science*, v. 281, p. 35-68.
- Koide, H., and Bhattacharji, S., 1975, Formation of fractures around magmatic intrusions and their role in ore localization: *Economic Geology*, v. 70, p. 781-799.
- Langton, J. M., 1973, Ore genesis in the Morenci-Metcalf district: Society of Mining Engineers, A.I.M.E. Transactions, v.254.
- Leeder, M. R., and Jackson, J. A., 1993, The interaction between normal faulting and drainage in active extensional basins, with examples from the western United States and central Greece: *Basin Research*, v.5, p.79-102.
- Leeder, M. R., and Gawthorpe, 1987, Sedimentary models for extensional tilt-block/half-graben basins, *in* Coward, M.P., Dewey, J.F., and Hancock, P.L., eds., Continental extensional tectonics: Geological Society of London, Special Publication No 28, p.39-152.
- Lindgren, W., 1905, The copper deposits of the Clifton-Morenci District, Arizona: U.S. Geological Survey, Professional Paper No. 43, 374 p.
- Lipman, P. W., 1981, Volcano-tectonic setting of Tertiary ore deposits, Southern Rocky Mountains, *in* Dickinson, W.R., and Payne, W.D., eds., Relations of tectonics to ore deposits in the Southern Cordillera: Tucson, Arizona Geological Society Digest 14, p.199-213.
- Lipman, P. W., Doe, B. R., Hedge, C. E., and Steven, T. A., 1978, Petrologic evolution of the San Juan volcanic field, southwestern Colorado: Pb and Sr isotope evidence: *Geological Society of America Bulletin*, v.89, p.59-82.

- Lipman, P. W., Prostka, H. J., and Christiansen, R. L., 1972, Cenozoic volcanism and plate tectonic evolution of the western United States: Part I, early and middle Cenozoic: Royal Society of London Philosophical Transactions, series A, v.271, p. 217-248.
- Lister, G. S., Etheridge, M. A., Symonds, P. A., 1986, Detachment faulting and the evolution of passive continental margins: *Geology*, v.14, p.246-250.
- Livaccari, R. F., 1991, Role of crustal thickening and extensional collapse in the tectonic evolution of the Sevier-Laramide orogeny, western United States: *Geology*, v.19, p.1104-1107.
- Livingston, D. E., Mauger, D. L., and Damon, P. E., 1968, Geochronology of the emplacement, enrichment and preservation of Arizona porphyry copper deposits: *Economic Geology*, v. 63, p.30-36.
- Lowell, J. D., 1983, Foreland deformation: in Rocky Mountain Association of Geologists symposium and field conference, p. 1-9.
- _____ 1974, Regional characteristics of porphyry copper deposits of the southwest: *Economic Geology*, v.69, p.601-617.
- Mack, G. H. and Clemons, R. E., 1988, Structural and stratigraphic evidence for the Laramide (early Tertiary) Burro uplift in Southwestern New Mexico, *in* Mack, G.H., Lawton, T.F., and Lucas, S.G., eds., Cretaceous and Laramide tectonic evolution of southwestern New Mexico: Socorro, New Mexico Geological Society 39th Annual Field Conference Guidebook, p.59-67.
- Mack, G. H., and Seager, W.R., 1990, Tectonic controls on facies distribution of the Camp Rice and Palomas Formations (Pliocene-Pleistocene) in the southern Rio Grande rift: *Geological Society of America Bulletin*, v.102., p.45-53.
- Marvin, R. F., Naeser, C. W., Bikerman, M., Mehnert, H. H., and Ratte, J. C., 1987, Isotopic age dates of post-Paleocene igneous rocks within and bordering the Clifton 1 x 2 quadrangle, Arizona - New Mexico: *New Mexico Bureau of Mines and Mineral Resources Bulletin* 118, 63p.
- Mayo, E. B., 1958, Lineament tectonics and some ore districts of the Southwest: *Mining Engineering*, p.1169-1175.
- Mayo, E. B., and Davis, G. H., 1976, Origin of the Red Hills-Piedmontite Hills uplift: *Arizona Geological Society Digest*, v.10, p.103-131.

- McCandless, T. E., and Ruiz, J., 1993, Rhenium-Osmium Evidence for Regional Mineralization in Southwestern North America: *Science*, v.261, p.1282-1286.
- McIntosh, W. C., Chapin, C.E., Ratte, J.C., and Sutter, J. F., 1992, Time-stratigraphic framework for the Eocene-Oligocene Mogollon-Datil volcanic field, southwest New Mexico: *Geological Society of America Bulletin*, v.104, p. 851-871.
- McIntosh, W. C., Kedzie, L. L., and Sutter, J. F., 1991, Paleomagnetism and $^{40}\text{Ar}/^{39}\text{Ar}$ ages of ignimbrites, Mogollon-Datil volcanic field, southwestern New Mexico: Socorro, New Mexico Bureau of Mines and Mineral Resources Bulletin 135, 99 p.
- McIntosh, W. C., Sutter, J. F., Chapin, C. E., and Kedzie, L. L., 1990, High precision $^{40}\text{Ar}/^{39}\text{Ar}$ sanidine geochronology of ignimbrites in the Mogollon-Datil volcanic field, southwestern New Mexico: *Bulletin of Volcanology*, v.52, p.584-601.
- McDowell, F. W., 1971, K-Ar ages of igneous rocks from the western United States: *Isochron/West*, no.2, p.1-17.
- Menges, C. M., and Pearthree, P. A., 1989, Late Cenozoic tectonism in Arizona and its impact on regional landscape evolution, in Jenney, J.P., and Reynolds, S.J., eds., *Geologic Evolution of Arizona: Tucson, Arizona Geological Society Digest 17*, p.649-680.
- Menges, C. M., and McFadden, L. M., 1981., Evidence for a latest Miocene to Pliocene transition from Basin-Range tectonic to post-tectonic landscape evolution in Southeastern Arizona, *in* Stone, Claudia, and Jenney, J.P., eds., *Geologic Evolution of Arizona: Tucson, Arizona Geological Society Digest 13*, p.151-160.
- Menzer, F. J., 1980, The Laramide intrusive complex at Morenci-Metcalf, Arizona: Arizona Conference A.M.I.E., Mining Geology Division, unpublished report on file in Phelps Dodge Morenci, Inc. geology office..
- Mohr, P., 1982, Musings on continental rifts, *in* Palmason, G., ed., *Continental and oceanic rifts: American Geophysical Union and Geological Society of America Geodynamics Series*, v.8, p.293-309.
- Molnar, P. M., and Lyon-Caen, H., 1988, Some simple physical aspects of the support, structure, and evolution of mountain belts, *in* Clark, S.P., Jr., Burchfiel, B.C., and Suppe, J., eds., *Processes in continental lithospheric deformation: Geological Society of America Special Paper 218*, p.179-207.

- Moolick, R. T. and Durek, J. J., 1966, The Morenci District, *in* Titley, S.R. and Hicks, C.L., eds., *Geology of the porphyry copper deposits southwestern North America*: University of Arizona Press, Tucson, Arizona, p.221-233.
- Nations, J. D., 1989, Cretaceous History of northeastern and east-central Arizona: *in* Jenny, J.P., & Reynolds, S.J., ed., *Geologic evolution of Arizona*, Arizona Geological Society Digest 17, p.435-447.
- Naruk, S. J., 1986. Strain and displacement across the Pinaleno Mountains shear zone, U.S.A.: *Journal of Structural Geology*, v.8, p.35-46.
- Nealey, D. L., and Sheridan, M. F., 1989, Post-Laramide volcanic rocks of Arizona and northern Sonora, Mexico, and their inclusions, *in* Jenny, J.P., and Reynolds, S.J., eds., *Geologic Evolution of Arizona: Arizona Geological Society Digest 17*, p.609-647.
- North, R. M., and Preece, R. K., 1993, Supergene ore-forming processes in the Morenci district: Arizona Conference A.M.I.E., Geology Division Spring Field Trip, Morenci, Arizona, unpublished Phelps Dodge Corp. extended abstract.
- Pawlowski, M. R., and Walker, M. A., 1993, Geology of the Morenci mining district: The regional context: Arizona Conference A.M.I.E., Geology Division Spring Field Trip, Morenci, Arizona, unpublished Phelps Dodge Corp. extended abstract.
- Pierce, H. W., 1985, Arizona's backbone: the transition zone: Arizona Bureau of Geology and Mineral Technology, Field Notes, v. 15, pp. 1-6.
- Pierce, H. W., Damon, P. E., and Shafiqullah, M., 1979, An Oligocene(?) Colorado Plateau edge in Arizona: *Tectonophysics*, v. 61. pp.1-24.
- Preece, R. K., 1984, Geology of the Morenci district: unpublished compilation map on file in Phelps Dodge Morenci, Inc. geology office., scale 1:9600.
- Preece, R. K., 1986, Intrusive-hosted alteration and mineralization within the Morenci porphyry copper deposit, [abs.]: *Geological Society of America, Abstracts with Programs*, v. 18, p. 722.
- Preece, R. K., Stegen, R. J., and Weiskopf, T. A., Hydrothermal alteration and mineralization of the Morenci porphyry copper deposit, Greenlee County Arizona: Arizona Conference A.I.M.E., Geology Division Spring Field Trip, Morenci, Arizona, unpublished Phelps Dodge Corp. extended abstract.

- Preece, R. K., 1985, Distribution of mineralization in the Morenci Mine: A geologic critique of proposed plan V final limits: unpublished report on file in Phelps Dodge Morenci, Inc. geology office.
- Preece, R. K., and Menzer, F. J., 1992, Geology of the Morenci copper deposit, Greenlee County, Arizona: unpublished Northwest Mining Association Short Course, Porphyry Copper Model-Regional Talks and Settings, Tucson, Arizona and Spokane, Washington.
- Preece, R. K., and Menzer, F. J., 1982, Geology and economic potential of the Western Copper Exchange (W.C.E. property): Unpublished report on file in Phelps Dodge Morenci, Inc. geology office.
- Ransome, F. L., 1903, Geology of the Globe copper district, Arizona: United States Geological Survey Professional Paper 12, 168 p.
- Ratte, J. C., 1989, Geologic map of the Bull Basin quadrangle, Catron County, New Mexico: U.S. Geological Survey, Geologic Quadrangle Map GQ-1651, scale 1:24,000.
- Ratte, J. C., McIntosh, W. C., and Houser, B. B., 1989, Geologic map of the Horse Springs West Quadrangle: U. S. Geological Survey, Open-file Report 89.201, scale 1:24,000.
- Ratte, J. C., Marvin, R. F., and Naeser, C. W., 1984, Calderas and ash-flow tuffs in the Mogollon Mountains: *Journal of Geophysical Research*, v.89, p. 8713-8732.
- Ratte, J. C., Landis, E. R., Gaskill, D. L., and Raabe, R. G., 1969, Mineral Resources of the Blue Range Primitive Area, Greenlee County Arizona and Catron County, New Mexico: United States Geological Survey Bulletin 1261-E, p.E1-E91, with geologic map, scale 1:62,500.
- Reber, L. R., 1916, The Mineralization at Clifton-Morenci: *Economic Geology*, v.11, p.528-573.
- Rehrig, W. A., 1986, Processes of regional Tertiary extension in the western Cordillera: Insights from the metamorphic core complexes: *Geological Society of America Special Paper* 208, p.97-122.
- Rehrig, W. A., and Heidrick, T. L., 1972, Regional fracturing in Laramide stocks of Arizona and its relationship to porphyry copper mineralization: *Economic Geology*, v. 67, p.198-213.

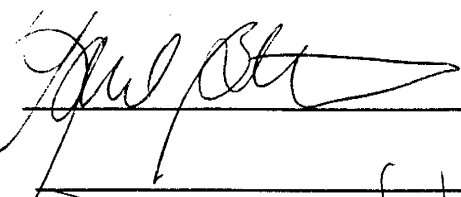
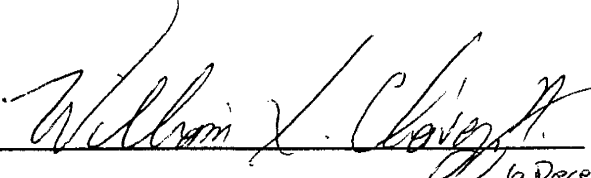
- _____. 1976, Regional tectonic stress during the Laramide and late Tertiary intrusive periods, Basin and Range province, *in* Wilt, J. C. and Jenny, J. P., eds., Tectonic digest: Tucson, Arizona Geological Society Digest 10, p.205-228.
- Rehrig, W. A., and Reynolds, S. J., 1980, Geologic and geochronologic reconnaissance of a northwest-trending zone of metamorphic core complexes in southern and western Arizona, *in* Crittenden, M., Coney, P.J., and Davis, G.H., eds., Cordilleran metamorphic core complexes: Geological Society of America Memoir 153, p.490.
- Reynolds, S. J., 1985, Geology of the South Mountains, central Arizona: Tucson, Arizona Bureau of Geology and Mineral Technology Bulletin 195, 61 p.
- Reynolds, S. J., Richard, S. M., Haxel, G. B., Tosdal, R.M., and Laubach, S.E., 1988, Geologic setting of Mesozoic and Cenozoic metamorphism in Arizona, *in* Ernst, W.G., ed., Metamorphism and crustal evolution of the Western United States, Volume 7: Prentice Hall, Englewood Cliffs, N.J.
- Reynolds, S. J., Florence, F. P., Welty, J. W., Roody, M. S., Currier, D. A., Anderson, A. V., and Keith, S. B., 1986, Compilation of radiometric age determinations in Arizona: Arizona Bureau of Geology and Mineral Technology, Geological Survey Branch. Bulletin 197.
- Reynolds, S. J., Spencer, J. E., Richard, S. M., and Laubach, S. E., 1986, Mesozoic structures in west-central Arizona: Arizona Geological Society Digest 16, p.35-51.
- Reynolds, S. J. and Spencer, J. E., 1985, Evidence for large-scale transport on the Bullard detachment fault, west- central Arizona: *Geology*, v.13, pp.353-356.
- Rosendahl, B. R., 1987, Architecture of continental rifts with special reference to East Africa: *Annual Revisions Earth and Planetary Sciences* 15, p. 445-503.
- Scarborough, R. B., and Peirce, H. W., 1978, Late Cenozoic basins in Arizona, *in* Callender, J.F., Wilt, J.C., and Clemons, R.F., eds., Land of Cochise: New Mexico Geological Society Guidebook, 29th Field Conference, Socorro, New Mexico, p.253-259.
- Schmitt, H. A., 1966, The porphyry copper deposits in their regional setting, *in*, Titley, S.R., and Hicks, C.L., eds., Geology of the porphyry copper deposits, Southwestern North America: Tucson, University of Arizona Press, p.17-33.
- Schumacher, D., 1978, Devonian stratigraphy and correlations in Southeastern Arizona, *in* Callender, J.F., Wilt, J.C., Clemons, R.E., & James, H.L., ed., Land of Cochise

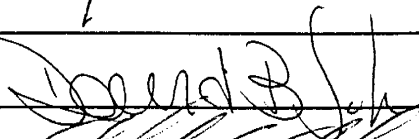

Southeastern Arizona: New Mexico Geological Society Guidebook, 29th Field Conference, Socorro, New Mexico, p.175-183.

- Seager, W. R., Shafiqullah, M., Hawley, J. W., and Marvin, R. F., 1984, New K-Ar dates from basalts and the evolution of the southern Rio Grande rift: Geological Society of America Bulletin, v.95, no.1, p.87-99.
- Shafiqullah, M., Damon, P. E., Lynch, D. J., Reynolds, S. J., Rehrig, W. A., and Raymond, R. H., 1980, K-Ar geochronology and geologic history of southwestern Arizona and adjacent areas, *in* Jenny, J. P., and Stone, Claudia, eds., Studies in western Arizona, Tucson, Arizona Geological Society Digest, p.201-260.
- Shafiqullah, M., Damon, P. E., and Kuck, P. H., 1978, Mid-Tertiary magmatism in southeastern Arizona, *in* Callender, J.F., Wilt, J.C., and Clemons, R.F., eds., Land of Cochise: New Mexico Geological Society Guidebook, 29th Field Conference, Socorro, New Mexico p.231-241.
- Sibson, R. H., 1977, Fault rocks and fault mechanisms: Journal of the Geological Society of London, v. 133, p. 191-213
- Silver, L. T., Williams, I. S., and Woodhead, J. A., 1981, Uranium in Granites from the Southwestern United States: Actinide parent-daughter system, sites and mobilization: U.S. Department of Energy Open File Report GJBX-45, p.315.
- Simons, F. S., 1964, Geology of the Klondyke quadrangle Graham and Pinal counties Arizona: Geological Survey Professional Paper 461.
- Spencer, J.E., and Reynolds, S. J., 1990, Relationship between Mesozoic and Cenozoic tectonic features in west-central Arizona and adjacent southeastern California: Journal of Geophysical Research, v.95, p.539-555.
- Spencer, J. E., and Reynolds, S. J., 1989, Middle Tertiary tectonics of Arizona and adjacent areas, *in* Jenney, J.P., and Reynolds, S.J., eds., Geologic Evolution of Arizona: Arizona Geological Society Digest 17, p.539-574.
- Spencer, J. E., 1984, Role of tectonic denudation in warping and uplift of low-angle normal faults: Geology, v.12, p.123-124.
- Strangway, D. W., Simpson, J., and York, D., 1976, Paleomagnetic studies of volcanic rocks from the Mogollon Plateau area of Arizona and New Mexico, *in* Elston, W.E., and Northrop, S.A., eds., Cenozoic volcanism in southwest New Mexico: New Mexico Geological Society Special Publication 5, p.119-124.

- Titley, S. R., 1976, Evidence for a Mesozoic linear tectonic pattern in southeastern Arizona: Arizona Geological Society Digest 10, pp. 71-101.
- _____, 1982, Geologic Setting of Porphyry Copper Deposits, Southeastern Arizona: *in* Titley, S. R., ed., Advances in Geology of the porphyry copper deposits, Southwestern North America: University of Arizona Press, Tucson, AZ., p.37-58.
- Titley, S. J., 1995, Geological summary and perspective of porphyry copper deposits in southwestern North America, *in*, Pierce, F.W., and Bolm, J.G., eds., Porphyry copper deposits of the American cordillera: Tucson, Arizona Geological Society Digest 20, p. 6-20.
- Tweto, O., 1975, Laramide (Late Cretaceous-Early Tertiary) Orogeny in the Southern Rocky Mountains: *in* Curtis, B.F., ed., Cenozoic History of the Southern Rocky Mountains, Geological Society America Memoir 144, p.1-45.
- Wahl, D. E., 1980, Mid-Tertiary volcanic geology in parts of Greenlee County, Arizona, and Grant and Hidalgo counties, New Mexico: Arizona State University Ph.D. Dissertation. 144 p.
- Wernicke, B., and Burchfiel, B. C., 1982, Modes of extensional tectonics: Journal of Structural Geology, v.4 no.2, p.105-115.
- Zoback, M. L., Anderson, R. E., and Thompson, G. A., 1981, Cenozoic evolution of the state of stress and the style of tectonism of the Basin and Range province of the western United States: Philosophical Transactions of the Royal Society of London, series A, v.300, p.189-434.
- Zoback, M. L., and Zoback, M., 1980, State of stress in the conterminous United States: Journal of Geophysical Research, v.85, no. 11, p.6113-6156.

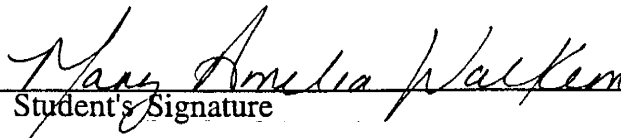
This thesis is accepted on behalf of the faculty
of the Institute by the following committee:

 _____
Advisor  _____
6 December, 1995

 _____
 _____

_____ *Dec. 6, 1995* _____
Date

I release this document to the New Mexico Institute of Mining and Technology.

 _____
Student's Signature *Dec 6 1995* _____
Date